# Stony Brook University

# Post-transcriptional Gene Regulation During Meiosis in *Schizosaccharomyces pombe*

A Dissertation Presented

by

**Kaustav Mukherjee**

to

The Graduate School

in Partial Fulfillment of the

Requirements

for the Degree of

**Doctor of Philosophy**

in

**Genetics**

**Stony Brook University**

**December 2015**
**Stony Brook University**

The Graduate School

**Kaustav Mukherjee**

We, the dissertation committee for the above candidate for the

Doctor of Philosophy degree, hereby recommend

acceptance of this dissertation.

**Dr. Janet Leatherwood**, Associate Professor
Department of Molecular Genetics and Microbiology
Dissertation Advisor

**Dr. Aaron Neiman**, Professor
Department of Biochemistry and Cell Biology
Chairperson of Defense

**Dr. Bruce Futcher**, Professor
Department of Molecular Genetics and Microbiology

**Dr. Wali Karzai**, Associate Professor
Department of Biochemistry and Cell Biology

**Dr. Charles Hoffman**, Professor
Department of Biology
Boston College

This dissertation is accepted by the Graduate School

**Charles Taber**
Dean of the Graduate School

# Abstract of the Dissertation

## Post-transcriptional Gene Regulation During Meiosis in *Schizosaccharomyces pombe*

by

**Kaustav Mukherjee**

**Doctor of Philosophy**

in

**Genetics**

**Stony Brook University**

**2015**

The fission yeast *Schizosaccharomyces pombe* grows by mitotic divisions as a haploid when nutrition is adequate. When starved for nitrogen, it mates with a cell of opposite mating type, undergoes meiosis and forms spores. When *S. pombe* cells switch from mitosis to meiosis, there is a massive rewiring of gene expression, controlled by both transcriptional and post-transcriptional gene regulation. I have studied two major post-transcriptional gene regulatory mechanisms during early meiosis in *S. pombe.*

A subset of early meiotic genes are actively transcribed even during vegetative growth, but an RNA binding protein called Mmi1 binds to their RNA and targets the RNA for degradation. We previously showed that two exonucleases of the exosome, Rrp6 and Dis3, are involved in degrading early meiotic RNAs. In my first project, I discovered

that Rrp6 plays a structural role in targeting early meiotic RNAs to the exosome. This function is very important for meiotic gene regulation even when Rrp6 itself lacks exonuclease activity to degrade RNAs. Unexpectedly, genome-wide analysis revealed that Rrp6 also targeted a subset of iron homeostasis mRNAs to the exosome, when sufficient iron was present. These mRNAs shared a nucleotide motif, indicating that they were possible targets of an unidentified RNA binding protein.

Induction of the early meiotic genes requires a specific RNA binding protein, Mei2. Mei2 is the master regulator of meiotic initiation in *S. pombe*, but the early steps controlled by Mei2 are unknown. In the next part of my dissertation research, I determined the RNAs bound to Mei2. Cells lacking Mei2 RNA binding activity cannot initiate meiosis. The only known partner of Mei2 is a noncoding RNA called meiRNA. However, Mei2 can trigger early meiotic events even in cells lacking meiRNA. This suggests that Mei2 must have additional RNA partners, which I aimed to determine in a genome-wide study. I found that Mei2 binds to the 5' UTR of two key meiotic inhibitors, *mmi1* and *rep2.* These results led to a model for meiotic induction by Mei2 and the hypothesis that initial meiotic induction by Mei2 is accomplished by down-regulating *mmi1* and *rep2.*

# To Mom and Dad

# TABLE OF CONTENTS

# List of Figures and Tables

## CHAPTER 1



## CHAPTER 2

## CHAPTER 3

# List of Abbreviations

5-FOA ..... 5-Fluoroorotic Acid
cAMP ..... cyclic Adenosine Mono-phosphate
cdc ..... Cell Division Cycle
CDK ..... Cyclin Dependent Kinase
DAPI ..... 4', 6-diamidino-2-phenylindole
DIC ..... Differential Interference Contrast
DNA ..... Deoxyribonucleic Acid
RNA ..... Ribonucleic Acid
dNTP ..... Deoxynucleoside Triphosphate
EDTA ..... Ethylenediaminetetraacetic Acid
EMM ..... Edinburgh Minimal Media
GEO ..... Gene Expression Omnibus
GO ..... Gene Ontology
HEPES ..... 4-(2-hydroxyethyl)-1-piperazineethanesulfonic acid
IGV ..... Integrative Genomics Viewer
IP ..... Immunoprecipitation
LAUH ..... Leucine, Adenine, Uracil, Histidine
MAPK ..... Mitogen Activated Protein Kinase
MBF ..... MCB-Binding Factor
ME ..... Malt Extract
*meu* ..... Meiotic Expression Upregulated
*mug* ..... meiotically upregulated gene
ts ..... Temperature Sensitive
CDS ..... Complementarity Determining Region
FPKM ..... Fragments per kilobase per Million
mRNA ..... messenger RNA
ncRNA ..... non coding RNA
RNase ..... Ribonuclease
ANOVA ..... Analysis of Variance
MEME ..... Multiple EM for Motif Elicitation
UTR ..... Untranslated Region
SDM ..... Site-Directed Mutagenesis
cDNA ..... complementary DNA
PAGE ..... Polyacrylamide Gel Electrophoresis

NLS ..... Nuclear Localization Signal
RIP ..... RNA Immunoprecipitation
CLIP ..... Cross-linking Immunoprecipitation
IgG ..... Immunoglobulin G
UV ..... Ultraviolet
RT ..... Reverse Transcriptase
CGH ..... Comparative Genome Hybridization
IGB ..... Integrated Genome Browser
PAP ..... Peroxidase Anti Peroxidase
PCR ..... Polymerase Chain Reaction
PKA ..... Protein Kinase A
PMSF ..... Phenylmethylsulfonyl Fluoride
qPCR ..... Quantitative PCR
SDS ..... Sodium Dodecyl Sulfate
Seq ..... Sequencing
TAP ..... Tandem Affinity Purification
WT ..... Wild-type
YES ..... Yeast Extract Supplemented
RRM ..... RNA Recognition Motif

# Acknowledgments

Graduate school at Stony Brook University has been memorable. Like any journey, there were ups and downs, but a vast majority of my experiences here have been positive. Now that I have reached my destination, I must thank all those who supported me and helped me achieve this lofty goal.

I would like to start by thanking Kathryn Bell, coordinator for the Genetics graduate program. I am not exaggerating when I say that she is the reason I am here. After my arrival, she took care of my every need, even without being asked to do so. She is a matronly figure, and loves the students and we love her. Saying “thank you” to her is an understatement. Without her, graduate school would not be as fun. I would also like to Dr. Jerry Thomsen and Dr. Martha Furie, previous and current directors of the Genetics graduate program.

I would like to thank my advisor Dr. Janet Leatherwood and co-mentor Dr. Bruce Futcher. In addition to being excellent scientists, they are wonderful people. Under their mentorship, I learnt that the main driving force of science is curiosity. They taught me to not be afraid of asking questions, or voicing opinions. They taught me to be critical of established dogmas until I have seen the evidence. They taught me to plan, design and execute elegant experiments. Most of all, they taught me to prioritize my work so that I could do answer the important questions first. They provided me the freedom to think and utilize all available resources. They treated me as a person of equal intellectual caliber,

although I have miles to go before I actually reach that level. I could go on and on, but the gist is – they taught me to be a scientist. For this, I will be forever grateful to them.

I thank my dissertation committee chair, Dr. Aaron Neiman. He has been patient and supportive, always willing to discuss and help. He is a brilliant scientist and I am grateful and lucky to have him as the chair of my dissertation committee. I also thank Dr. Wali Karzai and Dr. Charles Hoffman, for helping me with my dissertation. They provided some key ideas that helped me develop my project and explore new possibilities that I would not have thought of myself.

I must thank a number of my colleagues for not only supporting me during my stay in Stony Brook, but also helping me with my projects. I would like to thank my dear friends Angad, who was also my lab mate, and Disha. Angad and I spent a lot of time discussing and debating science in lab. He has a cynical, cautious approach to labwork, whereas I am more relaxed. Janet says we need to learn from each other, and thus I tried to adopt some of his caution. He also helped me with housing initially after my arrival, and made sure I settled in. I also thank another dear friend Justin. Justin has taught me many aspects of computational biology, and is a co-author on my paper. He and I are also good friends outside of lab. I also thank my friends Mansa Munshi and Sita Priya Moorthi for the good times we spent. Their friendship has truly made my life in Stony Brook enjoyable. All my friends helped me cope with the many stressful times that graduate school is bound to bring with it. In lab, I would like to thank Hong Wang and Alisa Yurovsky for their help with my work. I also thank all

professors and students in the Center for Yeast Molecular Biology and Genetics for their support during my PhD.

Above all, I would like to thank my parents. Nothing I say or write is enough to express how much they mean to me. Together, we have dreamed and achieved until I am here today. They are the only people that I completely trust. I know that, no matter what, they have my best interests in mind. They have been with me through the darkest times of my life. We have crossed all obstacles with each other's support and celebrated all achievements together. Though we are miles apart, they are always there for me, and I for them.

As I look forward to a new chapter in life, I thank everyone that has been a part of the previous chapters of my life. I wish to maintain the relationships I have developed during graduate school forever. Together, with their help, I will attempt in my scientific career to implement Tennyson's immortal line:

"To strive, to seek, to find, and not to yield"

# CHAPTER 1

## Introduction and Scope of Dissertation

## 1.1 Meiosis in *Schizosaccharomyces pombe*

*Schizosaccharomyces pombe,* also known as fission yeast, is a haploid that grows by mitotic division on nutrient-rich medium. However, when starved for nitrogen, *S. pombe* undergoes a specialized cell cycle called meiosis. Meiosis is a form of sexual differentiation in fission yeast. It results in the formation of spores, which are resistant to starvation and stress. Spores can remain dormant until the return of favorable conditions, when fission yeast can grow and divide again. Therefore, meiosis is a stress response leading to sexual differentiation in *S. pombe.* In higher eukaryotes, meiosis is used to make gametes for sexual reproduction. In both yeast and higher eukaryotes, mostly environmental signals lead to meiosis. In yeast, nutritional deprivation triggers cell-signaling events leading to meiosis. In higher eukaryotes, signals from surrounding cells initiate meiosis in specialized meiotic stem cells present in the reproductive organs.

Upon nitrogen starvation, haploid fission yeast of opposite mating types conjugate and their nuclei fuse (karyogamy) forming a diploid zygote. The zygote then undergoes one round of DNA replication during meiotic prophase, followed by two rounds of nuclear division. These are called the first and second meiotic divisions (meiosis I and II), forming four haploid nuclei. Spore membranes and spore walls then form around the nuclei producing four spores (Figure 1.1). This process is called 'zygotic' meiosis.

When diploids that have not committed to meiosis, are transferred to nutrient-rich media, they continue to grow vegetatively by mitosis. When such diploids are starved for nitrogen, they undergo 'azygotic' meiosis.

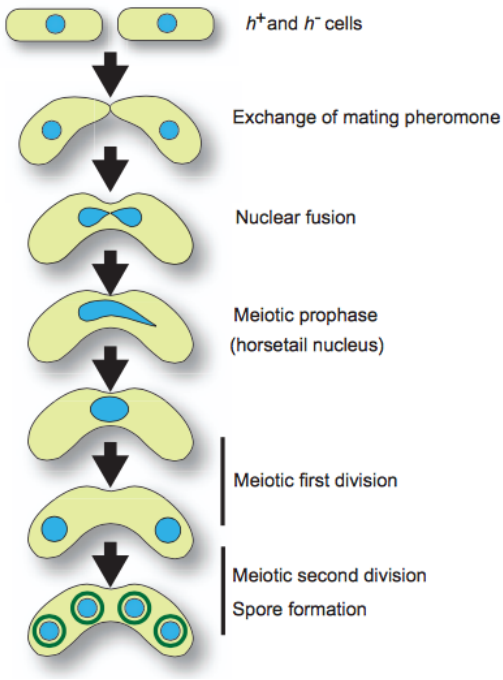


**Figure 1.1 Meiosis in S. pombe [image from (Asakawa, Haraguchi et al. 2007)]**

## 1.2 Molecular mechanisms that initiate meiosis – a tale of signaling, kinases, and transcription

### 1.2.1 Genetic studies to identify key meiosis genes

One of the earliest studies on meiosis screened for mutants of genes required for meiosis (Bresch, Muller et al. 1968). They found two major categories of mutants: a. mutants that could conjugate but not perform meiotic divisions called “mei” mutants b. mutants that could form four nuclei but not proper spores called “spo” mutants. Of the *mei* mutants, *mei1, mei2* and *mei3* genes are required before premeiotic S-phase, and *mei4* was found to be required for meiosis I but dispensable for S-phase (Shimoda, Hirata et al. 1985). The functions of these genes are discussed below. The function of *mei2* will be discussed in detail in later sections.

In a landmark screen for mutants that could initiate meiosis bypassing conjugation and nitrogen starvation, two groups simultaneously identified a gene they called, *pat1* and *ran1* respectively, that inhibited meiosis (Lino and Yamamoto 1985, Nurse 1985). *pat1* had a temperature-sensitive mutation that allowed even haploid cells to initiate meiosis. *pat1* codes for a protein kinase, and the *pat1* mutation was suppressed by a mutation in *mei3* (Beach, Rodgers et al. 1985). Further, a *mei2* mutant could also suppress the effect of the *pat1-ts* mutation (*pat1-114*), wherein either *mei3 pat1-114* or *mei2 pat1-114* double mutants could not initiate meiosis at the restrictive temperature of *pat1* (Beach, Rodgers et al. 1985, Lino and Yamamoto 1985). These studies suggested that *pat1* gene negatively regulates meiotic initiation, and *mei3* or *mei2* can initiate meiosis by counteracting the effect of *pat1* (Beach, Rodgers et al. 1985, Iino and Yamamoto 1985). Further studies showed that the meiosis initiation function is due to the Pat1 kinase, not altered *pat1* mRNA levels during meiosis (McLeod and Beach 1986). *mei3* was found to be essential in

starting meiosis by binding to Pat1 and inhibiting kinase activity (McLeod, Stein et al. 1987, McLeod and Beach 1988). *mei2* function is downstream of Pat1 and Mei3, and critical for meiosis initiation (Watanabe, Lino et al. 1988). *mei2* RNA levels increase upon nitrogen starvation and meiosis starts (Shimoda, Uehira et al. 1987).

### 1.2.2 Signaling pathways that initiate meiosis

Around this time, studies began to link cell signaling events with meiotic initiation. Meiosis is a response to change in environmental conditions and these changes are relayed into the cells by signaling. Early studies showed that cyclic AMP inhibited meiosis in fission yeast (Calleja, Johnson et al. 1980). Pat1 inactivation in vegetative cells without nitrogen starvation is lethal, and high levels of intracellular cAMP suppresses this lethality (Beach, Rodgers et al. 1985). *pat1* mutation kills cells by forcing them into meiosis, and high cAMP levels inhibit meiosis. cAMP inhibits meiosis by repressing *mei2* transcription, which is absolutely critical for starting meiosis. Upon nitrogen starvation cAMP levels go down, and that allows cells to initiate meiosis (Mochizuki and Yamamoto 1992). cAMP exerts its effect through cAMP-dependent protein kinase (PKA); high PKA activity also inhibits meiosis in fission yeast (Yu, Li et al. 1994). Thus both cAMP levels and PKA activity must decrease for nitrogen-starved cells to successfully begin meiosis.

A decrease in cAMP levels and PKA activity leads to expression of a transcription factor called *ste11* (Sugimoto, Iino et al. 1991). *ste11* was first isolated in screens for mutants that suppressed *pat1-114* and mutants that were defective in meiosis (Sipiczki

1988, Watanabe, Lino et al. 1988, Kitamura, Nakagawa et al. 1990). *ste11* transcription is induced by nitrogen starvation and inhibited by high cAMP (Sugimoto, Iino et al. 1991). Ste11 in an HMG-box transcription factor that upregulates many meiotic genes including mating type genes, *matP* and *matM* and the key meiosis initiator *mei2* (Sugimoto, Iino et al. 1991, Mata and Bahler 2006). *matP* and *matM* encode mating pheromones and their receptors. The binding of mating pheromones to their receptors triggers a MAP kinase cascade that leads to further upregulation of *ste11* in a positive regulatory loop. In summary, meiosis starts when nitrogen starvation leads to a reduction in cAMP levels and upregulates *ste11.* Ste11 transcribes *mei2,* and mating genes that start meiosis (Figure 1.2). However, several questions remained unanswered – what does Mei2 protein do, and how do Mei3 and Pat1 fit into the picture?

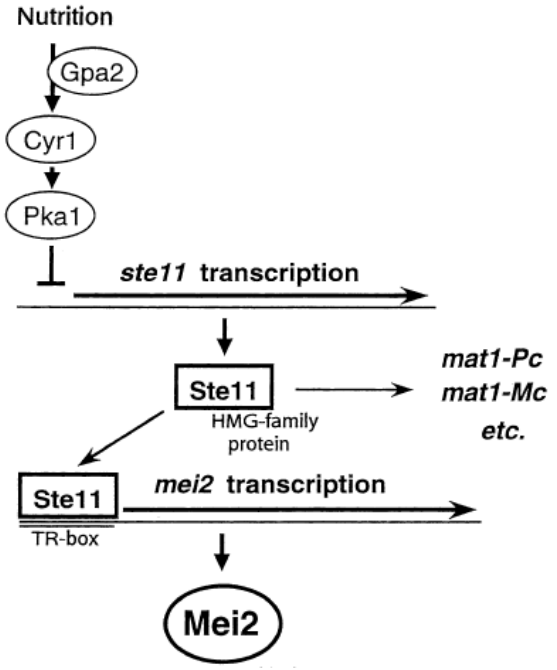


**Figure 1.2 Nitrogen starvation signals through cAMP and PKA and initiates meiosis by upregulating Ste11 and Mei2 [image modified from (Yamamoto 1996)]**

### 1.2.3 Pheromone signaling and kinases

A schematic of the major steps of meiosis initiation is shown in Figure 1.3. The first step of meiosis after nitrogen starvation is conjugation. Fission yeast has two mating types $h^+$ and $h^-$, which can conjugate and undergo meiosis; otherwise cells remain arrested at G1. The mating genes upregulated by Ste11 lead to the production of mating pheromones. $h^+$ cells secrete a pheromone called the P-factor which binds to the P-factor receptor on $h^-$ cells; $h^-$ cells secrete M-factor that binds to the M-factor receptor on $h^+$ cells. This triggers the MAP kinase pathway through a receptor coupled G-protein Gpa1 and MAP kinases Byr1, Byr2, and Spk1 (Obara, Nakafuku et al. 1991, Gotoh, Nishida et al. 1993, Neiman, Stevenson

et al. 1993). The Spk1 kinase activates Ste11 by phosphorylation so that Ste11 can upregulate its target genes (Kjaerulff, Lautrup-Larsen et al. 2005).

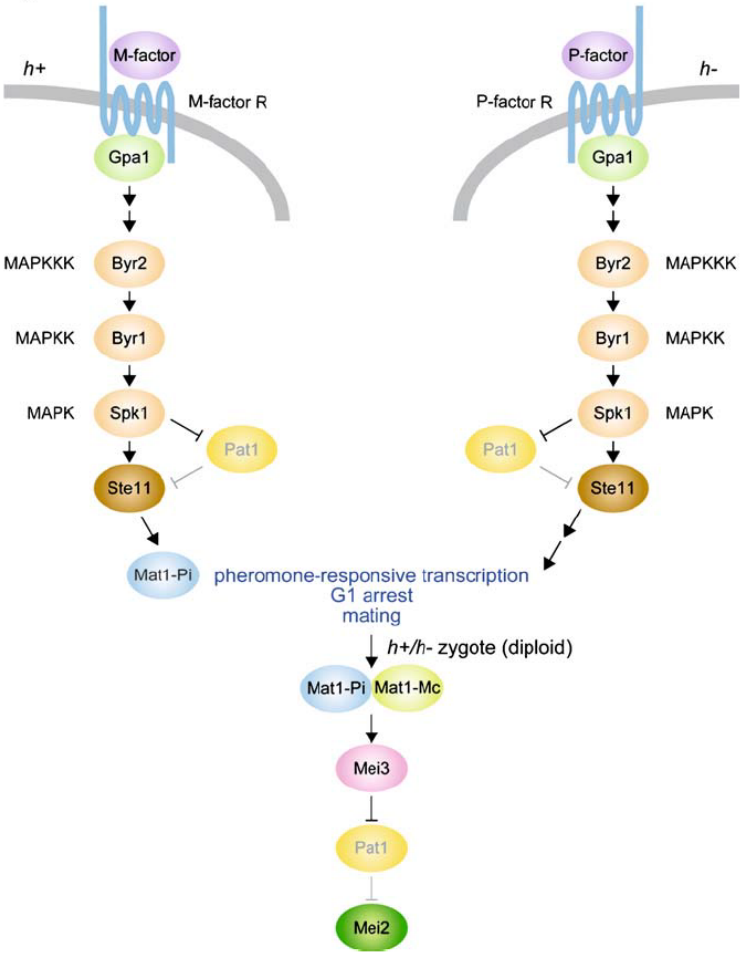


**Figure 1.3 Pheromone-induced MAP kinase signaling leads to initiation of meiosis [image from (Harigaya and Yamamoto 2007)]**

## 1.2.4 Role of Mei3 and Pat1 in meiosis initiation

The downstream targets of Ste11, Mat1-Pi in $h^+$ or Mat1-Mi in $h^-$ cells, are transcription factors (Kelly, Burke et al. 1988, Sinclair, Berta et al. 1990). Upon successful

conjugation and diploid formation, Mat1-Pi and Mat1-Mi are in the same cell and cooperatively induce Mei3 expression (Willer, Hoffmann et al. 1995). However, the role of Mat1-Mi in activating Mei3 maybe indirect since a later study showed that the Mei3 promoter has sites for Mat1-Mc, another $h^-$ cell-specific transcription factor (Van Heeckeren, Dorris et al. 1998). Nevertheless, Mei3 upregulation is a key step in meiosis induction. Mei3 acts as a pseudosubstrate inhibitor of Pat1 kinase (Li and McLeod 1996), which is the key inhibitor of meiosis. Pat1 inhibits meiosis by phosphorylating and inactivating both Ste11 and Mei2 (Li and McLeod 1996, Watanabe, Shinozaki-Yabana et al. 1997, Kitamura, Katayama et al. 2001). Upregulation of Mei3 relieves this inhibition and therefore initiates meiosis by derepressing Mei2. Mei2 is an RNA binding protein and a key meiosis initiator. The next section focuses on how Mei2 initiates meiosis.

## 1.3 How does Mei2 initiate meiosis?

*mei2* was identified as a crucially important meiotic gene in the earliest genetic screen (Bresch, Muller et al. 1968). Later studies showed that Pat1 inactivation and Mei2 upregulation were independent events, but both events were required to initiate meiosis (Beach, Rodgers et al. 1985, Watanabe, Lino et al. 1988). *mei2* mRNA was found to be upregulated by Ste11 upon nitrogen starvation (Sugimoto, Iino et al. 1991). Later, Mei2 was found to contain two RNA recognition motifs (RRMs) (Watanabe and Yamamoto 1994). This was an important study in understanding Mei2's role in meiosis initiation. They found that *mei2Δ* cells could not start premeiotic DNA replication (S-phase). However, a temperature-

sensitive allele of *mei2* with a mutation in the N-terminal RRM, completed S-phase but arrested before meiosis I (Figure 1.4).

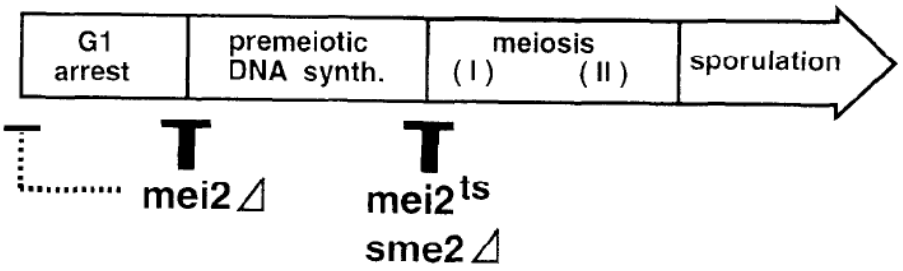


**Figure 1.4 mei2 starts premeiotic S-phase and plays a role meiosis I [image from (Watanabe and Yamamoto 1994)]**

They then screened for high-copy suppressors of the *mei2-ts* phenotype and found a suppressor that they called *sme2* (suppressor of *mei2*). They found that *sme2* was transcribed into a non-coding RNA that they named meiRNA. They showed that Mei2 directly bound meiRNA. In addition, the *sme2Δ* mutant phenocopied the *mei2-ts* mutant (Figure 1.4). However, they also found that a *mei2* allele with a point mutation in the C-terminal RRM phenocopied *mei2Δ.* Therefore, they hypothesized that Mei2 protein has yet other unidentified RNA partners that enable it to initiate premeiotic S-phase (Figure 1.5).

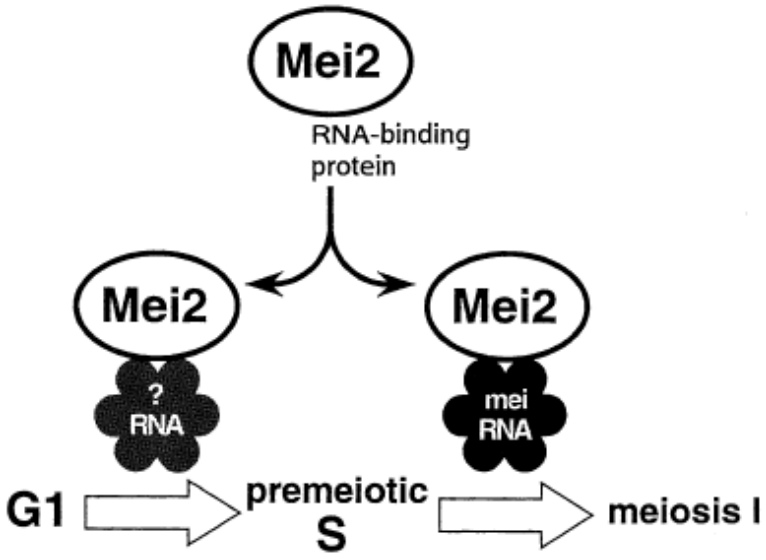


**Figure 1.5 Mei2 initiates S-phase by binding to an unidentified RNA species.** Mei2 and meiRNA cooperate to initiate meiosis I [image modified from (Yamamoto 1996)]

Further studies showed that a constitutively active form of Mei2, with Pat1 phosphorylation sites mutated, is able to start meiosis without the need for nitrogen starvation or Mei3 activation (Watanabe, Shinozaki-Yabana et al. 1997). Mei2 was shown to shuttle between the nucleus and cytoplasm, and this shuttling required its RNA binding activity (Sato, Shinozaki-Yabana et al. 2001). Mei2 nucleocytoplasmic shuttling was inhibited when it was phosphorylated by Pat1 kinase and bound by a 14-3-3 protein, Rad24 (Sato, Watanabe et al. 2002). Microscopy studies using fluorescent labeled Mei2 and meiRNA FISH revealed that Mei2 and meiRNA colocalized during meiosis and formed a dot in the nucleus (Yamashita, Watanabe et al. 1998, Shimada, Yamashita et al. 2003). The significance of the Mei2-meiRNA dot will be discussed in a later section. However, no studies found anything

that pointed to Mei2's role in initiation of meiosis by starting S-phase. This is one of the questions I have addressed in my dissertation and the results will be discussed Chapter 3.

## 1.4 Rewiring of gene expression during meiosis

To study gene expression during meiosis, one group used microarrays (Mata, Lyne et al. 2002). A *pat1-114* mutant diploid cell, when starved for nitrogen and shifted to its restrictive temperature, undergoes synchronized meiosis enabling studies on every stage of fission yeast meiosis (Iino and Yamamoto 1985). Mata et al. used this mutant along with wild type diploids (that enter meiosis somewhat asynchronously), to study gene expression during different stages of meiosis. They found that a total of around 2000 genes were upregulated at least two-fold during the course of meiosis. Strikingly, these genes were upregulated in the different phases of meiosis. The first set of 250 genes were involved in nutritional stress response and pheromone signaling. These included the '*mat*' genes, *ste11,* and m*ei2.*

The next set of 100 genes was called the 'early' genes, and were genes involved in premeiotic S-phase and recombination. Experimental analysis of cells deleted for early meiotic transcription factor *rep1* (Mata, Lyne et al. 2002), revealed that their transcription may be regulated by the meiotic S-phase transcription factor complex MBF comprising Cdc10, Res2 and Rep1 (Miyamoto, Tanaka et al. 1994, Sugiyama, Tanaka et al. 1994, Zhu, Takeda et al. 1994, Ding and Smith 1998). The early meiotic genes also include a key forkhead transcription factor, Mei4 that upregulates transcription of 'middle meiotic genes'

required for the next phase of meiosis – the meiotic nuclear divisions (Horie, Watanabe et al. 1998). Finally, Mata et al. found that Atf21 and Atf31 transcription factors accounted for transcriptional upregulation of 55% of genes in the 'late meiotic genes' category. These genes are involved in spore formation. Despite these advances in understanding how meiosis starts, a complete picture of the key events leading to premeiotic S-phase was still lacking. For instance, only about half the early meiotic genes were dependent on Rep1 for their expression, and *mei4* was not one (Mata, Lyne et al. 2002). This meant that *mei4* and other MBF-independent early meiotic genes could be upregulated by another transcription factor(s). A screen to find this transcription factor(s) led to extremely surprising results and uncovered novel mechanisms of posttranscriptional gene regulation, as discussed below.

## 1.5 Posttranscriptional regulation of early meiotic genes

### 1.5.1 Splicing regulation of early meiotic genes

First proof that a subset of early meiotic genes was post-transcriptionally regulated came from studies in our lab, where intron-containing early meiotic genes like *crs1, rec8,* and *meu13* were found to have regulated splicing (Averbeck, Sunder et al. 2005). Their mRNAs in vegetative cells were found to retain introns, whereas in meiosis, they were completely spliced. This also showed that transcription of early meiotic genes was not completely off during vegetative growth.

### 1.5.2 Role of RNA binding proteins Mmi1 and Mei2

To find putative transcription factors that upregulated a subset of Rep1 independent early meiotic genes, Harigaya et al. cloned a GFP reporter downstream of the *mei4* promoter (Harigaya, Tanaka et al. 2006). Surprisingly, they found that the GFP mRNA was detectable even in vegetative cells when *mei4* transcription should be off. They reasoned that although the *mei4* promoter was active in vegetative cells, the *mei4* mRNA sequence had some feature that prevented it from being stable. They found this region by deletion analysis and called it the "DSR" (determinant of selective removal). They found that if the DSR was added to a *ura4* reporter gene, its mRNA was undetectable during vegetative growth.

They used the DSR-containing *ura4* reporter to screen for mutants that could affect *ura4* mRNA accumulation in vegetative cells. They found that a YTH-domain RNA binding protein called Mmi1 was responsible for regulated turnover of DSR-containing transcripts. Further, they observed that Mmi1 formed foci in the nucleus in vegetative cells, but in meiosis it formed a nuclear dot that colocalized with the Mei2-meiRNA complex.

They also investigated possible mechanisms that were involved in early meiotic mRNA turnover. They found that only a temperature-sensitive *rrp6* mutant rescued the *sme2Δ* meiotic phenotype. *rrp6* codes for a 3'-5' exosome exonuclease and therefore this suggested that Rrp6 could be involved in early meiotic mRNA turnover in vegetative cells. They and others (McPheeters, Cremona et al. 2009) ruled out increased transcription, RNAi,

or cytoplasmic RNA decay mechanisms. Their model for early meiotic mRNA turnover regulation is shown in Figure 1.6. They postulated that Mei2-meiRNA complex sequesters Mmi1 during meiosis, thereby relieving the early meiotic mRNAs of targeted degradation. Later, it was shown that during meiosis, meiRNA had an extended 3' region with many Mmi1 binding sites (Shichino, Yamashita et al. 2014). These act as a sponge to sequester Mmi1 within a specific location in the nucleus. Although, meiRNA itself is an Mmi1 target in vegetative cells, during meiosis, Mei2 binds to the 5' region of meiRNA and possibly prevents its degradation by the exosome (Shichino, Yamashita et al. 2014).

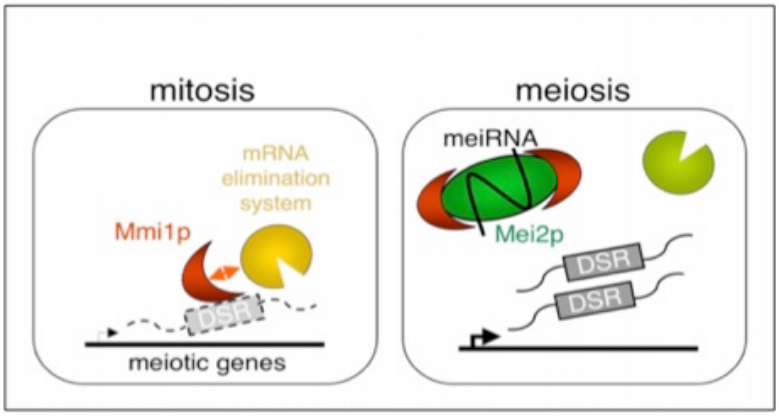


**Figure 1.6 Early meiotic mRNAs are bound by Mmi1 in vegetative cells and targeted for degradation.** In meiosis, Mei2-meiRNA sequesters Mmi1 and relieves early meiotic mRNAs from being degraded [Image from (Harigaya, Tanaka et al. 2006)]

### 1.5.3 Role of exosome exonucleases and Pab2

Further studies on the mechanism by which early meiotic mRNAs may be turned over showed that regulated splicing and polyadenylation plays an important role (McPheeters, Cremona et al. 2009). This study showed that in *mmi1* and *rrp6* mutants, the meiotic mRNA,

*crs1* accumulated as fully spliced in vegetative cells. This indicated that both Mmi1 and Rrp6 might regulate splicing by interacting with the splicing machinery. This study also showed that the splicing and polyadenylation of *crs1* mRNA maybe coupled and therefore coregulated. Additional studies implicated Pab2, a polyA binding protein, and Dis3, another exonuclease of the exosome (St-Andre, Lemieux et al. 2010, Yamanaka, Yamashita et al. 2010, Chen, Futcher et al. 2011). Yamanaka et al. showed that Mmi1 colocalizes with Pab2 and the exosome in vegetative cells. Further, I showed that a nucleotide motif was enriched in Mmi1 target RNAs (Chen, Futcher et al. 2011). Mmi1 bound to its target RNAs and induced formation of long polyA tails, which were bound by Pab2, and targeted the RNAs to the exosome exonucleases Rrp6 and Dis3 (Figure 1.7) (Chen, Futcher et al. 2011). This study also found that Mmi1 regulates intron-specific splicing of some early meiotic RNAs like *rec8*.

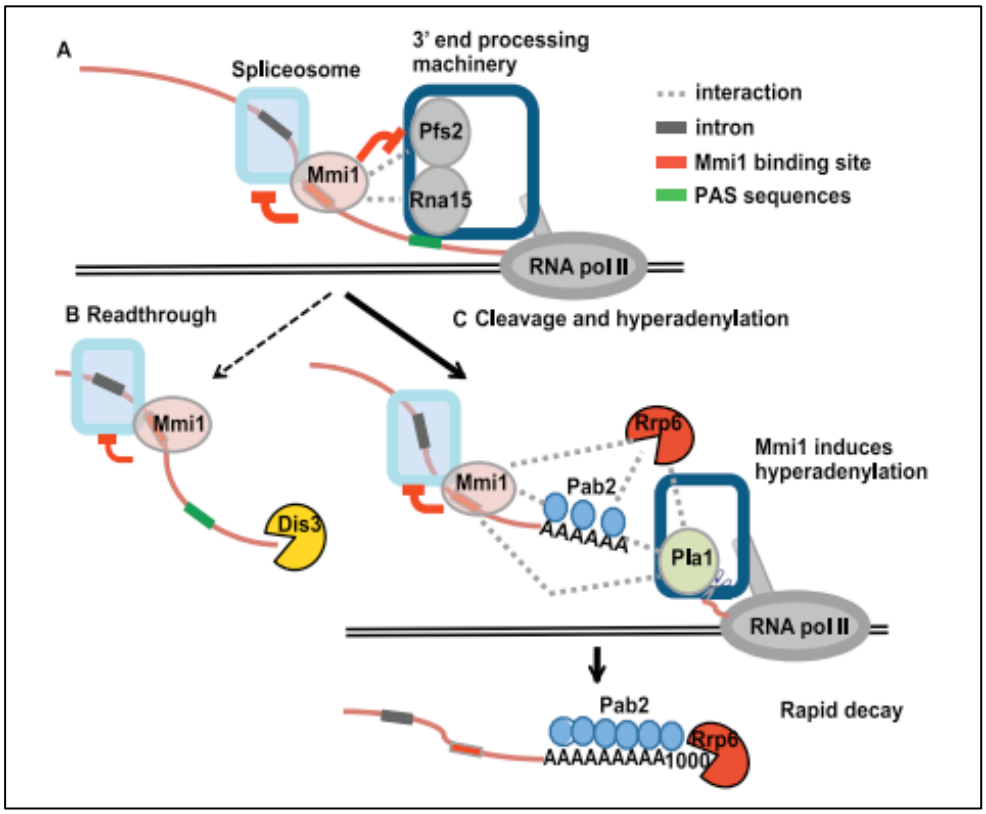


**Figure 1.7 Mmi1 mediated regulation early meiotic RNA turnover.** Mmi1 interacts with the spliceosome and 3' cleavage and polyadenylation complex to induce hyperadenylation in its target RNAs. These are then bound by Pab2 and degraded by the exosome exonucleases Rrp6 and Dis3 [Image from (Chen, Futcher et al. 2011)]

### 1.5.4 Role of the NURS complex in mediating protein-protein interactions

Additional screens identified more factors involved in the Mmi1 pathway such as Red1, Iss10, and Rhn1 (Sugiyama and Sugioka-Sugiyama 2011, Sugiyama, Sugioka-Sugiyama et al. 2012, Yamashita, Takayama et al. 2013). Some reports suggested that these factors interacted with Clr4 and resulted in H3K9 methylation and silencing of certain meiotic genes like *mei4* and *ssm4* (Hiriart, Vavasseur et al. 2012, Zofall, Yamanaka et al. 2012). These

reports showed that silencing involved the RNA-induced silencing complex (RITS) and required the functions of Mmi1, Rrp6 and Red1 (Tashiro, Asano et al. 2013).

The Red1-Iss10 containing complex was explored in further detail by coimmunprecipitation and additional factors of the complex were identified (Egan, Braun et al. 2014). They called this complex the 'NURS' complex, which is short for nuclear RNA silencing. This complex was found to mediate the interaction of Mmi1 and various other complexes such as the exosome, cleavage and polyadenylation machinery, the histone methylase complex and the cap binding complex (Figure 1.8).

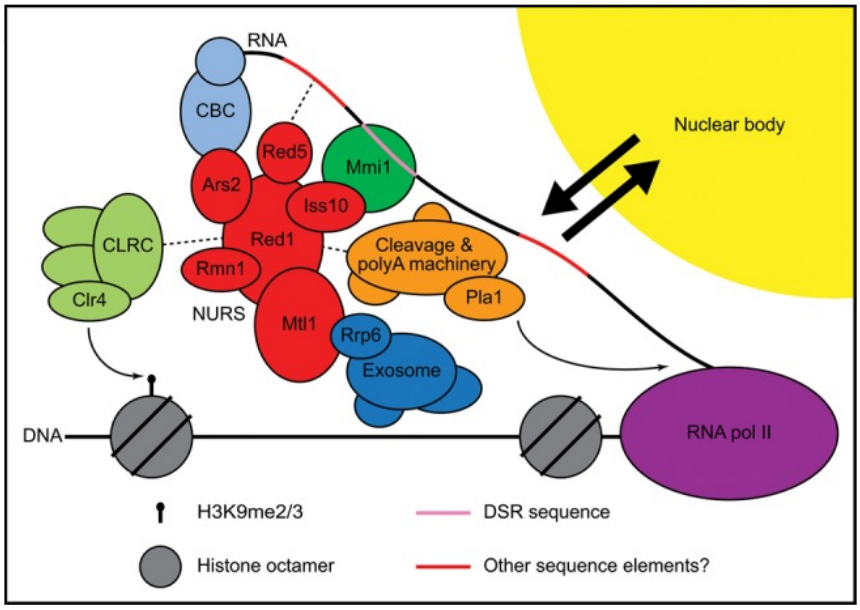


**Figure 1.8 The NURS complex mediates Mmi1 interaction with various other complexes involved in posttranscriptional processes [image from (Egan, Braun et al. 2014)].**

Importantly, this study showed that a subunit of this complex, Mtl1, directly interacted with Rrp6 of the exosome. This suggested that in addition to its catalytic functions as an exonuclease, Rrp6 also interacts with other proteins and possibly mediates

exosome recruitment. Further, in vitro studies (described below) have shown that Rrp6 protein, even with its exonuclease function lacking, is critical for exosome functions. I tested this hypothesis in vivo, and the results have been described in Chapter 2 of my thesis. In the next section, I have described the exosome and its components in further detail.

## 1.6 The Exosome structure and functions

### 1.6.1 Functions of the exosome

The Exosome is a macromolecular complex conserved from Archaea to eukaryotes. It was discovered in *S. cerevisiae* as a complex of essential proteins with similarities to bacterial 3'-5' exoribonucleases (Mitchell, Petfalski et al. 1997). Mutations in exosome core components led to defects in 5.8S rRNA processing (Mitchell, Petfalski et al. 1997), mRNA turnover (Anderson and Parker 1998), and snRNA and snoRNA processing (Allmang, Kufel et al. 1999). Indeed many of the core components of the exosome have 'rrp' names, meaning they were originally isolated as mutants of rRNA processing. In addition, coimmunoprecipitation showed that the yeast exosome exists as distinct nuclear and cytoplasmic complexes (Allmang, Petfalski et al. 1999). This study also found that the nuclear exosome contained 11 subunits with two exonucleases, Rrp6 and Dis3. Rrp6, a distributive enzyme was absent from the cytoplasmic exosome whereas Dis3, a processive enzyme was present in the nuclear and cytoplasmic exosomes (Allmang, Petfalski et al. 1999).

Studies on the exosome are difficult because most of the components are essential. However, yeast is a powerful model organism because conditional alleles can be easily generated. This led to a more detailed understanding of exosome functions. We now know that the exosome is involved in almost every aspect of RNA processing and turnover [extensively reviewed in (Schmid and Jensen 2008, Lykke-Andersen, Brodersen et al. 2009, Chlebowski, Lubas et al. 2013)]. A summary of exosome functions in RNA turnover is shown in Figure 1.9. The exosome is manly involved in RNA surveillance and degrades any species of aberrant RNAs in the cell. It is an important mediator of mRNA quality control.

The body of literature regarding exosome functions is vast and very well summarized in the reviews mentioned above. The specific functions of Rrp6 and Dis3 exonucleases in meiotic mRNA turnover in *S. pombe* were summarized in Subsection 1.5.3. Since a majority of my dissertation work tries to understand the structural role of Rrp6 in early meiotic RNA turnover, I will discuss the structure of the exosome and possible roles of Rrp6 and Dis3 with respect to this structure.

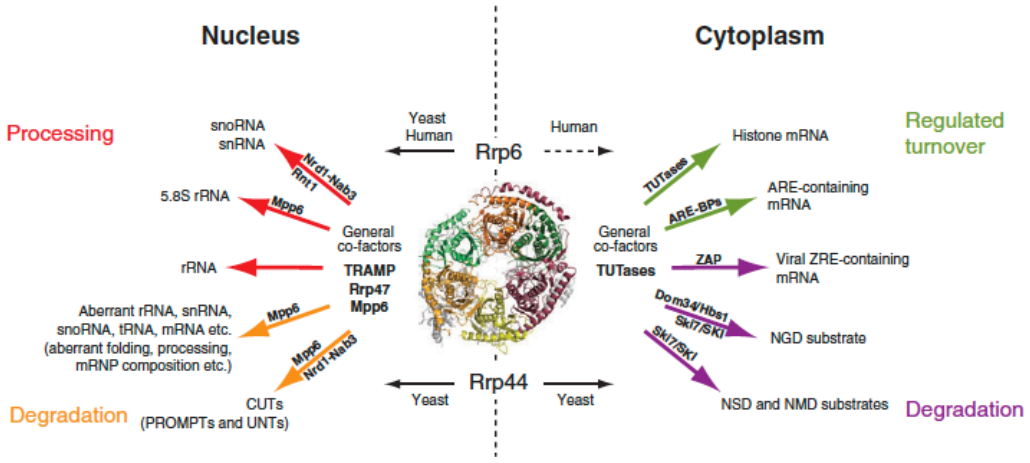


**Figure 1.9 Functions of the eukaryotic exosome.** The exosome is involved in processing and turnover of RNA making it a complex akin to the proteasome for proteins [image from (Lykke-Andersen, Brodersen et al. 2009)]. Dis3 (bottom) is also called Rrp44.

## 1.6.2 Structure of the exosome

Many groups have determined the crystal structure of the exosome with different RNA substrates coupled, or at different resolutions (Liu, Greimann et al. 2006, Makino, Baumgartner et al. 2013, Wasmuth, Januszyk et al. 2014, Makino, Schuch et al. 2015). The consensus structure (Figure 1.10) shows that the exosome has a set of 6 core subunits (grey) that form a hexamer and a central channel. The core is comprised of RNasePH-like subunits Rrp41, Rrp45, Rrp46, Rrp43, Mtr3, and Rrp42 (Liu, Greimann et al. 2006). Although the core exosome is formed of exonucleases, these are inactive because of mutations in their active sites, rendering them unable to degrade RNA in vitro (Dziembowski, Lorentzen et al. 2007). However, this study did not rule out that the core exosome could degrade RNA under regulated conditions.

RNA binding proteins with S1 and KH RNA binding domains, Rrp40, Csl4, and Rrp4, form a trimeric complex that associates with the top of the core (Figure 1.10). Rrp6 is at the top of the exosome above the trimeric RNA-binding complex, and in the absence of RNA, it covers the central channel formed by the core exosome (Wasmuth, Januszyk et al. 2014, Makino, Schuch et al. 2015). In the presence of RNA, Rrp6 undergoes a conformational change allowing the RNA to be threaded through the exosome core to Rrp4 (also called Dis3) (Makino, Schuch et al. 2015). Dis3 (purple in Figure 10, labeled Rrp44) is at the bottom of the exosome and its exonuclease domain faces the central channel of the exosome core (Makino, Baumgartner et al. 2013). The exonuclease domain of Rrp6 is exposed to solvent (Makino, Schuch et al. 2015).

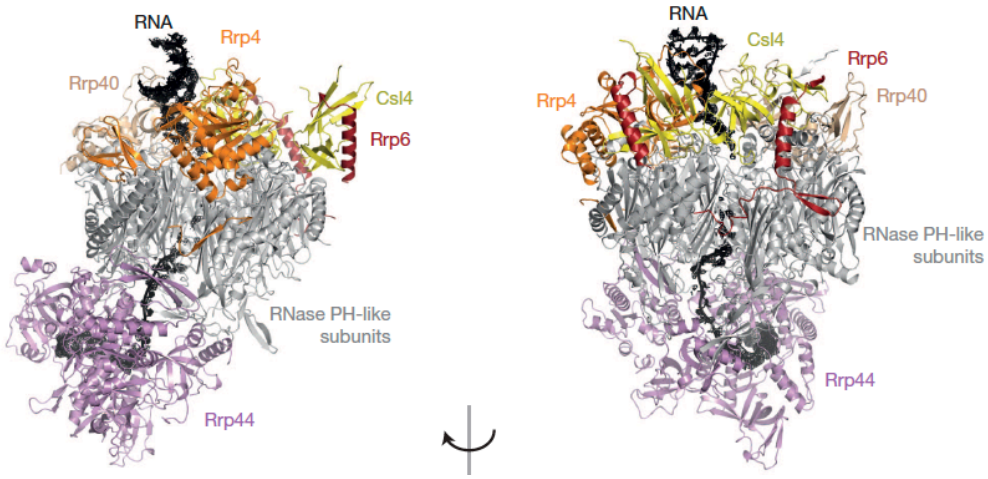


**Figure 1.10 Structure of the yeast exosome bound to RNA [image modified from (Makino, Baumgartner et al. 2013)]**

## 1.6.3 Interplay of Rrp6 and Dis3 in RNA degradation by the exosome

Recent structural studies have shed light into the interplay of Rrp6 and Dis3 in exosome mediated RNA degradation. Earlier studies showed that while Dis3 could degrade different species of RNAs in vitro, it could not degrade them when complexed with the exosome (Liu, Greimann et al. 2006). When Rrp6 was added to the reconstituted exosome, the RNAs were then degraded. Later, it was observed that Dis3 could degrade RNAs in the exosome even when Rrp6 was present but lacking its catalytic function (Wasmuth and Lima 2012). This result implied that the Rrp6 protein could enhance RNA degradation by the exosome, regardless of whether it was able to degrade RNA itself.

Makino et al. have solved the exosome structure with different RNA substrates and showed that there are two possible paths for the RNA (Figure 1.11). When the exosome is incubated with $AU_{18}$ RNA, it preferably uses an exosome core-independent path to access the active site of Dis3 (Figure 1.11, left). Rrp6 in this case is in 'RNA-binding mode' and may degrade some of the RNA or hand it over to Dis3 after processing it. The active site of Dis3 faces away from the central channel of the core exosome. Further, when they incubated the exosome with a structured $U_{31}$ duplex RNA, they found that it preferably uses an exosome core-dependent path to the active site of Dis3 (Figure 1.11, right). This was the case even with Rrp6 catalytic site mutated. Rrp6 undergoes a conformational change to allow the RNA to enter the exosome core channel. Therefore, the structural studies strongly suggest that Rrp6 protein is more important for exosome RNA degradation functions.

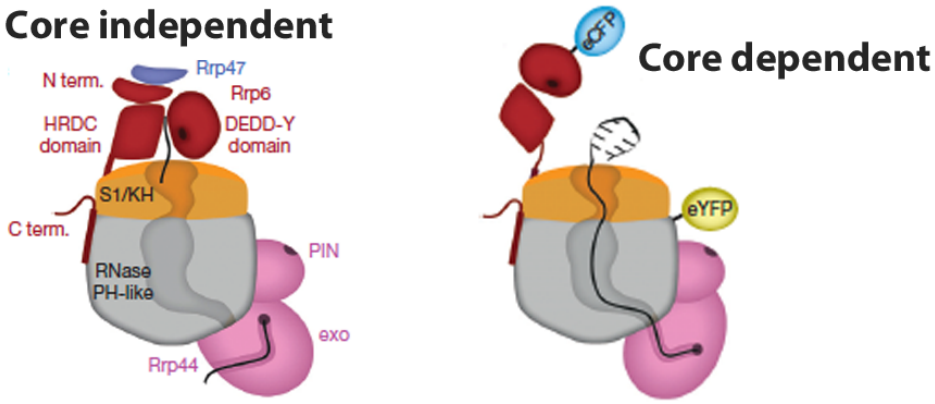


**Figure 1.11 Schematic view of possible paths taken by the RNA for exosome mediated degradation [images taken from (Makino, Schuch et al. 2015)]**

### 1.6.4 Importance of studying the RNA exosome

Given that most of the exosome components are essential in eukaryotes, and the exosome is critical for RNA surveillance, it is obvious that the exosome is vital for the normal functioning of a cell. Rrp6 was originally discovered as an autoantigen for the autoimmune disorder, Scleromyositis, and was called PM-Scl100 (Briggs, Burkard et al. 1998). Dis3 was long known to be critical for cell cycle regulation in yeast (Kinoshita, Goebl et al. 1991), and has recently been shown to be the most frequently mutated gene in multiple myelomas (Tomecki, Drazkowska et al. 2014, Weissbach, Langer et al. 2015). Dis3 is indirectly involved in the processing of the tumor suppressor miRNA, let-7, by reducing the stability of LIN28B, which is a pluripotency factor (Segalla, Pivetti et al. 2015) and results in unprocessed let-7 miRNAs leading to cancer. Therefore, detailed knowledge of various exosome targets and how this big complex recognizes and degrades a large variety of RNAs is extremely necessary even from a human disease perspective.

## 1.7 Scope of the dissertation

This dissertation studies posttranscriptional gene regulation mechanisms that are important for initiating meiosis in fission yeast. Since the Mei2-Mmi1-Exosome nexus forms a key to meiosis initiation, I have investigated two regulatory mechanisms pertinent to this system. The first study investigates in greater detail, the role of the exosome, particularly the role of Rrp6 in degrading early meiotic RNAs. I have also tried to investigate the role of Mei2 in meiosis initiation by determining its RNA targets.

**Chapter 2:** This chapter investigates the role of Rrp6 in early meiotic RNA turnover. Specifically, it investigates if Rrp6 directly degrades the early meiotic RNAs, or plays an indirect role in aiding RNA degradation by the exosome. The studies show that many of the meiotic RNAs that were believed to be Rrp6 catalytic targets, actually depend on a structural role of Rrp6 for their degradation by the exosome. This study also uncovered a novel role for Rrp6 in degrading mRNAs involved in iron assimilation in *S. pombe.*

**Chapter 3:** This chapter addresses how Mei2 is able to initiate meiosis. Since Mei2 is an RNA binding protein, what are the RNA targets of Mei2? How does Mei2 initiate meiosis after binding these targets? One of the known targets of Mei2 is meiRNA, but loss of meiRNA does not phenocopy loss of RNA binding ability of Mei2. This study showed that Mei2 binds to the 5' UTR of two meiotic inhibitors, *mmi1* and *rep2* mRNA. Further studies on how this binding helps Mei2 initiate meiosis, is underway.

**Chapter 4:** Concluding remarks - some future directions for studies described in Chapter 2 and 3.

# CHAPTER 2

## Exosome exonuclease Rrp6 plays a non-catalytic, structural role in degradation of meiotic and iron response mRNAs

## 2.1 Preface

The RNA Exosome is a conserved complex for RNA degradation, with Rrp6 and Dis3 as the catalytic subunits. However Rrp6 is involved in protein-protein interactions. To see whether Rrp6 has structural roles separate from its catalytic roles, I compared RNA levels in an *rrp6* deletion to an *rrp6* point mutant specifically defective in its exonuclease activity. I found that many mRNAs targeted by Rrp6 accumulated to high levels in the *rrp6* deletion mutant, but accumulated only slightly to moderately in the Rrp6 catalytic-null mutant. This suggested that Rrp6 catalytic activity was only partly responsible for their degradation. Instead, the Rrp6 protein was presumably directing these RNAs to the catalytic activity of Dis3 for degradation. I defined these RNAs as "protein dependent" targets of Rrp6. I found some Rrp6 protein dependent targets were expressed in meiosis, and were targets of the RNA binding protein Mmi1. Other protein dependent targets of Rrp6 were mRNAs of iron homeostasis genes. I found a motif enriched in the iron homeostasis mRNAs that an unknown RNA binding protein might recognize and bind. I report that Rrp6 acts as a structural adapter protein to target some RNAs to the exosome, possibly by interacting with sequence-specific RNA binding proteins.

## 2.2 Introduction

The RNA Exosome is a large complex conserved from archaea to higher eukaryotes. It functions in surveillance, processing, and degradation of RNAs including rRNA, tRNA and small RNAs (for reviews see (Schmid and Jensen 2008, Lykke-Andersen, Brodersen et al. 2009, Chlebowski, Tomecki et al. 2010)). In eukaryotes, the complex comprises a 9-subunit core of RNA-binding proteins associated with two ribonucleases, Rrp6 and Dis3 (Liu, Greimann et al. 2006, Dziembowski, Lorentzen et al. 2007). Dis3 is essential and has endonuclease activity and 3'-5' exonuclease activity. Rrp6 has only 3'-5' exonuclease activity, and is found in the nuclear but not the cytoplasmic form of the exosome (Allmang, Petfalski et al. 1999).

Crystal structures of exosome-RNA complexes reveal that Rrp6 and Dis3 are found at opposite ends of the exosome (Wasmuth and Lima 2012, Makino, Baumgartner et al. 2013, Wasmuth, Januszyk et al. 2014, Makino, Schuch et al. 2015). The exonuclease domain of Rrp6 is solvent-exposed even when associated with the exosome. By contrast, the exonuclease domain of Dis3 faces the inner core of the exosome, through which the RNA substrate is threaded. Although earlier studies showed that Rrp6 and Dis3 have distinct RNA targets (Kiss and Andrulis 2010), recent studies have shown that Rrp6 can regulate the catalytic activity of Dis3 *in vitro* (Wasmuth and Lima 2012). This may be because Rrp6 associates with the top of the exosome where the RNA enters, and possibly regulates RNA threading through the exosome core (Wasmuth and Lima 2012, Makino, Baumgartner et al. 2013, Makino, Schuch et al. 2015). Strikingly, even a catalytically inactive Rrp6 is able to

enhance RNA degradation by Dis3 *in vitro* (Wasmuth and Lima 2012). These studies show that, at least *in vitro,* Rrp6 has a structural role in the exosome in addition to its catalytic role.

In *Schizosaccharomyces pombe*, the RNA Exosome plays a crucial role in regulating meiosis. Many genes are upregulated during the switch from vegetative growth to meiosis (Mata, Lyne et al. 2002). During vegetative growth, some early meiotic genes are constitutively transcribed. The RNA binding protein Mmi1 binds these early meiotic mRNAs and targets them for degradation to keep meiosis off (Harigaya, Tanaka et al. 2006). Upon meiotic entry, Mmi1 is inactivated, allowing early meiotic transcripts to accumulate and be translated. Further studies on the mechanism of Mmi1-mediated RNA turnover showed the exosome degrades Mmi1-bound RNAs in vegetative cells, and is aided by polyadenylation of these RNAs (St-Andre, Lemieux et al. 2010, Yamanaka, Yamashita et al. 2010, Chen, Futcher et al. 2011). Previous studies have shown both *rrp6* and *dis3* mutations interfere with degradation of Mmi1 targets (Yamanaka, Yamashita et al. 2010, Chen, Futcher et al. 2011). Some Mmi1 targets, such as *rec8* mRNA, undergo Mmi1-dependent hyperadenylation and thus become a substrate for Rrp6. However, a small fraction of the *rec8* mRNA is read-through transcript that is targeted by Dis3 (Chen, Futcher et al. 2011). In summary, both Dis3 and Rrp6 keep many early meiotic mRNAs off in vegetative cells (Chen, Futcher et al. 2011).

Delivery of the mRNAs bound by Mmi1 to the exosome involves a multi-protein complex called NURS (Sugiyama and Sugioka-Sugiyama 2011, Sugiyama, Sugioka-Sugiyama

et al. 2012, Yamashita, Takayama et al. 2013). The NURS complex bridges Mmi1 and the exosome; it interacts with Mmi1 through Iss10 (Egan, Braun et al. 2014), and it interacts with Rrp6 through Mtl1 (Egan, Braun et al. 2014).

In *S. pombe*, it is currently believed that Rrp6 directly degrades Mmi1-bound RNAs. This is based on the observation that *rrp6Δ* mutants accumulate Mmi1-target RNAs. However, *dis3* mutants also accumulate Mmi1-target RNAs (Yamanaka, Yamashita et al. 2010, Chen, Futcher et al. 2011). One possibility is that Rrp6 and Dis3 are each partly responsible for degrading Mmi1-bound RNAs. Alternatively, loss of Rrp6 protein could result in defective recruitment of Mmi1-bound RNAs for degradation by Dis3. This led us to the question of whether Rrp6 has distinct catalytic and "structural" functions. The structural functions could include both an enhancement of Dis3 activity, and a recruitment activity via protein-protein interactions. To distinguish which RNAs are degraded by Rrp6, and which are somehow targeted to Dis3 via Rrp6, I made catalytic (*rrp6-cat*), null *(rrp6Δ)*, and *rrp6-cat dis3-4* (ts) mutants and measured the genome-wide abundance of RNAs.

## 2.3 Results

### 2.3.1 Analysis of phenotypes of exosome exonuclease mutants

To test whether Rrp6 has distinct catalytic and structural functions, I designed a mutant allele of *rrp6* (*rrp6-cat*) to abolish its 3'-5' exonuclease activity. When compared across species, the DEDD-Y exonuclease domain of Rrp6 is highly conserved (Figure 2.1A). I constructed *rrp6-cat* by mutating residues D243, E245, D303, Y366 and D370 to alanine. I

selected these residues based on reports showing these residues are required for processing 5.8S rRNAs, some snRNAs and snoRNA in yeast (Briggs, Burkard et al. 1998, Phillips and Butler 2003). I mutated all of them to increase the likelihood of obtaining a catalytically dead Rrp6 protein. All these amino acids are located inside the catalytic core of Rrp6 as shown in a homology model (Figure 2.1B).

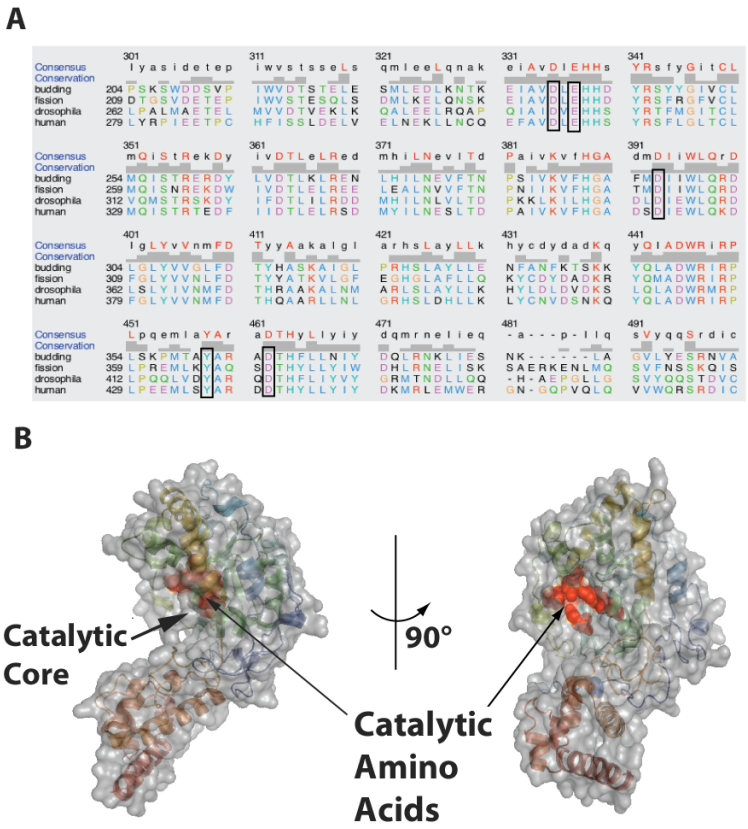


**Figure 2.1 Location of mutations in rrp6-cat** (A) Multiple sequence alignment of the conserved DEDD-Y exonuclease domain of Rrp6 in *S. cerevisiae* (budding), *S. pombe* (fission), *D. melanogaster* (drosophila) and *H. sapiens* (human). The catalytic (DEDD-Y) residues of Rrp6 are highlighted in black rectangles. The amino acids are numbered according to their position in *S. cerevisiae* Rrp6. In *S. pombe* they correspond to D243, E245, D303, Y366, and D370. (B) Homology model of *S. pombe* Rrp6 protein (http://swissmodel.expasy.org). The DEDD-Y catalytic residues (depicted in red) lie inside the catalytic core of Rrp6 (labeled)

The *rrp6-cat* mutant had a slight growth defect compared to wild type at all temperatures (Figure 2.2A). By contrast, the *rrp6Δ* mutant showed severe growth defects at all temperatures (Figure 2.2A). This shows that Rrp6-cat protein retains some functions of the wild type protein.

To further characterize the *rrp6-cat* mutant, I attempted to make double mutants with *dis3*, the core nuclease of the exosome. I first crossed to a cold-sensitive mutant, *dis3-54* (Kinoshita, Goebl et al. 1991). Despite dissecting 40 tetrads, I was unable to find any *rrp6-cat dis3-54* double mutants among the 11 complete tetrads ($p < 0.005$), suggesting that this double mutant is inviable even at the *dis3-54* permissive temperature. This is consistent with the idea that *rrp6-cat* lacks exonuclease activity. I then crossed *rrp6Δ* to *dis3-4* (ts), a different allele of *dis3* (Yamanaka, Yamashita et al. 2010), but was again unable to recover any double mutants, presumably because the *rrp6Δ dis3-4* (ts) double mutant is also inviable. However, I succeeded in generating the *rrp6-cat dis3-4* (ts) double mutant. This *rrp6-cat dis3-4* double mutant was temperature sensitive because of the *dis3-4* allele and also slightly cold sensitive like the *rrp6-cat* mutant (Figure 2.2A). This indicated that both Rrp6 and Dis3 functions were impaired in the *rrp6-cat dis3-4* double mutant.

The *dis3-4* allele was generated by error-prone PCR (Yamanaka, Yamashita et al. 2010), and is not well characterized. I sequenced it, and found three mutations: D307G, L642S, and F954S. These lie in the OB RNA binding region, the catalytic RNB region, and the

S1 RNA binding region, respectively. Thus, the molecular basis of the *dis3-4* defect is unclear.

Previous studies showed that Rrp6 is important for processing the 3' end of a fraction of 5.8S rRNA (Briggs, Burkard et al. 1998, Allmang, Mitchell et al. 2000). To test if *rrp6-cat* is defective for catalysis, I analyzed 5.8S rRNA processing by sequencing total RNA from wild type, *rrp6Δ,* and *rrp6-cat* mutants. I made the libraries by ligating a sequencing adapter to the 3' end of unfragmented total RNA (see methods) to determine 3' processing changes. I found that the *rrp6-cat* and *rrp6Δ* mutants each contained a substantial and similar amount of unprocessed 5.8S rRNA at both the 5' and 3' ends (Figure 2.2B); little or no such unprocessed 5.8S rRNA was seen in the WT strain (Figure 2.2B). Nevertheless, the total amount of mature 5.8S rRNA was similar in all three strains (Figure 2B – Y-axis). This result shows that mutating the five amino acids in the exonuclease domain did indeed abolish catalytic activity of Rrp6, since, for this phenotype, *rrp6-cat* phenocopies *rrp6Δ.* It also suggests that there are other, redundant mechanisms for producing the mature 5.8S rRNA. Finally, I found that Rrp6 protein levels were the same in wild type and the *rrp6-cat* mutant (Figure 2.2C). This result indicates that the mutant phenotype of *rrp6-cat* was due to the mutations, not an indirect effect of altered Rrp6 protein levels.

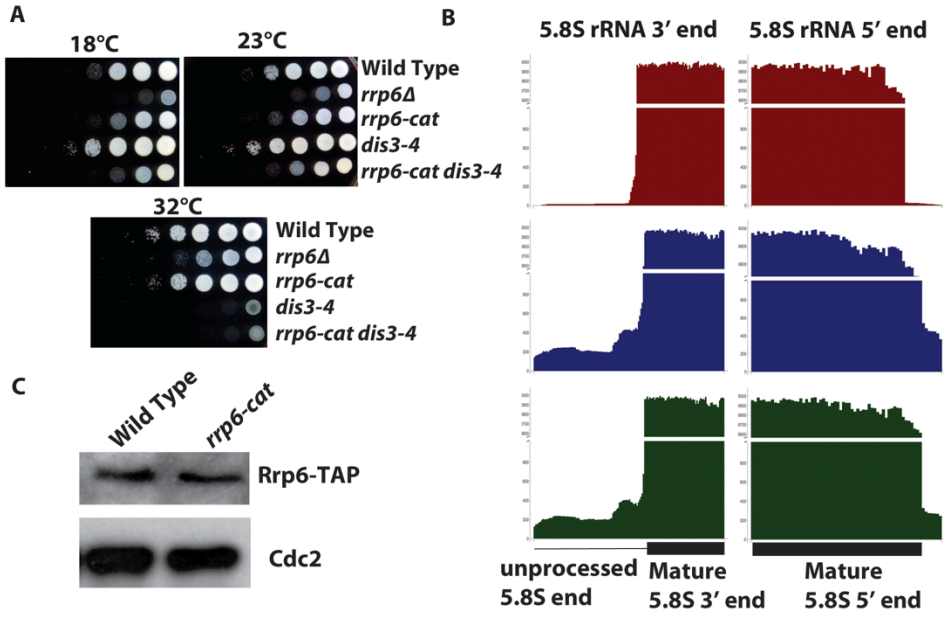


**Figure 2.2 Phenotypes of Rrp6 and Dis3 mutants.** (A) Growth assay for *rrp6* and *dis3* mutants on YES media at different temperatures. (B) Barchart showing RNA-Seq reads at one 5.8S rRNA locus (SPRRNA.51) at the 5' and 3' ends (direction of transcription is from right to left). The Y-axis was compressed to clearly show the unprocessed reads. (C) Western Blot showing the levels of TAP-tagged Rrp6 protein in wild type (CHP1365) and *rrp6-cat* mutant (JLP1708)

### 2.3.2 Rrp6 mostly plays a structural role in degrading its mRNA targets

I used RNA-Seq to determine the genome-wide RNA targets of Rrp6 and Dis3. The RNA-Seq libraries were made using polyA selected RNA from wild type and mutants *rrp6Δ, rrp6-cat, dis3-4*, and *rrp6-cat dis3-4,* with two biological replicates for each strain. The strains with *dis3-4* alleles were grown at permissive temperature (25°C) and then shifted to restrictive temperature (30°C) for 1h and RNA was isolated and sequenced from both conditions. I mapped the RNA-Seq reads to the *S. pombe* transcriptome and computed fragments per kilobase per million (FPKM) as a measure of RNA levels for each gene using

cuffnorm and cuffdiff (Trapnell, Hendrickson et al. 2013). The replicate experiments were highly correlated (Figure 2.3), with a correlation coefficient greater than 0.92 for all replicates.

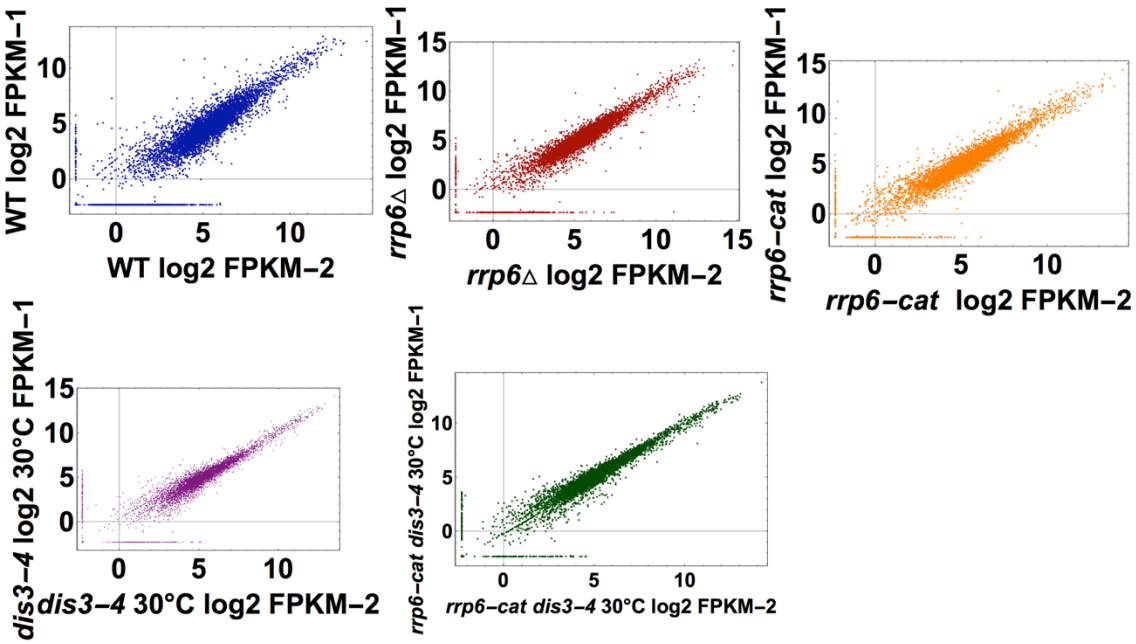


**Figure 2.3. RNA-Seq scatter plots for transcriptomes of rrp6 mutants.** The $\log_2$ fpkm values of all RNAs determined by RNA-Seq from biological replicates were plotted for each mutant. There was a high correlation (R>0.92) for all the replicates

First I compared the transcriptomes of wild type and the *rrp6Δ* mutant using cuffdiff to determine which RNAs were significantly different. When compared to wild type, many RNAs accumulated in the *rrp6Δ* mutant while few RNAs had lower levels in *rrp6Δ* (data not shown). This is consistent with the idea that deleting an exosome subunit should lead to RNA accumulation. I defined Rrp6 RNA targets as those RNAs that accumulated significantly ($p$<0.01) in the *rrp6Δ* mutant over wild type (Appendix - Table 1 - Rrp6 mRNA targets).

According to this definition, Rrp6 targets included 157 mRNAs and 103 non-coding RNAs (Appendix - Table 2 - Rrp6 ncRNA targets). (Note that since there are about 5,000 protein-coding genes in *S. pombe*, with a two-tailed p-value threshold of 0.01, there could be around 25 false positives amongst the 157 mRNAs accumulated.)

To compare the effect of the Rrp6 catalytic mutant to the null mutant for each mRNA, I plotted the *rrp6-cat/rrp6Δ* FPKM ratio for each Rrp6 target RNA as a frequency distribution (Figure 2.4A, Figure 2.5A). At one extreme, if the mRNA is extremely unstable in wild-type cells because of Rrp6 protein, but the catalytic mutation fails to stabilize the mRNA at all, this ratio could be as low as zero (i.e., very little mRNA in the catalytic mutant, a large amount of mRNA in the null mutant). At the other extreme, if degradation depends entirely on the Rrp6 exonuclease activity, so that the catalytic mutation stabilizes the mRNA by as much as the null mutation, then the ratio could be as high as one (ratios higher than one are likely due to noise). I found a roughly normal distribution of *rrp6-cat/rrp6Δ* ratios between 0 and 1, with a peak around 0.5, suggesting that for a large majority of Rrp6 targets, the catalytic mutation had a weaker effect on abundance than the null mutation. On average, over all mRNAs, the catalytic mutation had only about half the effect of the null mutation. In other words, overall, only about half of the effect of Rrp6 on mRNA degradation is due to its exonuclease activity.

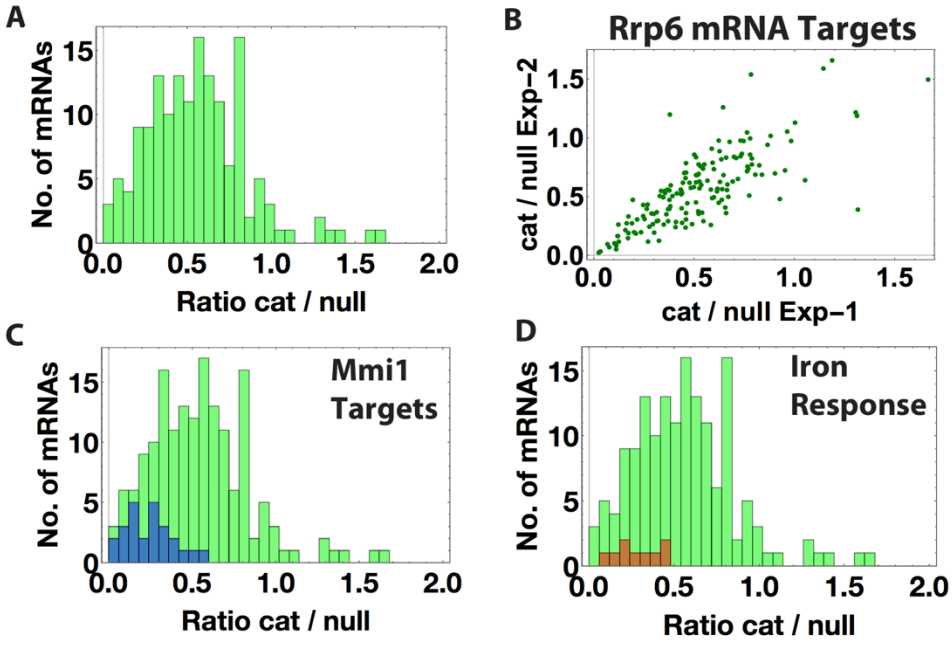


**Figure 2.4. Target mRNAs of Rrp6 protein.** (A) Frequency distribution of *rrp6-cat*/*rrp6Δ* FPKM ratios of mRNA targets of Rrp6, defined as accumulating significantly by Cuffdiff ($p$<0.01). The bin width is 0.05 (B) Scatterplot showing the correlation between replicate measurements of *rrp6*-cat/*rrp6Δ* FPKM ratios for Rrp6 target mRNAs. (C) Histogram showing the distribution of *rrp6-cat*/*rrp6Δ* FPKM ratios of Mmi1 target mRNAs (blue) and total mRNA targets of Rrp6 (green). (D) Frequency histogram showing the distribution of *rrp6-cat*/*rrp6Δ* FPKM ratios of iron homeostasis mRNAs (brown) and total mRNA targets of Rrp6 (green)

Rrp6 exonuclease activity could be distributed equally among its mRNA targets, or Rrp6 exonuclease could show a preference in degrading some targets over others. When I compared the *rrp6-cat/rrp6Δ* FPKM ratios of Rrp6 targets in the two replicate experiments, I found that they were highly correlated (Figure 2.4B). The correlation was smaller for non-coding RNA targets, likely due to polyA selection (Figure 2.5B). The fact that each mRNA gave essentially the same result in replicates 1 and 2 strongly suggests that the catalytic/null ratios in Figure 2.4A are accurate characterizations of each individual mRNA; that is, some mRNAs are “protein dependent” targets—their degradation depends on the Rrp6 protein,

but not its activity--while other mRNAs are “activity dependent” targets—their degradation depends on Rrp6 catalytic activity.

As further evidence that different mRNAs have different dependencies on the catalytic activity of Rrp6, I analyzed the replicate data shown in Figure 2.4A and 2.4B using ANOVA to test whether the mRNAs all come from a single population. ANOVA rejected this null hypothesis ($p < 10^{-31}$), showing that different mRNAs have different dependencies on the catalytic activity. Thus, there are some mRNAs efficiently degraded directly by Rrp6 (“activity dependent”), and other mRNAs that are not, but still require Rrp6 for degradation for some indirect reason (“protein dependent”) (e.g., targeting to Dis3 exonuclease).

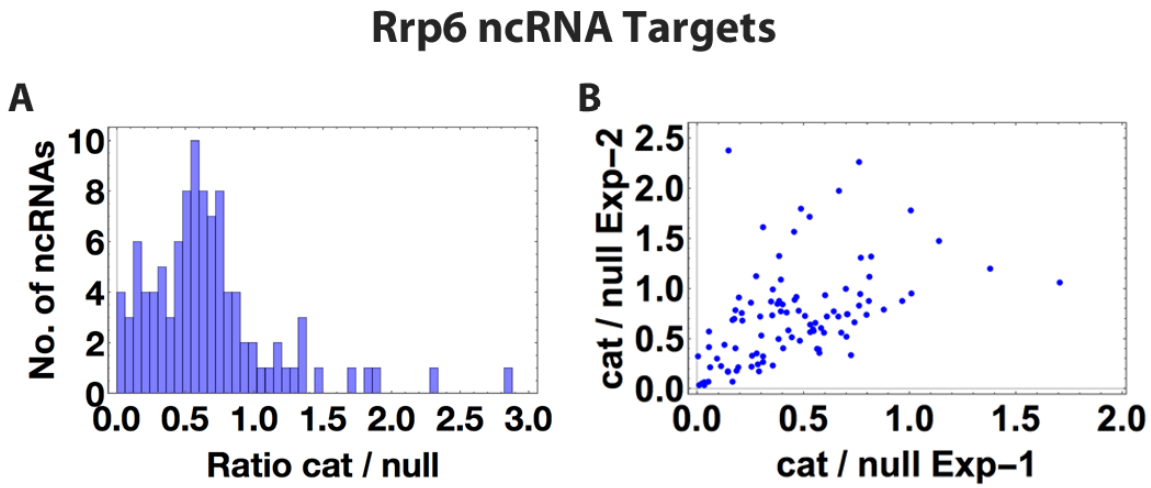


**Figure 2.5. Rrp6 noncoding RNA targets.** (A) Histogram showing the distribution of *rrp6-cat*/*rrp6Δ* fpkm ratios of noncoding RNA targets of Rrp6, defined as accumulating significantly by Cuffdiff ($p$<0.01). (B) Scatterplot showing the correlation between replicate measurements of *rrp6*-cat/*rrp6Δ* fpkm ratios for Rrp6 target noncoding RNAs. The ncRNA replicates were not well correlated

### 2.3.3 Protein-dependent targets of Rrp6 include Mmi1 targets and iron homeostasis mRNAs

To try to understand why degradation of some mRNAs might depend on the Rrp6 protein, but not its exonuclease activity, I applied Gene Ontology (GO) analysis (Ashburner, Ball et al. 2000) to the "protein dependent" targets. For this purpose, I defined "protein dependent" targets as those mRNAs with a catalytic/null ratio of 0.65 or less, which corresponds to the first (leftmost) 13 bars of Figure 2.3A. This analysis revealed two functional groups. The first significant category of genes was involved in meiosis (Table 2.1, Appendix – Table 2.3), and the genes were immediately recognizable as those coding for early meiotic mRNAs targeted by Mmi1 (Figure 2.4C – blue). The second and non-overlapping group contained genes involved in iron ion homeostasis, mostly iron transport (Figure 2.4D, Table 2.1, Appendix – Table 2.3).

**Table 2.1. GO analysis of protein dependent mRNA targets of Rrp6**

| GO ID | GO TERM | *P*-VALUE | No. of Annotations Rrp6 targets | Total no. of Annotations in Category |
|---|---|---|---|---|
| GO:0055072 | Iron Ion Homeostasis | 2.13 e-7 | 9 | 22 |
| GO:0051321 | Meiotic Cell Cycle | 4.86 e-4 | 19 | 236 |

Previously I identified a set of 30 mRNAs targeted by the RNA-binding protein Mmi1 for degradation by the exosome during vegetative growth (Chen, Futcher et al. 2011). In our current experiments, I obtained no sequence reads for 4 of them, *mcp6, mug1, mcp5,* and SPAC6C3.05. When I calculated the *rrp6-cat/rrp6Δ* FPKM ratios of the remaining 26 Mmi1

targets, I found that they accumulated much more in *rrp6Δ* than in *rrp6-cat* (Figure 2.4C - blue, Figure 2.6B, Table 2.2); that is, they had very low cat/null ratios. Thus, the Rrp6 protein may be channeling Mmi1 target-mRNAs to Dis3 for degradation. I speculate that this occurs because Rrp6 is indirectly bound to the RNA-binding protein Mmi1, and Mmi1 is bound to these particular mRNAs (Egan, Braun et al. 2014).

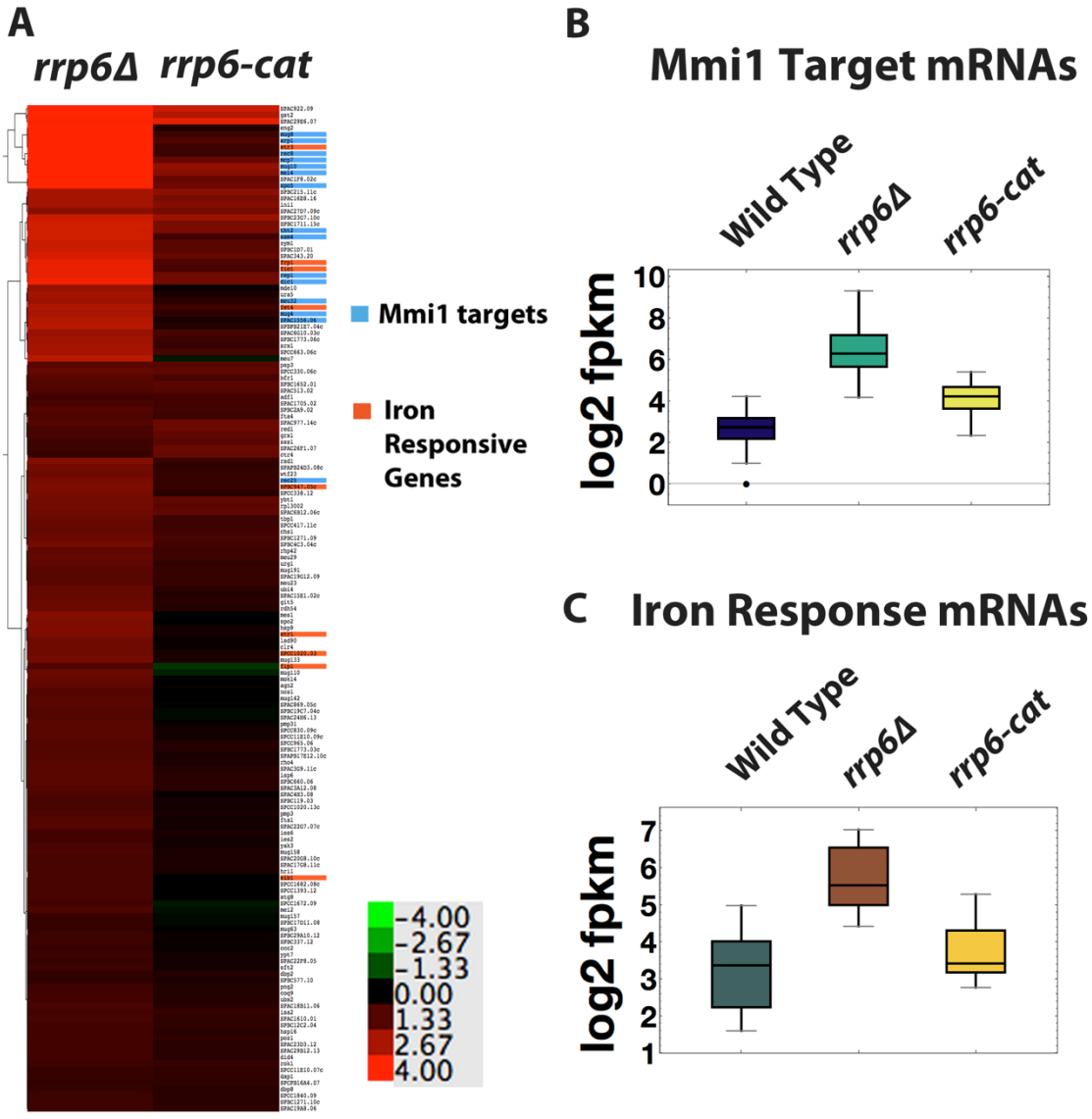

**Figure 2.6. RNA accumulation of Rrp6 target mRNAs in *rrp6* deletion and catalytic mutants.** (A) Hierarchical clustering of the $\log_2$ (mutant/WT) FPKM ratio of the 157 Rrp6 target mRNAs, in *rrp6Δ* and *rrp6-cat*. Mmi1 target RNAs are highlighted in blue and iron homeostasis mRNAs are highlighted in orange. (B) Median log2 FPKM values for Mmi1 target mRNAs and (C) iron response mRNAs in wild type and *rrp6* mutants

**Table 2.2. Effect of Rrp6 null and catalytic mutations on Mmi1 target RNAs**

| Systematic Name | Common name | *rrp6-cat*/*rrp6Δ* fpkm ratio |
|---|---|---|
| SPAC17A5.18c | *rec25* | 0.47 |
| SPAC458.04c | *dli1* | 0.53 |
| SPBC1347.12 | *arp1* | 0.12 |
| SPBC582.06c | *mcp6* | Fpkm N/A |
| SPAC25G10.04c | *rec10* | 0.41 |
| SPCC11E10.03 | *mug1* | Fpkm N/A |
| SPBC2D10.06 | *rep1* | 0.27 |
| SPBC216.02 | *mcp5* | Fpkm N/A |
| SPAC32A11.01 | *mug8* | 0.11 |
| SPAC14C4.03 | *mek1* | 0.32 |
| SPCC1393.07c | *mug4* | 0.27 |
| SPAC27D7.13c | *ssm4* | 0.21 |
| SPAP27G11.08c | *meu32* | 0.30 |
| SPAC1556.06 | *meu1* | 0.19 |
| SPAC57A10.04 | *mug10* | 0.15 |
| SPBC32H8.11 | *mei4* | 0.15 |
| SPCC70.09c | *mug9* | 0.16 |
| SPAC13A11.03 | *mcp7* | 0.09 |
| SPAC6C3.05 | | Fpkm N/A |
| SPBC577.05c | *rec27* | 0.36 |
| SPAC222.15 | *meu13* | 0.16 |
| SPBC2G2.09c | *crs1* | 0.07 |
| SPCC4E9.01c | *rec11* | 0.28 |
| SPBC646.17c | *dic1* | 0.24 |
| SPBP8B7.04 | *mug45* | 0.58 |
| SPBC29A10.02 | *spo5* | 0.03 |
| SPBC29A10.14 | *rec8* | 0.03 |
| SPAC23C4.07 | *tht2* | 0.40 |
| SPBC1921.04c | | 0.33 |
| SPNCRNA.103 | *sme2* | 0.05 |

Similarly, degradation of a set of iron response mRNAs was dependent on the Rrp6 protein, but not on its catalytic activity (Figure 2.4D - brown, Figure 2.6C and Table 2.1). The results from RNA-Seq were confirmed by qPCR for several of the genes (Figure 2.7A). The genes in this category and their functions are listed in Table 2.3 and their expression levels are in (Appendix – Table 4).

Prior studies on iron metabolism genes suggest that they are upregulated during iron depletion, but repressed when iron is present in the growth medium (Roman, Dancis et al. 1993, Pelletier, Beaudoin et al. 2003, Mercier, Pelletier et al. 2006). Since I grew cells in YES (nutrient-rich) medium, it is unlikely that these genes were upregulated due to iron depletion. Thus, our results suggest that in addition to transcriptional regulation, these genes are post-transcriptionally regulated by exosome-mediated RNA degradation during high iron conditions.

By analogy to the Mmi1 targets, I hypothesize that Rrp6 mediates interaction of the RNA Exosome with these iron homeostasis mRNAs via some unknown RNA-binding protein. This idea suggests that these mRNAs could contain a nucleotide motif for recognition by this hypothetical RNA binding protein. Motif analysis using MEME found that 8 of the 9 iron homeostasis Rrp6 targets had a total of 30 copies of a purine-rich motif (Figure 2.7B) with an E-value of 0.015. This suggests that there may a sequence-specific RNA binding protein binding to iron homeostasis mRNAs and regulating their turnover by the exosome.

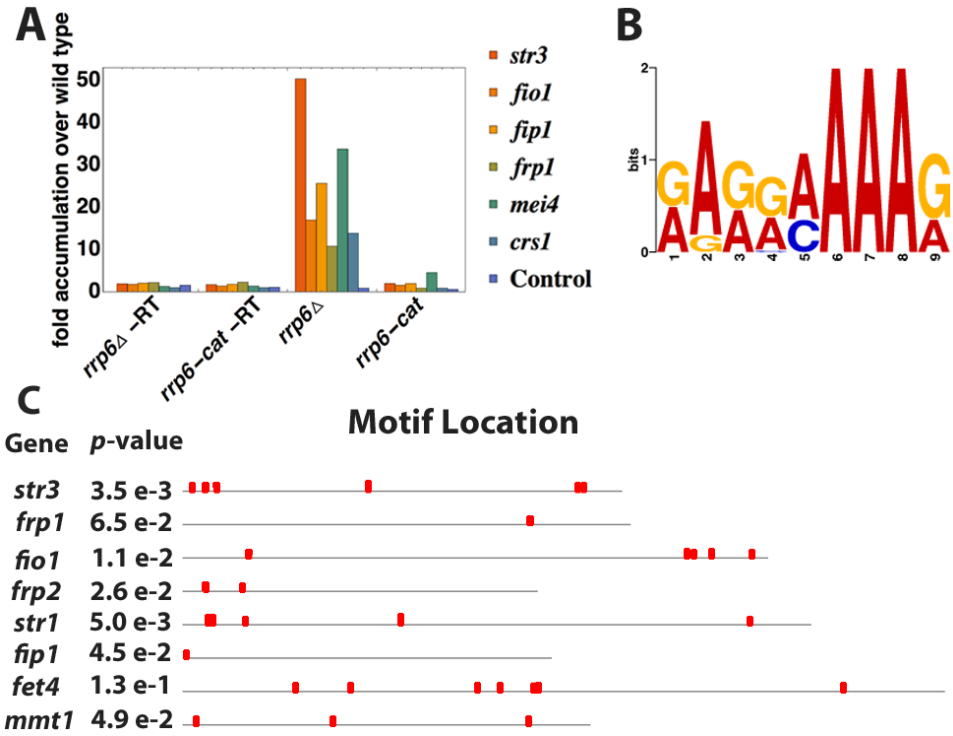


**Figure 2.7. Iron response mRNAs are protein dependent targets of Rrp6.** (A) qPCR showing fold accumulation of selective mRNA targets of Mmi1 (*mei4* and *crs1*) and iron homeostasis mRNAs (*str3, fio1, fip1, frp1*), specifically in *rrp6Δ* but not *rrp6-cat. adh1* mRNA levels were tested as internal control and labeled as "control". (B) An enriched purine-rich motif, (G/A)A(G/A)(G/A)(A/c)AAA(G/A) was found in the sequences of 8 of the 9 iron homeostasis mRNAs targeted by Rrp6. (C) Locations of the motif in each of the 8 mRNAs

**Table 2.3. Rrp6 target iron homeostasis mRNAs (*http://pombase.org*)**

| SYSTEMATIC ID | NAME | FUNCTION |
|---|---|---|
| SPAC1F7.07c | *fip1* | iron permease Fip1 |
| SPAC1F7.08 | *fio1* | iron transport multicopper oxidase Fio1 |
| SPAC1F8.03c | *str3* | siderophore-iron transporter Str3 |
| SPAC23G3.02c | *sib1* | ferrichrome synthetase Sib1 |
| SPBC1683.09c | *frp1* | ferric-chelate reductase Frp1 |
| SPBC4F6.09 | *str1* | siderophore-iron transmembrane transporter Str1 |
| SPBC947.05c | *frp2* | ferric-chelate reductase Frp2 (predicted) |
| SPBP26C9.03c | *fet4* | iron/zinc ion transmembrane transporter (predicted) |
| SPCC1020.03 | *mmt1* | mitochondrial iron ion transmembrane transporter Mmt1 (predicted) |

### 2.3.4 Effects of *dis3-4*

As described above, I was able to make *rrp6-cat dis3-4* double mutants, but not *rrp6Δ dis3-4, rrp6-cat dis3-54*, or *rrp6Δ dis3-54* double mutants. I investigated mRNA levels at permissive and restrictive temperatures in the *dis3-4* mutant and the *rrp6-cat dis3-4* double mutant. However, by RNA-Seq, these had about the same mRNA levels at both temperatures (Figure 2.8), suggesting that the biochemical activity of Dis3-4 is not highly dependent on temperature.

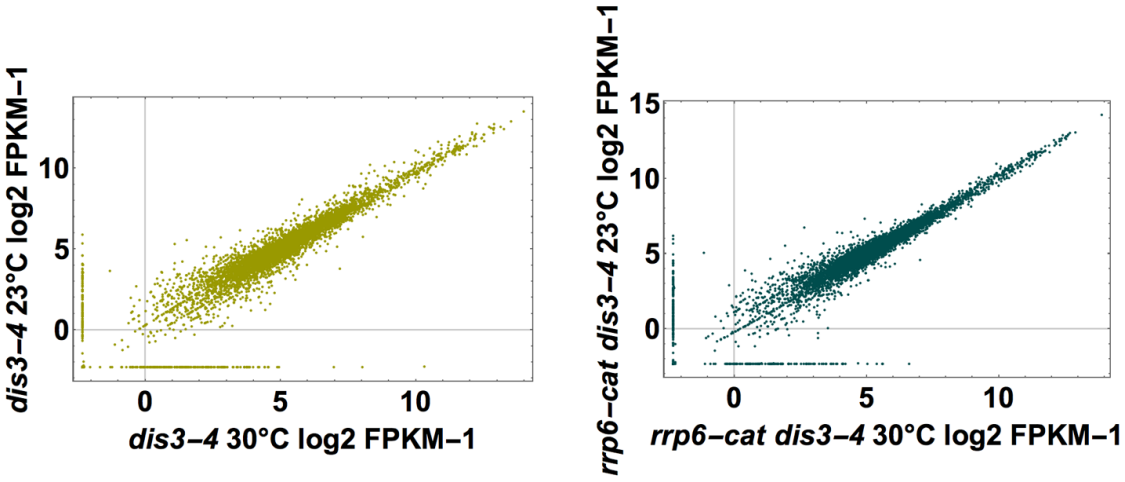


**Figure 2.8. Correlation plot of the dis3-4 mutant transcriptome at 23° and 36°C.** The $\log_2$ fpkm values of all RNAs determined by RNA-Seq from *dis3-4* at 23°C and 30°C were plotted. The RNA levels in the *dis3-4* mutant at both these temperatures were highly correlated

I clustered the mRNA abundances from RNA-Seq in the *rrp6Δ, rrp6-cat, dis3-4* and *rrp6-cat dis3-4* mutants (Figure 2.9). I found that the Mmi1 targets accumulated at a higher

level in *dis3-4* than in *rrp6-cat* (Figure 2.9A, 2.9B). However, this result is difficult to interpret because the specific defect of Dis3-4 mutant protein is uncharacterized.

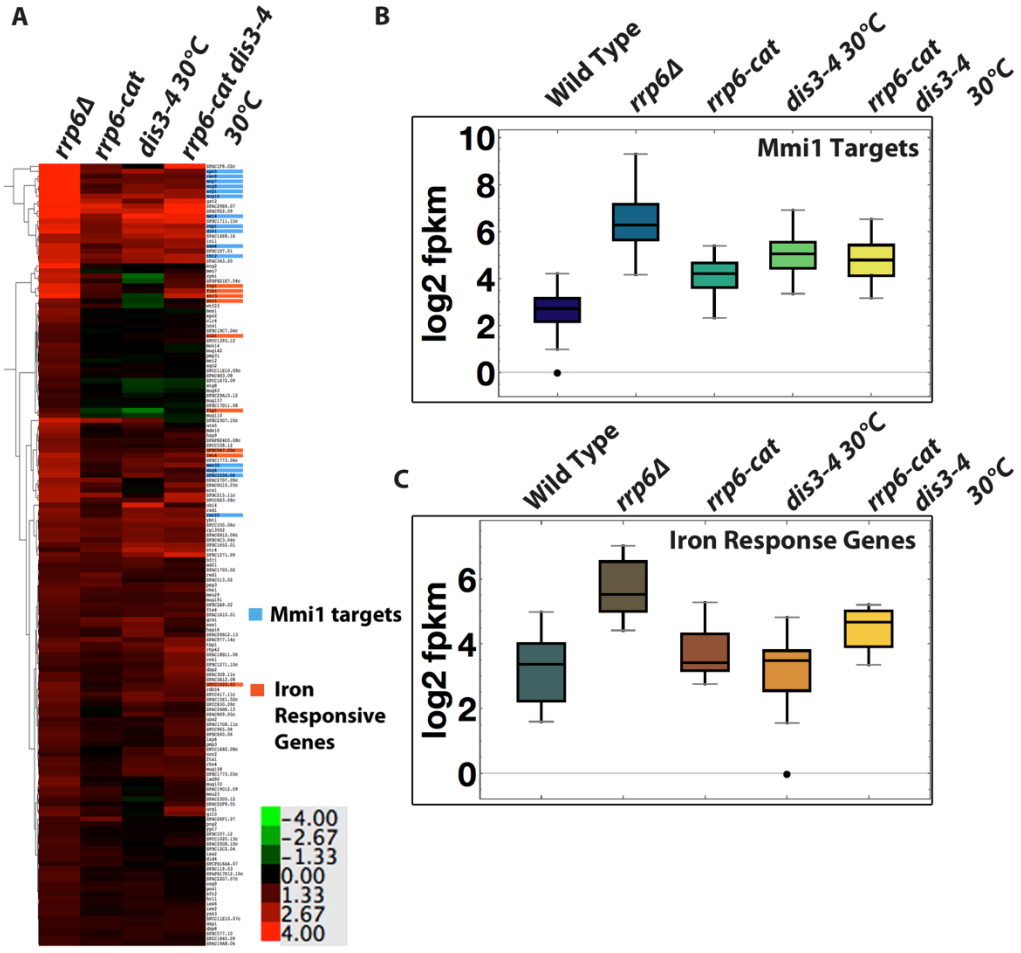


**Figure 2.9. Comparison of RNA accumulation of Rrp6 target mRNAs in exosome exonuclease mutants.** (A) Hierarchical clustering of the log2 (mutant/WT) fpkm ratio of the 157 Rrp6 target mRNAs, in all exonuclease mutants in this study. Mmi1 target RNAs are highlighted in blue and iron homeostasis mRNAs are highlighted in orange. (B) Median log2 fpkm values for Mmi1 target mRNAs and (C) iron response mRNAs in wild type and different exonuclease mutants. Most of the Rrp6 protein dependent target mRNAs accumulate higher when dis3 is mutated than in the rrp6 exonuclease mutant

## 2.4 Discussion

I determined the *in vivo* RNA targets of the exosome exonuclease Rrp6 using *rrp6* deletion and *rrp6* catalytic mutants by RNA-Seq. I found that degradation of many mRNAs depended strongly on the presence of Rrp6 protein, but less so on Rrp6 exonuclease activity. Therefore, I called them Rrp6 "protein dependent" mRNA targets, with the idea that some of the role of Rrp6 was to channel these mRNAs to Dis3 for degradation. Further, many of the Rrp6 protein dependent targets fell into two major functional groups – meiotic mRNAs that are targets of the Mmi1 RNA binding protein, and iron homeostasis mRNAs.

I suggest that in wild type cells, the exosome is recruited to the Mmi1-bound RNAs through the NURS-Mtl1-Rrp6 interaction. The exosome then degrades these RNAs using Dis3 (Figure 2.10A). However, as indicated by the dotted line, Rrp6 also has some catalytic role given that the Mmi1 targets accumulated somewhat (about 4-fold) in *rrp6-cat* (Figure 2.6B). Our results are also consistent with structural studies showing that the presence of Rrp6 protein in the exosome enhances RNA degradation by the exosome (Wasmuth and Lima 2012).

I found that Rrp6 targets 9 mRNAs required for iron transport in *S. pombe.* Most of them code for cell surface transporters of iron, and these mRNAs are upregulated during low iron conditions (Roman, Dancis et al. 1993, Askwith and Kaplan 1997, Pelletier, Beaudoin et al. 2003). In mammals and budding yeast, iron-responsive elements (IREs) in the mRNAs of iron metabolism genes control either stability or translation of those mRNAs (Hentze, Caughman et al. 1987, Rouault, Hentze et al. 1988, Hentze, Rouault et al. 1989). Analogous to the Mmi1 pathway, in *S. pombe* there may be one or more RNA binding

proteins bound to these mRNAs during high-iron conditions that targets them to the exosome using Rrp6 as an adapter (Figure 2.10B). Supporting this model, I found a nucleotide motif shared by these mRNAs. An alternative model would be analogous to the regulation of iron starvation mRNAs in budding yeast by the Cth1, Cth2 RNA-binding proteins (Martinez-Pastor, Vergara et al. 2013). Under high iron conditions, Rrp6 processes the 3' end of the CTH2 pre-mRNA resulting in mature CTH2 mRNA (Ciais, Bohnsack et al. 2008). Cth2 recognizes AU-rich elements in the 3' UTR of iron starvation mRNAs and targets them for degradation (Puig, Askeland et al. 2005, Puig, Vergara et al. 2008). However, Cth1 and Cth2 have no homologs in *S. pombe.*

Although they did not fall into large enough functional groups to emerge in our analysis, there are "protein dependent" targets of Rrp6 that are neither Mmi1 targets nor iron transport genes. These may likewise be recruited to the exosome via an Rrp6-RNA binding protein interaction, and subsequently degraded largely by Dis3.

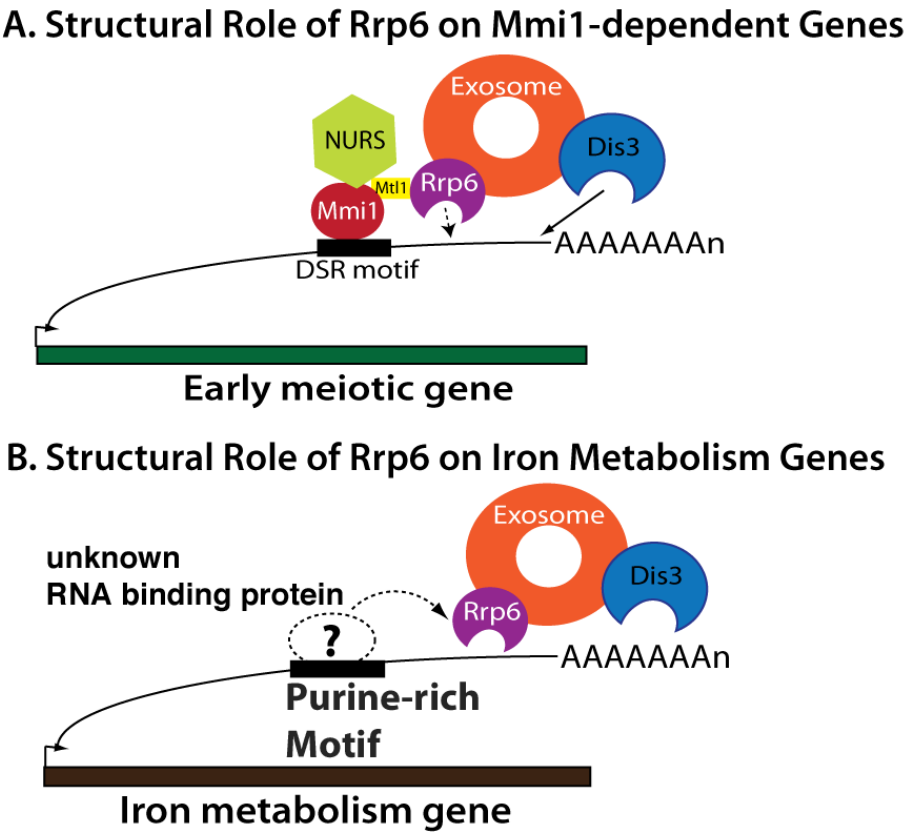


**Figure 2.10. A schematic model for the role of Rrp6 as a structural adapter protein.** (A) Rrp6 associates with the NURS complex through its interaction with Mtl1. NURS complex associates with Mmi1 bound to early meiosis RNAs during mitosis. Therefore, exosome recruitment to these RNAs is possible and these RNAs are degraded mostly by Dis3. Rrp6 degrades only some of the Mmi1 target RNA (depicted by dotted line). (B) Rrp6 facilitates the degradation of iron homeostasis mRNAs during high-iron conditions. It does so presumably by interacting with yet unidentified RNA binding proteins that bind to the discovered purine-rich motif in my study

## 2.5 Materials and Methods

### 2.5.1 Yeast strains, media and growth conditions

*S. pombe* culture methods were used as described in (Forsburg and Rhind 2006). When required, cells were grown in Edinburgh Minimal Media (EMM) with supplements. For RNA isolation and spot assays, cells were grown in liquid YES at 32°C, until they reached

O.D.600 = 0.5 to 0.6. Temperature-sensitive mutants (*dis3-4*) were grown at 23°C before shifting to 30°C for 1h. For RNA isolation, cells were harvested at 4°C, washed with ice-cold water, frozen in liquid nitrogen, and stored at -80°C. For spot assays, wild type (CHP1365), *rrp6Δ* (JLP1704), *rrp6-cat* (JLP1708), *dis3-4* (JT449), and *rrp6-cat dis3-4* (JLP1863) strains were grown in liquid YES at 32°C until they reached an optical density (600nm) of 0.6. Cells were then suspended in water at a density of $2 \times 10^6$ cells/ml. 10-fold serial dilutions were made and 5µl of each dilution was spotted on YES-agar plates and incubated at the temperatures indicated. For transformation, cells were grown in liquid YES at 32°C overnight and then diluted in equal volume of fresh YES media. Cells were grown another 3h before harvesting.

### 2.5.2 Cloning and site-directed mutagenesis of *rrp6* exonuclease domain

A region containing the exonuclease domain of *rrp6* was PCR amplified. The PCR product was T-A cloned and the resulting plasmid, pKM-rrp6-ex2, was mutagenized by site-directed mutagenesis to give plasmid pKM-rrp6-cat. Site-directed mutagenesis was performed using Stratagene QuikChange Multi Site-Directed Mutagenesis kit according to instructions.

### 2.5.3 Construction of *rrp6Δ, rrp6-cat,* and *rrp6-cat dis3-4* mutants

The *rrp6* gene was disrupted using *ura5-lys7* cassette as described in (Mudge, Hoffman et al. 2012). *ura5-lys7* was PCR amplified, with 250 nucleotide overhangs homologous to exon2 of *rrp6,* from plasmid pUL57. This PCR product was transformed into

CHP1365 (kindly provided by Dr. Charles Hoffman) using a protocol described in (Bahler, Wu et al. 1998). Cells were plated on EMM with leucine, adenine and histidine to select for *ura+ lys7+* colonies resulting in the *rrp6::ura5-lys7* (*rrp6Δ*) strain, JLP1704. JLP1704 was then transformed with a PCR product from pKM-*rrp6-cat* generated using primers rrp6-exon2F and rrp6-exon2R. Transformants were counter-selected on EMM media containing 0.1% 5-FOA. Mutants were screened by colony PCR, and sequencing the *rrp6* gene. The resulting *rrp6-cat* mutant, JLP1708, was crossed to the *dis3-4* (ts) mutant (JT449, kindly provided by Dr. Masayuki Yamamoto, (Yamanaka, Yamashita et al. 2010)) and tetrads were dissected to obtain the *rrp6-cat dis3-4* mutant (JLP1863).

### 2.5.4 RNA isolation and Illumina RNA-Seq

RNA was extracted from cells using RiboPure Yeast kit (Ambion) according to manufacturer's instructions. 20µg of total RNA was DNase-treated using Turbo DNase (Ambion). 1µl of DNase-treated RNA was used for PCR using srp7F and srp7R primers to ascertain whether there was no genomic DNA contamination. The integrity of total RNA was measured using Agilent Bioanalyzer 2100.

*RNA-Seq library preparation for total RNA using 3' ligation* - 1µg of unfragmented total RNA was end repaired using polynucleotide kinase. A modified oligonucleotide adapter from the Illumina Art-Seq/Riboprofile kit was ligated to the 3' end. 1$^{st}$ strand cDNA was made using reagents provided with this kit. 2$^{nd}$ strand cDNA was made using reagents from NuGen Ovation Universal RNA-Seq System according to manufacturer's instructions. cDNA was

sonicated using a Misonix 3000 sonicator at amplitude 60, for 10 minutes on ice. Following sonication, the libraries were prepared using reagents and instructions from the NuGen Ovation Universal RNA-Seq system but with the following modification. Only 5' adapter was ligated to the fragmented, end-repaired cDNA. The libraries were PCR amplified using forward and reverse primers provided in the Illumina Art-Seq/Riboprofile kit. The libraries were purified using 0.8X Ampure XP beads and sequenced on Illumina MiSeq.

*RNA-Seq library preparation for polyA selected RNA* - 30µg of DNase-free RNA was used for polyA selection using Poly(A)Purist kit (Ambion). 100ng of polyA selected RNA was used as starting material for making strand-specific cDNA-Seq libraries using Ovation Universal RNA-Seq Library System (NuGen) according to manufacturer's instructions. cDNA was sonicated using a Misonix 3000 sonicator at amplitude 60, for 10 minutes on ice. Strand-specific cDNA was PCR-amplified for 12 cycles and sequenced on Illumina MiSeq by paired-end sequencing.

### 2.5.5 Computational Methods

*Clustal Alignment* – The Rrp6 exonuclease domain amino acid sequences from *S. cerevisiae, S. pombe, D. melanogaster,* and *H. sapiens* was aligned by Clustal X multiple sequence alignment using default parameters (Thompson, Gibson et al. 2002). Jalview was used to visualize and annotate the results (Waterhouse, Procter et al. 2009).

*Homology Modeling* – A homology model for *S. pombe* Rrp6 was created based on the crystal structure of *S. cerevisiae* Rrp6 using the server at http://swissmodel.expasy.org

(Arnold, Bordoli et al. 2006). Pymol was used to visualize and annotate the Rrp6 homology model.

*Bowtie* – Reads from total RNA libraries made by end-ligation were aligned using Bowtie2. Reads mapping to the chromosome coordinates corresponding to SPRRNA.51 (5.8S rRNA) were extracted using Samtools mpileup and plotted using Mathematica.

*Tophat* - Reads were aligned to the *S. pombe* transcriptome (ASM294v2.26) using Tophat2 (Kim, Pertea et al. 2013). Discordant mapping of pairs was not allowed and minimum and maximum intron lengths were set to 29 and 1000 respectively (all Tophat options used will be provided upon request). The mapping did not allow for discovery of novel intron junctions. Mapped reads were sorted and indexed using Samtools (Li, Handsaker et al. 2009) and visualized on Integrative Genomics Viewer (IGV) (Robinson, Thorvaldsdottir et al. 2011, Thorvaldsdottir, Robinson et al. 2013).

*Cuffquant, Cuffnorm* and *Cuffdiff* - For differential gene expression, Cuffquant was used to estimate abundances for each transcript. To estimate correlation between replicate experiments, Cuffnorm was used to generate normalized fragments per kilo base per million (FPKM) by considering each replicate as an independent sample (Trapnell, Roberts et al. 2012). To determine targets of Rrp6, I used Cuffdiff (Trapnell, Hendrickson et al. 2013) to compare the transcriptomes of wild type and *rrp6Δ* mutant by pooling the replicate data for each sample. Cuffdiff provided the expression level (FPKM) as well as a measure of differential expression, for each gene in wild type and *rrp6Δ*.

*Analysis of rrp6 mutants' transcriptome and RNA target determination:* From the Cuffdiff analysis, the RNAs that accumulated significantly in *rrp6Δ*/WT ($p<0.01$) were considered Rrp6 target RNAs. All genes with 0 FPKM in all samples were removed from the analysis. A pseudo count of 1 was added to FPKM of all genes in all conditions to enable $\log_2$ transformation and ratio calculation. For the Rrp6 targets, I determined their Rrp6-cat dependence by calculating their FPKM ratio in *rrp6-cat*/*rrp6Δ.* All plots were generated using Mathematica.

*Cluster* – ($\log_2$ FPKM mutant – $\log_2$ FPKM WT) for each gene, was clustered by hierarchical clustering with Euclidian distance as the similarity metric using Cluster 3.0 (de Hoon, Imoto et al. 2004). The clusters were visualized and analyzed by Java TreeView (Saldanha 2004).

GO analysis was done using http://go.princeton.edu/cgi-bin/GOTermFinder as described in (Ashburner, Ball et al. 2000).

*MEME* – The motif search in iron assimilation mRNAs was done using MEME motif finder. I allowed for multiple repetitions of motifs in each sequence. Only the CDS (including UTRs) was used for the analysis. A similar search using the shuffled sequences of the same genes gave a motif with a significantly higher E-value (not shown).

### 2.5.6 Western Blot

Cells were lysed according to the procedure mentioned in (Forsburg and Rhind 2006) and equal amounts of protein from each sample were resolved by 10% SDS-PAGE. Rrp6-TAP

was detected by chemiluminescence using a 1:5000 dilution of peroxidase anti-peroxidase antibody.

# CHAPTER 3

## Determining the RNAs bound to Mei2 during early meiosis

## 3.1 Preface

Mei2 is an RNA binding protein and the master initiator of meiosis. Meiosis is blocked prior to S-phase of meiosis if Mei2 is either absent, or if it is unable to bind RNA. Mei2 is known to bind *meiRNA* and this binding helps the cells initiate meiotic nuclear divisions. How Mei2 initiates early meiotic events is still unclear, but we know that Mei2 likely binds to some RNA(s) and accomplishes this function. Therefore, I determined the RNAs bound to Mei2 during early meiosis using both RNA Immunoprecipitation and Crosslinking Immunoprecipitation, followed by microarray or sequencing respectively. I found that Mei2 binds to the mRNAs of meiotic inhibitor *mmi1,* mitotic MBF transcription factor *rep2,* and *mug110. mug110* is a meiosis upregulated gene whose role in meiosis is unknown. Deleting *mug110* had no apparent effect on sporulation. Further, deleting *mug110* could not rescue the *mei2Δ* meiosis initiation defect. Preliminary investigation revealed that depleting *rep2* or *mmi1* might rescue the meiosis initiation defect of *mei2Δ.*

## 3.2 Introduction

Mei2 is critical for initiating meiosis in *S. pombe.* It is an RNA binding protein and its only known partner is *meiRNA,* a non-coding RNA (Watanabe and Yamamoto 1994). Mei2 has two RNA recognition motifs, and the RRM closer to the C-terminus is required for meiosis initiation (Watanabe, Shinozaki-Yabana et al. 1997). During vegetative growth, the meiotic program is kept off because Pat1 kinase phosphorylates Mei2 (Watanabe, Shinozaki-Yabana et al. 1997) and Mei2 is degraded by the proteasome (Kitamura,

Katayama et al. 2001). Mutants of Mei2 that cannot be phosphorylated initiate meiosis without nitrogen starvation (Watanabe, Shinozaki-Yabana et al. 1997).

Mei2 localizes at a specific locus in the nucleus during meiosis forming a 'dot' (Watanabe and Yamamoto 1994), even before karyogamy of meiosis (Yamashita, Watanabe et al. 1998). *meiRNA* is required to form the Mei2 dot, and Mei2-*meiRNA* complex is formed at the *sme2* locus (*meiRNA* coding locus) (Shimada, Yamashita et al. 2003). Mei2 apparently shuttles between the cytoplasm and nucleus, and *meiRNA* is required to keep Mei2 in the nucleus during meiosis (Sato, Shinozaki-Yabana et al. 2001, Sato, Watanabe et al. 2002). However, adding an NLS to Mei2 is also sufficient to allow it to localize to the nucleus, and form a dot, even in the absence of *meiRNA* (Yamashita, Watanabe et al. 1998). Importantly, the C-terminal RRM of Mei2 is critical for Mei2-*meiRNA* complex formation; even addition of an NLS to Mei2 C-terminal RRM mutants, does not allow it to localize in the nuclear dot (Yamashita, Watanabe et al. 1998). Thus Mei2 is required in a specific location in the nucleus to initiate meiosis, and this localization requires its RNA binding ability.

The significance of the Mei2 dot was revealed when Mei2-*meiRNA* was found to colocalize with Mmi1 in the nucleus during meiosis. This released the Mmi1 bound early meiotic RNAs so that they could be translated (Harigaya, Tanaka et al. 2006). Mmi1 binds to a hexanucleotide motif on its target RNAs (Chen, Futcher et al. 2011, Yamashita, Shichino et al. 2012). *meiRNA* has a number of these motifs at its 3' end that act as an Mmi1 decoy to keep it localized to the *sme2* locus during meiosis (Chen, Futcher et al. 2011, Shichino, Yamashita et al. 2014). During vegetative growth, a shorter form of *meiRNA* lacking the

excess Mmi1 motifs is made, and this form of *meiRNA* is bound by Mmi1 and degraded by the exosome (Shichino, Yamashita et al. 2014). Therefore *meiRNA* is unable to sequester Mmi1 during vegetative growth. Mei2 binds to the 5' end of *meiRNA,* but the significance of this binding is not entirely clear (Shichino, Yamashita et al. 2014).

*meiRNA* is required for meiosis I but dispensable for initiating meiosis. Mei2p and its RNA binding function are required for initiating meiotic S-phase. Thus Mei2 must have additional RNA binding partners that allow it to initiate meiotic S-phase. In this chapter, I have investigated what RNAs Mei2 binds, and how they may help Mei2 initiate meiosis.

## 3.3 Results

To determine the targets of Mei2, I used a technique called RIP (Figure 3.1). For immunoprecipitating Mei2, I added a TAP tag to the Mei2 protein. As a control, I used a strain with Mei2 lacking a TAP tag. Both strains had an $h^{90}$ genotype, so when starved for nitrogen, they mated and underwent meiosis. When starved for nitrogen on ME medium, the Mei2-TAP strain was able to sporulate as well as the strain with no tag on Mei2 (data not shown). This indicated that the TAP tag did not interfere with Mei2 function in meiosis.

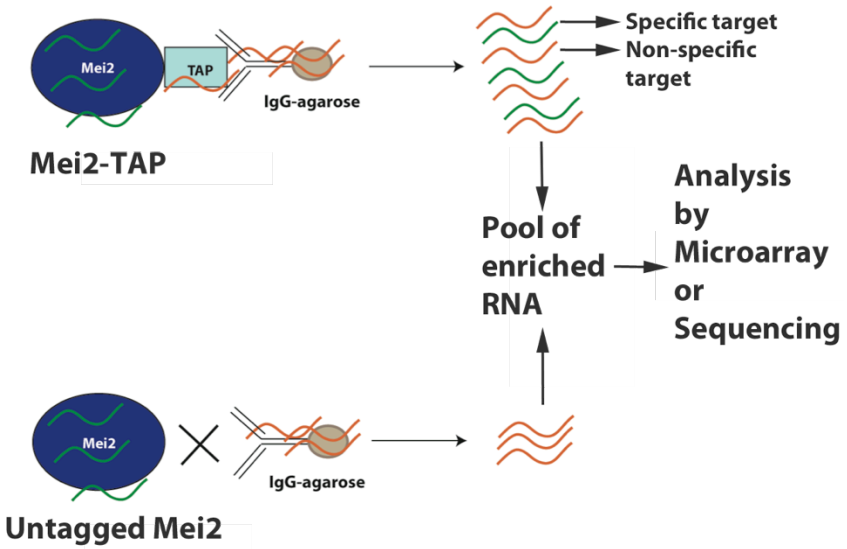


**Figure 3.1 Schematic of RIP-CHIP.** Mei2-TAP and untagged Mei2 are immunoprecipitated with IgG antibodies. The bound RNAs are then eluted and analyzed by microarray or sequencing

### 3.3.1 Mei2 expression during meiosis

To determine when Mei2 protein was being expressed in meiosis, I used western blotting to detect Mei2-TAP expression at different times after nitrogen starvation. I found two bands corresponding to full-length Mei2 from 3h to 6h after nitrogen starvation (Figure 3.2A). I found by microscopy that during these times, most cells had conjugated (data not shown). Further, I found that Mei2 levels were higher at 3h and 6h and lower at other times. This could be either because Mei2 levels actually increase and decrease during meiosis, or because different populations of cells entered meiosis at different times. The second cause is likely because meiosis was asynchronous in these cultures. The reason for the two full-length bands is unclear.

I also found multiple bands that were shorter than full-length Mei2 (Figure 3.2). These were most probably degradation products of Mei2 protein. This was not surprising given that protease levels in meiotic cells are very high.

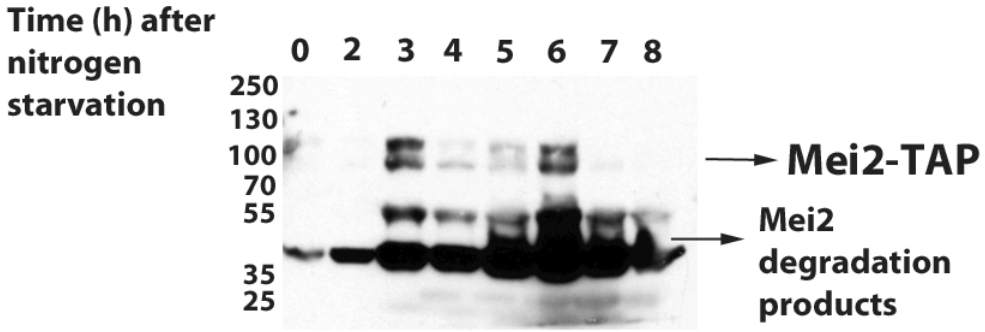


**Figure 3.2 Mei2 is expressed in early meiosis.** (A) Western blot showing Mei2 protein levels at different times after $h^{90}$ Mei2-TAP cells are starved for nitrogen. Full length Mei2-TAP is around 100kDa. (B) Western blot using lysates prepared from nitrogen starved $h^{90}$Mei2-TAP strain with either 5µg/ml or 10µg/ml of protease inhibitors.

### 3.3.2 RIP-CHIP suggests Mei2 maybe bound to *mmi1* and *rep2* mRNA

I used the samples with high Mei2 expression (between 4-5h after nitrogen starvation) to immunoprecipitate Mei2 and determine its RNA targets by RIP-CHIP. I used IgG coupled to agarose beads for immunoprecipitation since IgG binds to the TAP tag. After immunoprecipitation, I used western blot to detect Mei2 enrichment and found that Mei2 was highly enriched in the IgG beads before and after elution (Figure 3.3A, lanes 6,8). This indicated that the IgG beads efficiently immunoprecipitated Mei2-TAP. Mei2 was not detectable in lysates from the untagged Mei2 strain (Figure 3.3A, lanes 1,3,5,7), indicating that the IgG antibody was specifically binding to Mei2-TAP.

I eluted RNA from the IgG-Mei2-TAP beads and also isolated total RNA from a fraction of the lysate used for immunoprecipitation, and used this to normalize for enrichment. Since, Mei2 is known to bind *meiRNA,* I first tested *meiRNA* enrichment using qRT-PCR (Figure 3.3B). I found that *meiRNA* was specifically enriched in Mei2-TAP immunoprecipitation (Figure 3.3B). I also tested for enrichment of *srp7* RNA, which should not bind Mei2, and found that it was not enriched (Figure 3.3B). This indicated that I was successfully able to immunoprecipitate Mei2 and enrich for its known RNA target using RIP.

Next, I determined the targets of Mei2 by hybridizing the extracted RNAs to a microarray (see methods). I used a tiling array chip with 50 nucleotide strand-specific probes covering fifty percent of the genome. I analyzed the genome for Mei2 targets manually and found 13 mRNAs specifically enriched in Mei2-TAP and not untagged Mei2 immunoprecipitation (Table 3.1). *mmi1, rep2* and *mug110* mRNAs were among the specifically enriched mRNAs (Figure 3.4). However, I was unable to successfully repeat the RIP-CHIP experiment and confirm this result. This was probably because Mei2 was losing its RNA-protein interactions ex vivo and its RNA targets were being degraded. Therefore, I decided to use an alternative strategy to increase the strength of Mei2-RNA interactions during immunoprecipitation (below).

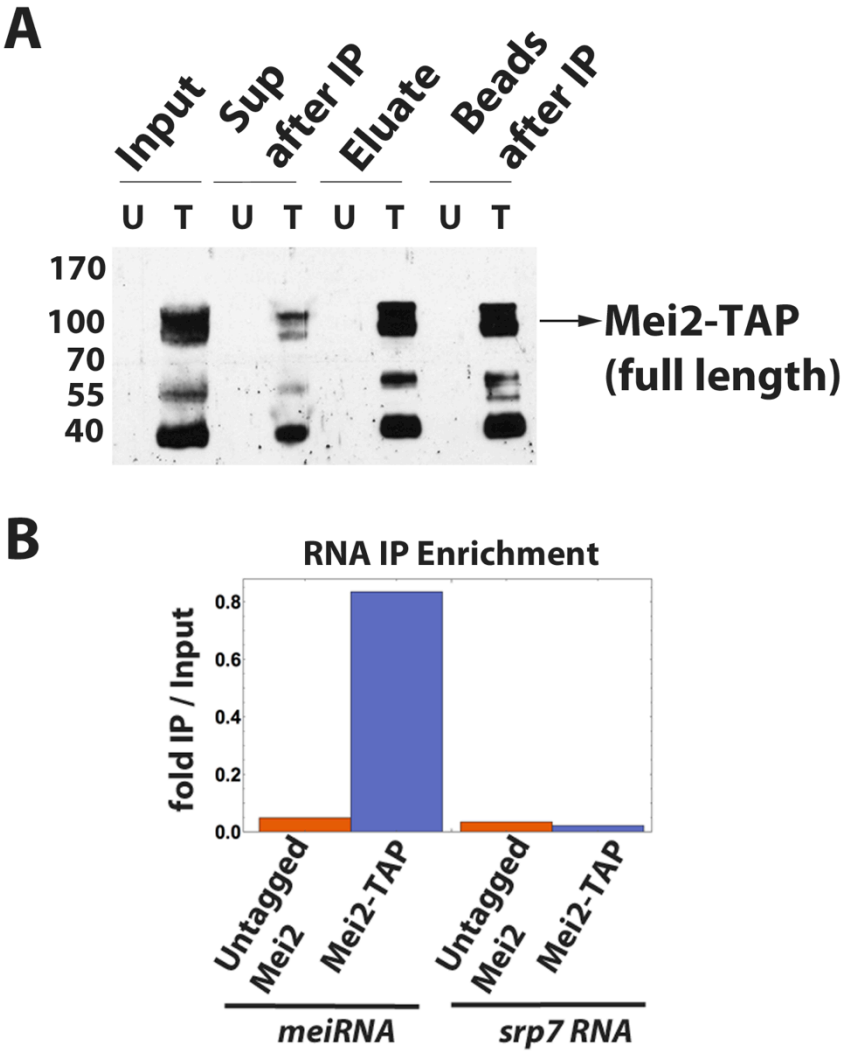


**Figure 3.3 Immunoprecipitation of Mei2-TAP.** (A) Western blot showing specific enrichment of Mei2 in Mei2-TAP (T). "Input": total lysate before IP; "Sup after IP": lysate after IP; "Eluate": after elution with 1% SDS; "Beads": beads after IP (B) qRT-PCR showing *meiRNA* enrichment specifically in Mei2-TAP, compared to a non-specific RNA, *srp7*

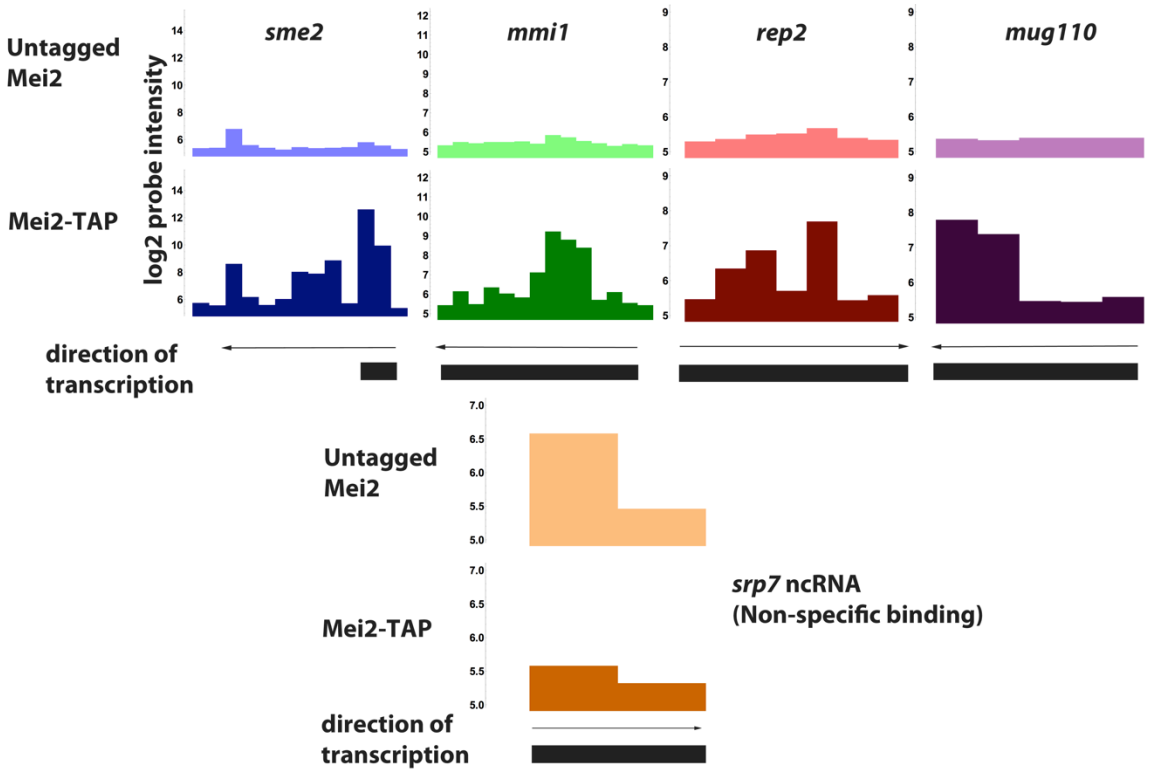


**Figure 3.4 RIP-CHIP showing specific enrichment of mmi1, rep2 and mug110 mRNA in Mei2-TAP.** Mei2 targets were analyzed by Agilent CGH microarray. *srp7* RNA intensities are shown as a control for non-specific enrichment

**Table 3.1 Mei2 targets determined by RIP-CHIP**

| Gene | Function | Meiosis RNA expression |
|---|---|---|
| SPACUNK4.17 | NAD binding dehydrogenase family protein | Up in middle meiosis |
| sme2 | non coding RNA | Up in early meiosis |
| mug110 | unknown | Up in early meiosis |
| efc25 | Ras1 guanyl-nucleotide exchange factor | slightly down |
| SPBC32F12.07c | E3 ligase | slightly up |
| snoU14 | unknown | no change |
| but2 | protein neddylation with Uba3 | no change |
| rep2 | MBF TF | Down in early meiosis |
| SPBP23A10.11c | cell wall biosynthesis | Up in middle meiosis |
| yox1 | MBF regulatory subunit | Slightly up |
| mmi1 | meiotic RNA turnover | Down |

| | | |
|---|---|---|
| SPCC1223.14 | chorismate synthesis | Down |
| SPCC757.12 | alpha amylase homolog | Down in late meiosis |

### 3.3.3 UV crosslinking and immunoprecipitation (CLIP) of Mei2 and Msa1

To increase the strength of Mei2-RNA interactions, I decided to use UV crosslinking before immunoprecipitation. UV crosslinking is not as strong as formaldehyde crosslinking, and therefore there are fewer non-specific crosslinks. Moreover, UV crosslinking procedures have been optimized to study yeast RNA binding proteins (Granneman, Kudla et al. 2009). Many groups that study RNA-protein interactions have observed that some RNAs are prone to bind multiple RNA binding proteins (personal communication). These RNAs are specifically enriched after immunoprecipitation of most RNA binding proteins. These non-specific RNA-protein interactions may further increase after UV crosslinking. Therefore, to control for such noise, I added a TAP tag to Msa1, another RNA binding protein that is expressed in meiosis. Msa1 has some meiotic phenotypes, so this experiment would also help me determine Msa1 RNA targets, if any. I used Western blot to determine the expression of Msa1-TAP and found that it was highly expressed in meiosis (Figure 3.5). Like Mei2, Msa1 also had some level of protein degradation in meiosis (Figure 3.5).

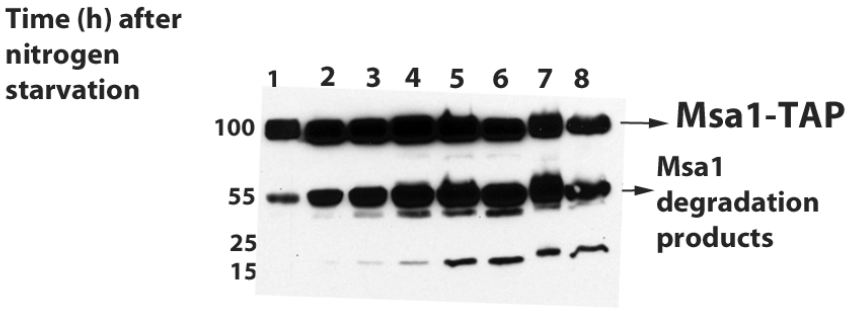


**Figure 3.5 Msa1 is highly expressed during meiosis**

Next I repeated the immunoprecipitation after UV crosslinking of nitrogen starved Mei2-TAP, Msa1-TAP and untagged strains (see methods for details). The lysates were lightly sonicated after crosslinking to break up potential UV-induced big complexes. I determined the efficiency of immunoprecipitation by Western blot (Figure 3.6A). I found that full length Mei2-TAP was reasonably well immunoprecipitated, but Msa1-TAP was less efficiently immunopreciptated (Figure 3.6A, lanes 5,6). I found consistently, that Mei2-TAP bands in the lysate after crosslinking (input in Figure 3.6A) were not as sharp compared to RIP (Figure 3.3A). This was probably due to UV crosslinking.

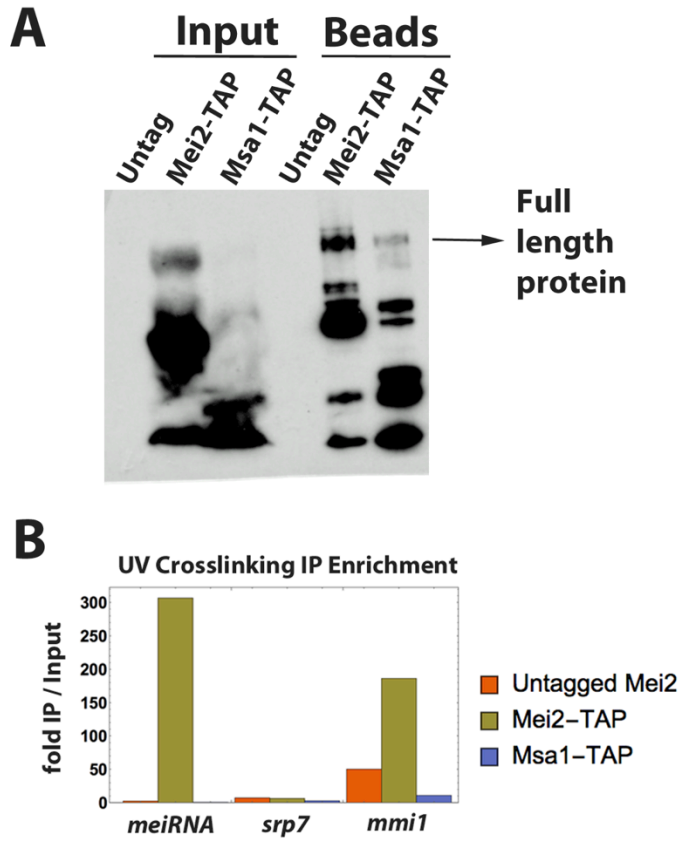


**Figure 3.6 UV crosslinking and Immunoprecipitation of Mei2-TAP and Msa1-TAP.** (A) Western blot showing the immunoprecipitation efficiency of Mei2 and Msa1. "Input" indicates total lysate before immunoprecipitation and "Beads" indicates amount of protein present on IgG beads after immunoprecipitation (B) Enrichment of *meiRNA, srp7* and *mmi1* after CMIP, detected by qRT-PCR

To determine whether CLIP was successful, I tested the enrichment of *meiRNA* by qPCR (Figure 3.6B). I found that both *meiRNA* and *mmi1* were specifically enriched in Mei2-TAP but not in untagged or Msa1-TAP, but non-specific RNA, *srp7,* was not enriched specifically in any of the samples (Figure 3.6B). CLIP was also more reproducible than RIP, so I then continued with target determination.

### 3.3.4 Mei2 binds the 5' UTR of *mmi1* and *rep2* mRNAs

To determine the targets of Mei2 and Msa1, I extracted RNA from the eluates of the CLIP experiment and sequenced them using Illumina MiSeq. I used random-primed cDNA to make the RNA-Seq libraries for sequencing. I mapped the sequencing reads to the *S. pombe* transcriptome, and visualized the alignments using Integrative Genomics Viewer (IGV). I then analyzed the genome for RNAs specifically enriched in Mei2-TAP but not in Msa1-TAP.

Initially, I looked at the known targets of Mei2 from previous studies and my RIP-CHIP data – *meiRNA, mmi1, rep2,* and *mug110*. I calculated and plotted the counts over each nucleotide in these loci using Samtools mpileup (Figure 3.7, see methods). I found that, even from CLIP, all four RNAs were targets of Mei2 (Figure 3.7). Therefore, I concluded that these are definitely Mei2 RNA targets since they were repeatedly enriched in different experiments. I also found a few other Mei2 targets using CLIP (Table 3.2), but these were not enriched in Mei2-TAP in the RIP experiment. Similarly, there were some Mei2 targets that were determined only by RIP but not by CLIP. I could not classify either of these RNAs as high confidence Mei2 targets. Many RNAs were enriched in both Mei2-TAP and Msa1-TAP IPs and I considered these non-specific targets.

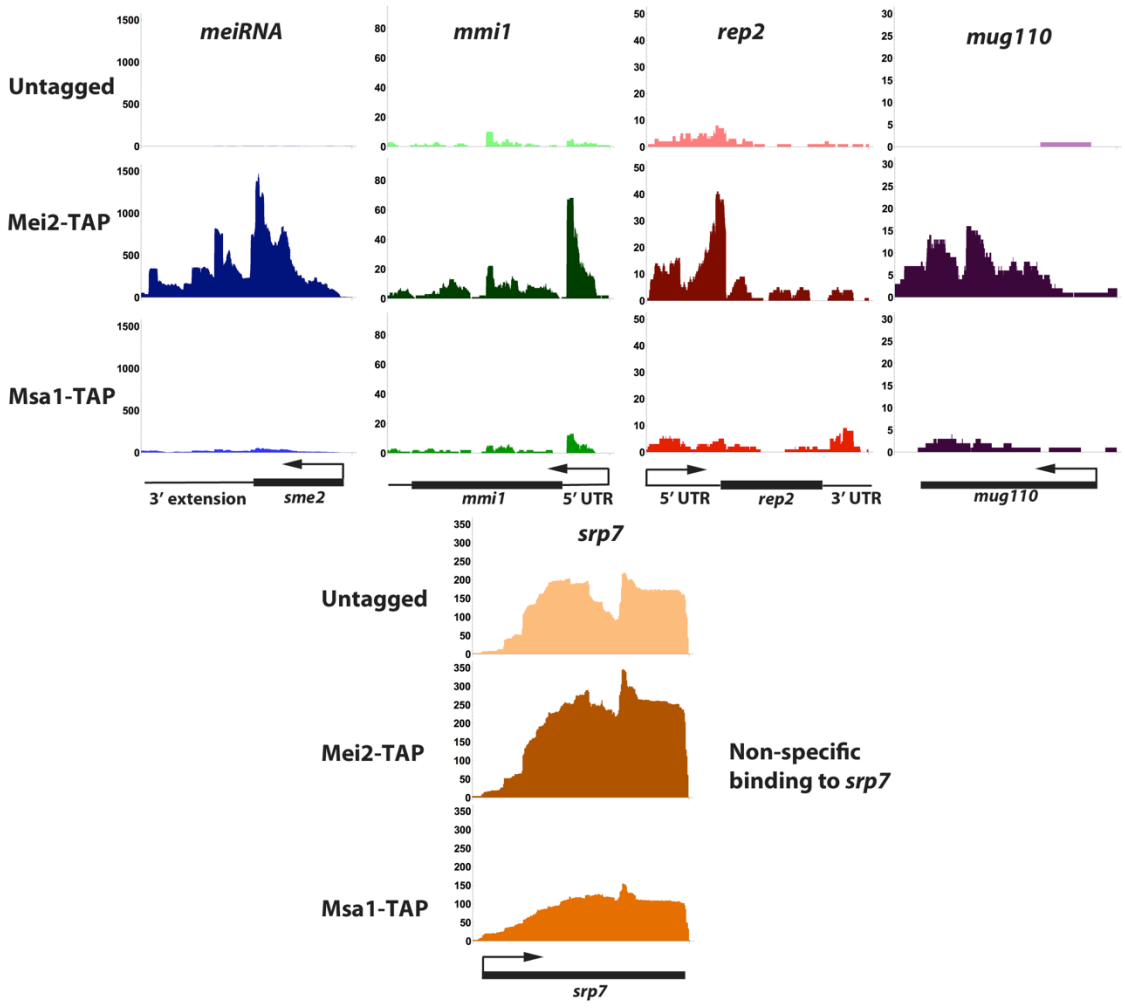


**Figure 3.7 RNA targets of Mei2.** Mei2 binds to *meiRNA, mug110* mRNA and possibly the 5' UTR of *mmi1* and *rep2. srp7* ncRNA binds non-specifically and is enriched in all IP samples

**Table 3.2 Mei2 targets determined by CLIP-Seq**

| GENE | EXPRESSION | FUNCTION |
|---|---|---|
| | **Up in Meiosis** | |
| sme2 | middle | ncRNA – Mmi1 bait |
| ubc7 | S-phase | Ub conjugating enzyme |
| mug110 | middle | Unknown |

| Down in meiosis | |
|---|---|
| mmi1 | RNA binding of meiosis genes |
| rep2 | MBF TF |
| SPAC19B12.06c | Rhomboid family protease |

*meiRNA* is a non coding RNA that is critical for meiosis I. It was shown that *meiRNA* has a 3' extension of its RNA in meiosis, and Mei2 binds to the 5' end (Shichino, Yamashita et al. 2014). I found that the *meiRNA* bound to Mei2-TAP after CLIP was the meiotic full-length *meiRNA* (Figure 3.7, panel 1). However, more reads aligned to the 5' end of *meiRNA,* so my results are consistent with (Shichino, Yamashita et al. 2014). Strikingly, for *rep2* and *mmi1* RNAs, I found more reads aligning to the 5' UTR (Figure 3.7, panel 2,3). This could indicate that Mei2 binds specifically to the 5' UTR of *rep2* and *mmi1*, so it is protected from degradation during CLIP. However, it is also possible that the pileups are restricted to the 5' UTR due to an artifact of library preparation using random hexamers. I did not find the same bias for all enriched RNAs when I looked at the reads using Integrative Genomics Viewer (IGV), suggesting that the pileups may be due to preferential Mei2 binding. Since the RNA was not fragmented significantly during the IP process, I am unable to explain why full-length *mmi1* and *rep2* RNA is not detected even if Mei2 preferentially binds to their 5' UTR. Finally, I found that for *mug110* mRNA, reads aligned to the entire gene indicating that Mei2 bound to the entire RNA without any binding preference (Figure 3.7, panel 4).

### 3.3.5 Functions of Mei2 RNA targets

The functions of all Mei2 targets determined by RIP and CLIP are summarized in Table 1 and Table 2. *meiRNA* is a noncoding RNA, thought to act as an Mmi1 sponge during meiosis. Mmi1 binds and targets early meiotic RNAs for degradation during vegetative growth. Further Mei2, *meiRNA* and Mmi1 colocalize in the nucleus during meiosis. My results show that Mei2 also binds to the 5' UTR of *mmi1* RNA.

Mug110 is a meiosis upregulated gene (mug is an abbreviation of this) of unknown function. *mug110* mRNA was also found to bind another RNA binding protein, Crp79 (Amorim, Cotobal et al. 2010). It is possible that *mug110* promiscuously binds to RNA binding proteins ex vivo. However, *mug110* mRNA was not enriched in Msa1-TAP CLIP suggesting that this might not be the case. I found that Mei2 specifically bound *mug110* mRNA, and I made a *mug110Δ mei2Δ* double mutant to test whether it can rescue the meiosis initiation defect of *mei2Δ.* I found that the phenotype of *mug110Δ mei2Δ* was indistinguishable from *mei2Δ,* and *mug110Δ mei2Δ* double mutant did not initiate meiosis.

Rep2 is a transcription factor of the MBF complex (Nakashima, Tanaka et al. 1995). The MBF complex comprises Res1, Res2, Cdc10 and Rep2 in vegetative cells, and is responsible for transcription of S-phase genes (Aves, Durkacz et al. 1985, Tanaka, Okazaki et al. 1992, Miyamoto, Tanaka et al. 1994, Sugiyama, Tanaka et al. 1994, Nakashima, Tanaka et al. 1995). During meiosis, Rep2 levels decrease, and Rep1, another transcription factor, replaces it in the MBF complex. Rep1 is required for the transcription of S-phase genes during meiosis.

Mmi1 is inhibitory towards meiosis, and *mmi1* mutants try to undergo meiosis even without nitrogen starvation but fail (Harigaya, Tanaka et al. 2006). Both *rep2* and *mmi1* RNA levels decrease during meiosis. Rep2 may also be inhibitory towards meiosis since it needs to be replaced by Rep1. Since I found that Mei2 may bind to both *rep2* and *mmi1* 5' UTR, its binding may cause their destabilization or block translation, thus promoting meiosis. Thus I hypothesized that Mei2 may initiate meiosis by blocking Rep2 or Mmi1 mediated inhibition of meiosis. I then did a preliminary experiment to test this hypothesis.

### 3.3.6 Mei2 may initiate meiosis by destabilizing *rep2* and *mmi1* mRNA

To test the hypothesis that Mei2 initiates meiosis by somehow inactivating *mmi1* and *rep2*, I asked whether *mei2Δ* could not initiate meiosis because *mmi1* and *rep2* mRNA are stable and the proteins are present. This suggests that, depleting Rep2 or Mmi1 (or perhaps both) would rescue the meiotic initiation phenotype of *mei2Δ* and allow cells to initiate premeiotic S-phase. I constructed diploids of *mei2Δ rep2Δ* double mutant and *mei2Δ mmi1-ts3* double mutants. Mmi1 is essential, and its temperature sensitive mutant strain (*mmi1-ts3*) is growth sensitive at 36°C (Yamamoto).

I starved *mei2Δ mmi1-ts3* and *mei2Δ rep2Δ* double mutant diploids for nitrogen, and tested whether they replicated their DNA by DAPI staining (Figure 3.8). When *S. pombe* cells successfully complete pre-meiotic S-phase, the nucleus undergoes "horsetail" nuclear movements, which can be observed by nuclear staining (Saito, Tougan et al. 2005). *mei2Δ* when starved for nitrogen is able to conjugate but blocks at the diploid stage of meiosis

(Watanabe 1994). The *sme2Δ* mutant is able to initiate meiosis and complete premeiotic S-phase. Therefore, I used *sme2Δ* diploid as a positive control to observe horsetail nuclear movement indicating successful DNA replication, and *mei2Δ* diploid as a negative control (Figure 3.8). The wild type diploid had cells in different stages of meiosis, including some that had sporulated completely (Figure 3.8, left top). I found a substantial number of horsetail nucleus containing diploids in the *sme2Δ* mutant (~ 10%), but none of the *mei2Δ* mutants had horsetail nuclei (Figure 3.8, left bottom and middle). Strikingly, I found that the *mei2Δ mmi1-ts3* double mutant diploid had horsetail nuclei at both permissive and restrictive temperature (Figure 3.8, right top and middle). I also found that the *mei2Δ rep2Δ* double mutant had horsetail nuclei. These results suggest that depleting either *mmi1* or *rep2* can possible rescue the meiosis initiation defect of *mei2Δ* mutants. I am currently quantifying the nuclear phenotypes and designing further experiments to test this premise.

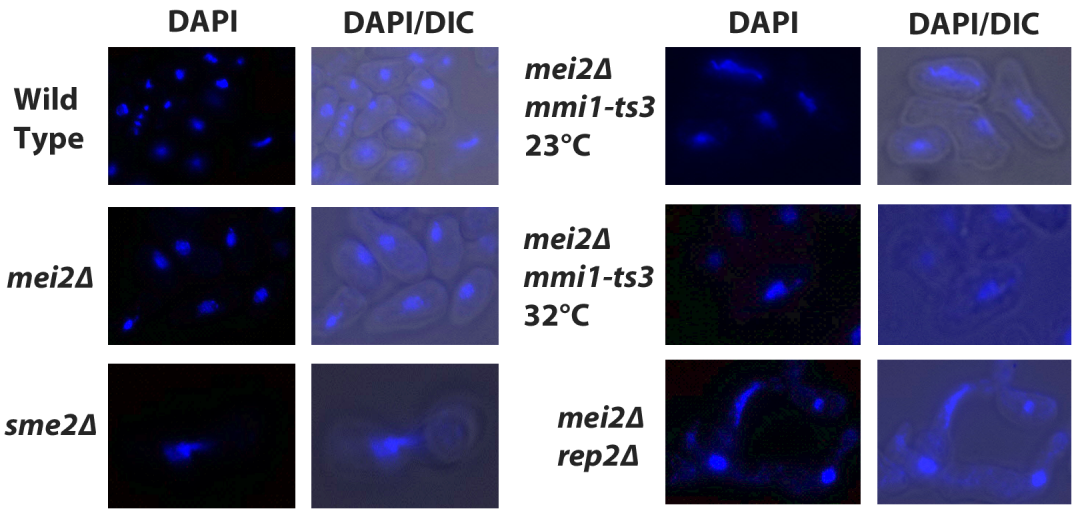


**Figure 3.8 Depletion of rep2 and mmi1 can rescue the meiosis initiation defect of mei2Δ.** Diploid strains with genotypes indicated in the figure were nitrogen starved on Spa plates and allowed to sporulate for 24h before ethanol fixation and DAPI staining to observe 'horsetail nucleus' indicating successful DNA replication

## 3.4 Discussion

I found three novel RNA targets of RNA binding protein Mei2 using both RIP-CHIP (RNA Immunoprecipitation and microarray) and CLIP-Seq (cross-linking immunoprecipitation and RNA sequencing). They were mRNAs of *mug110, mmi1* and *rep2.* Mug110 is a protein of unknown function and Mmi1 and Rep2 are possible meiotic inhibitors. I had limited success with RIP-CHIP, but I was able to successfully overcome that by crosslinking Mei2 to its RNA targets. I used UV crosslinking because the crosslinking efficiency is relatively low compared to formaldehyde crosslinking, so there is less noise. In my experience, RNA IP experiments are only successful when the noise is significantly low -

something that is incredibly hard to achieve. However, I only considered the targets from both experiments as high-confidence Mei2 targets.

First, I tried to investigate the significance of Mei2 binding to *mug110* mRNA. *mug110Δ* is viable, and undergoes normal meiosis (Martin-Castellanos, Blanco et al. 2005). Localization experiments with GFP-tagged Mug110 suggest it maybe a membrane protein (Matsuyama, Arai et al. 2006). However, Martin-Castellanos et al. had already found that *mug110* was dispensable for a normal meiosis. Therefore, I attempted to test if *mug110* genetically interacted with *mei2* by making a *mug110Δ mei2Δ* double mutant. I found that its meiotic phenotype was indistinguishable from *mei2Δ* indicating no apparent negative interaction. One possibility is that *mug110* cooperates with Mei2. An experiment to test this would be to overexpress *mug110* in a *mei2Δ* mutant and see if it rescues the *mei2Δ* phenotype. So far, none of the overexpression screens for rescuing *mei2* mutant phenotypes have reported *mug110* as a hit.

Both *rep2* and *mmi1* were more understandable Mei2 targets than *mug110.* Mmi1 is known to bind and target early meiotic mRNAs for degradation (discussed extensively in Chapter 1.5.2). Rep2 is a MBF complex subunit that activates transcription of S-phase genes in vegetative growth (Nakashima, Tanaka et al. 1995). This group also reported that *rep2Δ* had a slight meiotic defect. The MBF complex is made of subunits *cdc10, res1, res2* and either *rep2* or *rep1* (Aves, Durkacz et al. 1985, Tanaka, Okazaki et al. 1992, Miyamoto, Tanaka et al. 1994, Sugiyama, Tanaka et al. 1994, Nakashima, Tanaka et al. 1995). Rep1 is specifically required for transcription of meiotic recombination genes (Ding and Smith

1998). *rep1* transcript levels increase during meiosis at the same time that *rep2* transcript decreases (Watanabe, Shinozaki-Yabana et al. 1997). Although many studies have tried to elucidate the functions of the different subunits of MBF, a clear picture has not emerged. The general idea is that Res1, Res2 and Cdc10 are always bound to the DNA of S-phase genes. Rep2 activates transcription during mitosis and Rep1 activates transcription during meiosis. Hence the presence of Rep2 may not allow cells to initiate meiosis successfully because it may compete with Rep1 for binding to MBF. Therefore, I hypothesized that Mei2 binding to the 5' UTR of *rep2* mRNA inhibits its expression somehow, and helps in initiating meiosis. Indeed I found some preliminary evidence for this possibility, because *rep2Δ* cells are able to rescue some of the meiosis initiation defect of *mei2Δ*. Similarly, I showed that *mmi1* mutant cells are able to do the same.

To study these effects more completely and accurately, I will use flow cytometry to follow DNA replication of *mei2Δ mmi1-ts3* and *mei2Δ rep2Δ* diploids. I am currently quantifying the horsetail nuclei in the different mutants. I will also study the global gene expression changes indicative of meiotic progression in *mei2Δ rep2Δ* and *mei2Δ mmi1-ts3* diploids, using RNA-Seq.

## 3.5 Materials and methods

### 3.5.1 Yeast strains, media and growth conditions

*S. pombe* culture methods were used as described in (Forsburg and Rhind 2006). When required, cells were grown in Edinburgh Minimal Media (EMM) with supplements. For

transformation, cells were grown in liquid YES at 32°C overnight and then diluted in equal volume of fresh YES media. Cells were grown another 3h before harvesting. For nitrogen starvation, Spa and ME media were used (Forsburg and Rhind 2006).

For immunoprecipitation experiments using $h^{90}$ strains (untagged, Mei2-TAP and Msa1-TAP), cells were grown at 32°C on YES up to $OD_{600}$ = 0.6 – 0.8. Then they were harvested, washed in water and inoculated into ME media for 4 – 5h at 23°C. They were harvested in ice, washed with cold lysis buffer (see below), frozen in liquid nitrogen and stored at -80°C.

### 3.5.2 Construction of TAP-tagged Mei2 and Msa1 strains

The TAP tag cassette was amplified from plasmid pFA-6a-TAP-Kan with 300 nucleotide 5' and 3' sequences complementary to either Mei2 C-terminus or Msa1 C-terminus. This was transformed using the protocol by (Bahler, Wu et al. 1998). Kanamycin resistant transformants were selected on YES-G418 plates, and TAP tag integration was confirmed by colony PCR and sequencing.

### 3.5.3 Western Blot

Cells were lysed according to the procedure mentioned in (Forsburg and Rhind 2006) and equal amounts of protein from each sample were resolved by 10% SDS-PAGE. Mei2-TAP and Msa1-TAP was detected by chemiluminescence using a 1:5000 dilution of peroxidase anti-peroxidase antibody.

### 3.5.4 RNA Immunoprecipitation (RIP)

RIP was done according to the protocol in (Gerber, Herschlag et al. 2004) with the following modifications. All steps were done using cold reagents in a cold room. Protease inhibitors Leupeptin, Pepstatin, Bestatin, Aprotinin were added to a final concentration of 2µg/ml of Lysis buffer. PMSF was added to a final concentration of 1mM and 100 U/ml of SuperaseIn (Ambion) was also added to Lysis Buffer. Cells were lysed by bead beating using 0.7mm Zirconia beads in a Fast Prep at maximum speed for 2 pulses of 20s and incubation for 5 min on ice in between pulses. 20µl of lysate was frozen in liquid nitrogen for Western, and 50µl was stored in liquid nitrogen as input. IgG-Agarose beads (Sigma) were used for immunoprecipitation at 4°C for 2h. Three sets of three washes with wash buffers B and C were performed for a total of 9 washes after immunoprecipitation. RNA was eluted from the beads using 1% SDS dissolved in 1X TE with SuperaseIn. RNA was extracted by phenol:chloroform extraction and ethanol precipitation.

### 3.5.5 Microarray

Microarray Labeling and Hybridization was performed using a two-color Quick Amp Labeling Kit (Agilent). Labeled cDNAs were hybridized onto Agilent Comparative Genome Hybridization arrays for *S. pombe* (Agilent). IP RNAs were labeled with Cy3 and Input RNAs were labeled with Cy5. The CGH array had 50 nucleotide probes with 50 nucleotide gaps on each strand. Therefore the genome coverage is roughly 50%. Cy3 intensities were visualized on IGB (Integrated Genome Browser - UCSC) and intensities were plotted using Mathematica.

### 3.5.6 Crosslinking Immunoprecipitation

Crosslinking Immunoprecipitation of Mei2-TAP and Msa1-TAP were done according to (Selth, Gilbert et al. 2009) with some modifications. Cells were UV crosslinked using Stratalinker with power 100 and default time settings. Protease inhibitors and RNase inhibitors were added to the lysis buffer as mentioned in 3.4.4. Lysates were sonicated using a Misonix sonicator at 80 Amplitude for 30s. Immunoprecipitation, washes and elution was done as in 3.4.4. Following elution, 1µl of 20mg/ml proteinase K was added to the eluates and incubated for 1h at 42°C. RNA was extracted by phenol chloroform and precipitated by 1/10$^{th}$ volume of sodium acetate and 100% ethanol at -80°C overnight.

### 3.5.7 RNA Sequencing of immunoprecipitated RNA and data analysis

Immunoprecipitated RNA was DNase treated and libraries were made using Nugen Ovation Universal RNA-Seq system with random primers. Strand specificity is maintained using this method. cDNA was sonicated using a Misonix 3000 sonicator at 60 amplitude for 10 minutes on ice. Strand-specific cDNA libraries were PCR-amplified for 12 cycles. The quality of libraries was checked using Bioanalyzer and Qubit and sequenced on Illumina MiSeq by paired-end sequencing.

Reads were mapped to *S. pombe* reference transcriptome version ASM294v2.26 using STAR (Dobin, Davis et al. 2013). Discordant mapping was not allowed and only annotated splice junctions were mapped. Alignments were sorted and indexed using Samtools and visualized

on Integrative Genomics Viewer (IGV). Pileups at the *sme2, mmi1, rep2,* and *mug110* loci were generated using samtools mpileup, and plotted using Mathematica.

### 3.5.8 Quantitative RT-PCR

For qRT-PCR was performed to test *meiRNA* enrichment after immunoprecipitation. Input and IP RNAs were used to make first strand cDNA using Superscript RT III (Invitrogen Life Technologies) according to manufacturer's instructions. cDNA was used for quantitative PCR using Roche LightCycler 480 SYBR Green Master kit with gene specific primers.

# CHAPTER 4

## Concluding Remarks

## Impact of this dissertation

I have studied two key aspects of posttranscriptional gene regulation in *S. pombe.* I have uncovered a novel class of mRNAs targeted by the exosome. I have also discovered novel targets of Mei2, which was a long unanswered question in the field. Below I have summarized the results from each of these studies, as well as discussed the significance of the findings. I have also discussed some possible future research directions, some of which I am planning to pursue.

## 4.1 Chapter 2: Exosome exonuclease Rrp6 plays a non-catalytic, structural role in degradation of meiotic and iron response mRNAs

The exosome is a complex of proteins that processes and degrades RNA in all eukaryotes. There are similar complexes in bacteria and archaea as well. Studies on the exosome have been hard in yeast, and harder in higher eukaryotes. One reason is that most subunits of the exosome are essential. Of the two exonucleases of the exosome in yeast, Dis3 is essential for cell survival, but Rrp6 is not. The interplay of Rrp6 and Dis3 in degrading exosome target RNAs was poorly understood. In recent years, X-ray crystallographic studies of the exosome structure have provided a better understanding (Makino, Baumgartner et al. 2013, Wasmuth, Januszyk et al. 2014). Indeed these studies indicate that Dis3 is responsible for degrading most of the RNA, with Rrp6 playing a secondary role.

Previous studies showed that mutations in both *rrp6* and *dis3* affected turnover of early meiotic RNAs targeted by Mmi1 (Harigaya, Tanaka et al. 2006, Yamanaka, Yamashita et al. 2010, Chen, Futcher et al. 2011). However, it was not clear which exonuclease was degrading the RNA, partly because these studies used *rrp6Δ* and *dis3* mutants that were not specifically lacking in their exonuclease activity. For *dis3* the mutations were generated by error-prone PCR, and the mutations thus induced were not well characterized. Since *rrp6Δ* mutants accumulated high levels of Mmi1 target mRNAs, and Rrp6 has 3'-5' exonuclease activity, the general consensus was that Rrp6 must be degrading these RNAs. However, mutations in *dis3* also affected Mmi1 target RNAs. Rrp6 and Dis3 possibly had overlapping functions in degrading meiotic mRNAs. However, because we knew that Rrp6 mediated protein-protein interactions between the Mmi1-NURS and the exosome, it was possible that Rrp6 was playing a structural adapter role. Therefore deleting Rrp6 would lead to loss of exosome recruitment to the Mmi1 bound mRNAs resulting in their accumulation.

We previously showed that Mmi1 induces hyperadenylation in its target RNAs, and this leads to Rrp6 mediated degradation (Chen, Futcher et al. 2011). The evidence for this was that *rrp6* deletion and *rrp6-ts* mutants accumulated Mmi1 targets RNAs with long polyA tails. This could either mean that Rrp6 was recognizing and degrading RNAs with long polyA tails or the long polyA tails were generated because of deleting *rrp6.* In any case, I found using Northern blots that the *rrp6-cat* mutant accumulated little RNA from Mmi1 targets, and these were not hyperadenylated (data not shown). My results point to a new way of looking at Rrp6 function in degrading Mmi1 targets.

My genome-wide analysis of Rrp6 targets also showed a novel category of iron homeostasis mRNAs. These were mostly mRNAs coding for iron transport proteins. My data suggest that these are constitutively transcribed and degraded by the exosome during high iron conditions, when they are not required. Their mode of regulation seemed to mirror Mmi1 targets because they require Rrp6 protein but not its exonuclease activity to keep their levels low. Therefore I hypothesized that an unknown RNA binding protein might be regulating their turnover during high iron conditions. I also found a purine-rich motif using MEME in the mRNAs of iron transport genes. This suggests that there may indeed be an RNA binding protein regulating iron transport mRNA turnover in high iron conditions.

I intend to conduct preliminary experiments to discover this RNA binding protein. One idea is to fuse *str3* (the most responsive iron transport mRNA) with a nutritional marker like *ura4* or *his5* to make a fusion mRNA. This strain should be $ura^-$ or $his^-$ on iron-rich medium but $ura^+$ $his^+$ on iron depleted medium. I can then screen for mutants that make them $ura^+$ or $his^+$. I also plan to test the motif that these mRNAs share. Mutating all copies of this motif in *str3* should make the *str3* RNA stable on iron-rich medium.

From yeast to mammals, iron metabolism is known to be posttranscriptionally regulated, so such a mechanism existing in *S. pombe* can be expected. Keeping transcription of genes responsive to nutrition deficiency on, but regulating the stability of their transcripts seems to be a key theme in *S. pombe.*

## 4.2 Chapter 3: Determining the RNAs bound to Mei2 during early meiosis

One key mechanism of meiosis initiation has long been unknown – how does Mei2 initiate meiosis? Although researches knew early on that Mei2-*meiRNA* did not tell the entire story, no studies were done to find out the other RNA partners of Mei2. I show in Chapter 3, that Mei2 binds probably in the 5' UTR of *rep2* and *mmi1* mRNA. I also have preliminary results showing that depleting either Rep2 or Mmi1, may allow the cells to initiate premeiotic DNA synthesis. However, due to lack of time and funding I was unable to complete this study in the course of my Ph.D. I plan to finish some key experiments to complete this study in the near future. The first would be to starve *mei2Δ rep2Δ* and *mei2Δ mmi1-ts3* mutant diploids for nitrogen and test if they are able to initiate meiosis. I already did a preliminary experiment (Figure 3.8) that indicated that this might be true. However, the critical test would be to test the nitrogen starved diploids using Flow Cytometry for initiation of DNA replication. Nitrogen starved *mei2Δ* cells arrest with 1N DNA content. If *rep2Δ* or *mmi1-ts3* mutations compensate for the loss of Mei2, then we expect that the *rep2Δ mei2Δ* and *rep2Δ mmi1-ts3* double mutants will accumulate 2N DNA (since they will be able to replicate their DNA). I also intend to overexpress *meiRNA* in the *rep2Δ mei2Δ* and *mmi1-ts3 mei2Δ* double mutants to test if they can sporulate.

I will also test for upregulation of early meiotic genes in *mei2Δ rep2Δ* and *mei2Δ mmi1-ts3* diploids starved for nitrogen. *mei2Δ* mutant is not expected to have early meiotic

gene expression. If depleting Rep2 or Mmi1 allows nitrogen-starved cells to initiate meiosis, I expect to see the early meiotic genes upregulated in *mei2Δ rep2Δ* and *mei2Δ mmi1-ts3* cells.

Interestingly, I found that Mei2 bound to the 5' UTR of *rep2* and *mmi1* RNA as determined by CLIP-Seq. This could be due to sequencing bias, but I did not see a strong 5' bias for all the mRNAs that were enriched. To test if Mei2 binding to the 5' UTR of *rep2* and *mmi1* is functionally significant, I intend to delete specifically the 5' UTR of these genes and test meiotic effects in the presence and absence of Mei2. I could also use western blot to test for levels of Rep2 and Mmi1 protein, with and without the 5' UTR after nitrogen starvation. For Mmi1, this will only be possible if the 5' UTR deletion is not lethal. Therefore I will delete the 5' UTR in a diploid first to test this.

The role of *mug110* remains a mystery. My studies show that it binds specifically to Mei2-TAP but not Msa1-TAP. One possibility is that its function is redundant with *meiRNA* and thus deleting *mug110* does not have any apparent effects. To test this hypothesis, I intend to make a *mug110Δ sme2Δ* double mutant. The *sme2Δ* mutant is able to form spores at a very low frequency (~1%, unpublished observations). I will test if deleting *mug110* in a *sme2Δ* mutant, results in an increase or decrease in sporulation efficiency.

Nevertheless, this study has answered a key long-standing question of how exactly Mei2 maybe initiating meiosis in *S. pombe.*

## 4.3 Perspective

Posttranscriptional gene regulation is critical for meiotic initiation in *S. pombe.* Meiosis is a form of sexual development in response to stress in *S. pombe*. There are many parallels with higher eukaryotes such as nematodes, insects and mammals. In these organisms posttranscriptional gene regulation is crucial for sexual development. A recently discovered novel class of small RNAs, called piRNAs (Piwi-interacting RNAs), regulates sexual development and sex determination in many higher eukaryotes [reviewed in (Kim, Han et al. 2009, Malone and Hannon 2009, Peng and Lin 2013, Watanabe and Lin 2014)]. piRNAs interact with Piwi proteins of the Argonaute family and silence gene expression from transposable elements in germline cells (Brennecke, Aravin et al. 2007, Gunawardane, Saito et al. 2007). piRNAs also regulate sex determination in silkworm (Kiuchi, Koga et al. 2014). These numerous studies show the importance of posttranscriptional gene regulation as a vital gene regulation mechanism.

Studying the molecular mechanisms driving meiosis in *S. pombe* lets us appreciate the fascinating interplay of two RNA binding proteins, Mmi1 and Mei2 in posttranscriptional gene regulation. RNA binding proteins are found in all organisms. A recent census estimates that humans may have approximately 1500 RNA binding proteins (Gerstberger, Hafner et al. 2014). Some RNA binding proteins, like FMRP (fragile-X mental retardation protein) are involved in neuronal diseases. Understanding the fundamental mechanisms of regulation by RNA binding proteins is a necessity to complete our understanding of all aspects of gene regulation. Recently, with the development of techniques like HITS-CLIP and PAR-CLIP, significant progress has been made in understanding some RNA binding proteins and their

targets (Licatalosi, Mele et al. 2008, Hafner, Landthaler et al. 2010). However, a lot of progress is required to fully understand the role of the 1542 RNA binding proteins in humans, as well as those in other organisms.

# BIBLIOGRAPHY

Allmang, C., J. Kufel, G. Chanfreau, P. Mitchell, E. Petfalski and D. Tollervey (1999). "Functions of the exosome in rRNA, snoRNA and snRNA synthesis." EMBO J **18**(19): 5399-5410.
Allmang, C., P. Mitchell, E. Petfalski and D. Tollervey (2000). "Degradation of ribosomal RNA precursors by the exosome." Nucleic Acids Res **28**(8): 1684-1691.
Allmang, C., E. Petfalski, A. Podtelejnikov, M. Mann, D. Tollervey and P. Mitchell (1999). "The yeast exosome and human PM-Scl are related complexes of 3' --> 5' exonucleases." Genes Dev **13**(16): 2148-2158.
Amorim, M. J., C. Cotobal, C. Duncan and J. Mata (2010). "Global coordination of transcriptional control and mRNA decay during cellular differentiation." Mol Syst Biol **6**: 380.
Anderson, J. S. and R. P. Parker (1998). "The 3' to 5' degradation of yeast mRNAs is a general mechanism for mRNA turnover that requires the SKI2 DEVH box protein and 3' to 5' exonucleases of the exosome complex." EMBO J **17**(5): 1497-1506.
Arnold, K., L. Bordoli, J. Kopp and T. Schwede (2006). "The SWISS-MODEL workspace: a web-based environment for protein structure homology modelling." Bioinformatics **22**(2): 195-201.
Asakawa, H., T. Haraguchi and Y. Hiraoka (2007). "Reconstruction of the kinetochore: a prelude to meiosis." Cell Div **2**: 17.
Ashburner, M., C. A. Ball, J. A. Blake, D. Botstein, H. Butler, J. M. Cherry, A. P. Davis, K. Dolinski, S. S. Dwight, J. T. Eppig, M. A. Harris, D. P. Hill, L. Issel-Tarver, A. Kasarskis, S. Lewis, J. C. Matese, J. E. Richardson, M. Ringwald, G. M. Rubin and G. Sherlock (2000). "Gene ontology: tool for the unification of biology. The Gene Ontology Consortium." Nat Genet **25**(1): 25-29.
Askwith, C. and J. Kaplan (1997). "An oxidase-permease-based iron transport system in Schizosaccharomyces pombe and its expression in Saccharomyces cerevisiae." J Biol Chem **272**(1): 401-405.
Averbeck, N., S. Sunder, N. Sample, J. A. Wise and J. Leatherwood (2005). "Negative control contributes to an extensive program of meiotic splicing in fission yeast." Mol Cell **18**(4): 491-498.
Aves, S. J., B. W. Durkacz, A. Carr and P. Nurse (1985). "Cloning, sequencing and transcriptional control of the Schizosaccharomyces pombe cdc10 'start' gene." EMBO J **4**(2): 457-463.
Bahler, J., J. Q. Wu, M. S. Longtine, N. G. Shah, A. McKenzie, 3rd, A. B. Steever, A. Wach, P. Philippsen and J. R. Pringle (1998). "Heterologous modules for efficient and versatile PCR-based gene targeting in Schizosaccharomyces pombe." Yeast **14**(10): 943-951.
Beach, D., L. Rodgers and J. Gould (1985). "ran1+ controls the transition from mitotic division to meiosis in fission yeast." Curr Genet **10**(4): 297-311.
Brennecke, J., A. A. Aravin, A. Stark, M. Dus, M. Kellis, R. Sachidanandam and G. J. Hannon (2007). "Discrete small RNA-generating loci as master regulators of transposon activity in Drosophila." Cell **128**(6): 1089-1103.
Bresch, C., G. Muller and R. Egel (1968). "Genes involved in meiosis and sporulation of a yeast." Mol Gen Genet **102**(4): 301-306.

Briggs, M. W., K. T. Burkard and J. S. Butler (1998). "Rrp6p, the yeast homologue of the human PM-Scl 100-kDa autoantigen, is essential for efficient 5.8 S rRNA 3' end formation." J Biol Chem **273**(21): 13255-13263.
Calleja, G. B., B. F. Johnson and B. Y. Yoo (1980). "Macromolecular changes and commitment to sporulation in the fission yeast Schizosaccharomyces pombe." Plant and Cell Physiology **21**(4 %U http://pcp.oxfordjournals.org/content/21/4/613.abstract): 613-625.
Chen, H. M., B. Futcher and J. Leatherwood (2011). "The fission yeast RNA binding protein Mmi1 regulates meiotic genes by controlling intron specific splicing and polyadenylation coupled RNA turnover." PLoS One **6**(10): e26804.
Chlebowski, A., M. Lubas, T. H. Jensen and A. Dziembowski (2013). "RNA decay machines: the exosome." Biochim Biophys Acta **1829**(6-7): 552-560.
Chlebowski, A., R. Tomecki, M. E. Lopez, B. Seraphin and A. Dziembowski (2010). "Catalytic properties of the eukaryotic exosome." Adv Exp Med Biol **702**: 63-78.
Ciais, D., M. T. Bohnsack and D. Tollervey (2008). "The mRNA encoding the yeast ARE-binding protein Cth2 is generated by a novel 3' processing pathway." Nucleic Acids Res **36**(9): 3075-3084.
de Hoon, M. J., S. Imoto, J. Nolan and S. Miyano (2004). "Open source clustering software." Bioinformatics **20**(9): 1453-1454.
Ding, R. and G. R. Smith (1998). "Global control of meiotic recombination genes by Schizosaccharomyces pombe rec16 (rep1)." Mol Gen Genet **258**(6): 663-670.
Dobin, A., C. A. Davis, F. Schlesinger, J. Drenkow, C. Zaleski, S. Jha, P. Batut, M. Chaisson and T. R. Gingeras (2013). "STAR: ultrafast universal RNA-seq aligner." Bioinformatics **29**(1): 15-21.
Dziembowski, A., E. Lorentzen, E. Conti and B. Seraphin (2007). "A single subunit, Dis3, is essentially responsible for yeast exosome core activity." Nat Struct Mol Biol **14**(1): 15-22.
Egan, E. D., C. R. Braun, S. P. Gygi and D. Moazed (2014). "Post-transcriptional regulation of meiotic genes by a nuclear RNA silencing complex." RNA **20**(6): 867-881.
Forsburg, S. L. and N. Rhind (2006). "Basic methods for fission yeast." Yeast **23**(3): 173-183.
Gerber, A. P., D. Herschlag and P. O. Brown (2004). "Extensive association of functionally and cytotopically related mRNAs with Puf family RNA-binding proteins in yeast." PLoS Biol **2**(3): E79.
Gerstberger, S., M. Hafner and T. Tuschl (2014). "A census of human RNA-binding proteins." Nat Rev Genet **15**(12): 829-845.
Gotoh, Y., E. Nishida, M. Shimanuki, T. Toda, Y. Imai and M. Yamamoto (1993). "Schizosaccharomyces pombe Spk1 is a tyrosine-phosphorylated protein functionally related to Xenopus mitogen-activated protein kinase." Mol Cell Biol **13**(10): 6427-6434.
Granneman, S., G. Kudla, E. Petfalski and D. Tollervey (2009). "Identification of protein binding sites on U3 snoRNA and pre-rRNA by UV cross-linking and high-throughput analysis of cDNAs." Proc Natl Acad Sci U S A **106**(24): 9613-9618.

Gunawardane, L. S., K. Saito, K. M. Nishida, K. Miyoshi, Y. Kawamura, T. Nagami, H. Siomi and M. C. Siomi (2007). "A slicer-mediated mechanism for repeat-associated siRNA 5' end formation in Drosophila." Science **315**(5818): 1587-1590.
Hafner, M., M. Landthaler, L. Burger, M. Khorshid, J. Hausser, P. Berninger, A. Rothballer, M. Ascano, Jr., A. C. Jungkamp, M. Munschauer, A. Ulrich, G. S. Wardle, S. Dewell, M. Zavolan and T. Tuschl (2010). "Transcriptome-wide identification of RNA-binding protein and microRNA target sites by PAR-CLIP." Cell **141**(1): 129-141.
Harigaya, Y., H. Tanaka, S. Yamanaka, K. Tanaka, Y. Watanabe, C. Tsutsumi, Y. Chikashige, Y. Hiraoka, A. Yamashita and M. Yamamoto (2006). "Selective elimination of messenger RNA prevents an incidence of untimely meiosis." Nature **442**(7098): 45-50.
Harigaya, Y. and M. Yamamoto (2007). "Molecular mechanisms underlying the mitosis-meiosis decision." Chromosome Res **15**(5): 523-537.
Hentze, M. W., S. W. Caughman, T. A. Rouault, J. G. Barriocanal, A. Dancis, J. B. Harford and R. D. Klausner (1987). "Identification of the iron-responsive element for the translational regulation of human ferritin mRNA." Science **238**(4833): 1570-1573.
Hentze, M. W., T. A. Rouault, J. B. Harford and R. D. Klausner (1989). "Oxidation-reduction and the molecular mechanism of a regulatory RNA-protein interaction." Science **244**(4902): 357-359.
Hiriart, E., A. Vavasseur, L. Touat-Todeschini, A. Yamashita, B. Gilquin, E. Lambert, J. Perot, Y. Shichino, N. Nazaret, C. Boyault, J. Lachuer, D. Perazza, M. Yamamoto and A. Verdel (2012). "Mmi1 RNA surveillance machinery directs RNAi complex RITS to specific meiotic genes in fission yeast." EMBO J.
Horie, S., Y. Watanabe, K. Tanaka, S. Nishiwaki, H. Fujioka, H. Abe, M. Yamamoto and C. Shimoda (1998). "The Schizosaccharomyces pombe mei4+ gene encodes a meiosis-specific transcription factor containing a forkhead DNA-binding domain." Mol Cell Biol **18**(4): 2118-2129.
Iino, Y. and M. Yamamoto (1985). "Negative control for the initiation of meiosis in Schizosaccharomyces pombe." Proc Natl Acad Sci U S A **82**(8): 2447-2451.
Kelly, M., J. Burke, M. Smith, A. Klar and D. Beach (1988). "Four mating-type genes control sexual differentiation in the fission yeast." EMBO J **7**(5): 1537-1547.
Kim, D., G. Pertea, C. Trapnell, H. Pimentel, R. Kelley and S. L. Salzberg (2013). "TopHat2: accurate alignment of transcriptomes in the presence of insertions, deletions and gene fusions." Genome Biol **14**(4): R36.
Kim, V. N., J. Han and M. C. Siomi (2009). "Biogenesis of small RNAs in animals." Nat Rev Mol Cell Biol **10**(2): 126-139.
Kinoshita, N., M. Goebl and M. Yanagida (1991). "The fission yeast dis3+ gene encodes a 110-kDa essential protein implicated in mitotic control." Mol Cell Biol **11**(12): 5839-5847.
Kiss, D. L. and E. D. Andrulis (2010). "Genome-wide analysis reveals distinct substrate specificities of Rrp6, Dis3, and core exosome subunits." RNA **16**(4): 781-791.
Kitamura, K., S. Katayama, S. Dhut, M. Sato, Y. Watanabe, M. Yamamoto and T. Toda (2001). "Phosphorylation of Mei2 and Ste11 by Pat1 kinase inhibits sexual

differentiation via ubiquitin proteolysis and 14-3-3 protein in fission yeast." Dev Cell **1**(3): 389-399.
Kitamura, K., T. Nakagawa and C. Shimoda (1990). "Novel sterile mutants of the fission yeast Schizosaccharomyces pombe which are defective in their response to starvation." Current Genetics **18**(4): 315-321.
Kiuchi, T., H. Koga, M. Kawamoto, K. Shoji, H. Sakai, Y. Arai, G. Ishihara, S. Kawaoka, S. Sugano, T. Shimada, Y. Suzuki, M. G. Suzuki and S. Katsuma (2014). "A single female-specific piRNA is the primary determiner of sex in the silkworm." Nature **509**(7502): 633-636.
Kjaerulff, S., I. Lautrup-Larsen, S. Truelsen, M. Pedersen and O. Nielsen (2005). "Constitutive activation of the fission yeast pheromone-responsive pathway induces ectopic meiosis and reveals ste11 as a mitogen-activated protein kinase target." Mol Cell Biol **25**(5): 2045-2059.
Li, H., B. Handsaker, A. Wysoker, T. Fennell, J. Ruan, N. Homer, G. Marth, G. Abecasis, R. Durbin and S. Genome Project Data Processing (2009). "The Sequence Alignment/Map format and SAMtools." Bioinformatics **25**(16): 2078-2079.
Li, P. and M. McLeod (1996). "Molecular mimicry in development: identification of ste11+ as a substrate and mei3+ as a pseudosubstrate inhibitor of ran1+ kinase." Cell **87**(5): 869-880.
Licatalosi, D. D., A. Mele, J. J. Fak, J. Ule, M. Kayikci, S. W. Chi, T. A. Clark, A. C. Schweitzer, J. E. Blume, X. Wang, J. C. Darnell and R. B. Darnell (2008). "HITS-CLIP yields genome-wide insights into brain alternative RNA processing." Nature **456**(7221): 464-469.
Lino, Y. and M. Yamamoto (1985). "Mutants of Schizosaccharomyces pombe which sporulate in the haploid state." Mol Gen Genet **198**(3): 416-421.
Liu, Q., J. C. Greimann and C. D. Lima (2006). "Reconstitution, activities, and structure of the eukaryotic RNA exosome." Cell **127**(6): 1223-1237.
Lykke-Andersen, S., D. E. Brodersen and T. H. Jensen (2009). "Origins and activities of the eukaryotic exosome." J Cell Sci **122**(Pt 10): 1487-1494.
Makino, D. L., M. Baumgartner and E. Conti (2013). "Crystal structure of an RNA-bound 11-subunit eukaryotic exosome complex." Nature **495**(7439): 70-75.
Makino, D. L., B. Schuch, E. Stegmann, M. Baumgartner, C. Basquin and E. Conti (2015). "RNA degradation paths in a 12-subunit nuclear exosome complex." Nature **524**(7563): 54-58.
Malone, C. D. and G. J. Hannon (2009). "Small RNAs as guardians of the genome." Cell **136**(4): 656-668.
Martin-Castellanos, C., M. Blanco, A. E. Rozalen, L. Perez-Hidalgo, A. I. Garcia, F. Conde, J. Mata, C. Ellermeier, L. Davis, P. San-Segundo, G. R. Smith and S. Moreno (2005). "A large-scale screen in S. pombe identifies seven novel genes required for critical meiotic events." Curr Biol **15**(22): 2056-2062.
Martinez-Pastor, M., S. V. Vergara, S. Puig and D. J. Thiele (2013). "Negative feedback regulation of the yeast CTH1 and CTH2 mRNA binding proteins is required for adaptation to iron deficiency and iron supplementation." Mol Cell Biol **33**(11): 2178-2187.

Mata, J. and J. Bahler (2006). "Global roles of Ste11p, cell type, and pheromone in the control of gene expression during early sexual differentiation in fission yeast." Proc Natl Acad Sci U S A **103**(42): 15517-15522.
Mata, J., R. Lyne, G. Burns and J. Bahler (2002). "The transcriptional program of meiosis and sporulation in fission yeast." Nat Genet **32**(1): 143-147.
Matsuyama, A., R. Arai, Y. Yashiroda, A. Shirai, A. Kamata, S. Sekido, Y. Kobayashi, A. Hashimoto, M. Hamamoto, Y. Hiraoka, S. Horinouchi and M. Yoshida (2006). "ORFeome cloning and global analysis of protein localization in the fission yeast Schizosaccharomyces pombe." Nat Biotechnol **24**(7): 841-847.
McLeod, M. and D. Beach (1986). "Homology between the ran1+ gene of fission yeast and protein kinases." EMBO J **5**(13): 3665-3671.
McLeod, M. and D. Beach (1988). "A specific inhibitor of the ran1+ protein kinase regulates entry into meiosis in Schizosaccharomyces pombe." Nature **332**(6164): 509-514.
McLeod, M., M. Stein and D. Beach (1987). "The product of the mei3+ gene, expressed under control of the mating-type locus, induces meiosis and sporulation in fission yeast." EMBO J **6**(3): 729-736.
McPheeters, D. S., N. Cremona, S. Sunder, H. M. Chen, N. Averbeck, J. Leatherwood and J. A. Wise (2009). "A complex gene regulatory mechanism that operates at the nexus of multiple RNA processing decisions." Nat Struct Mol Biol **16**(3): 255-264.
Mercier, A., B. Pelletier and S. Labbe (2006). "A transcription factor cascade involving Fep1 and the CCAAT-binding factor Php4 regulates gene expression in response to iron deficiency in the fission yeast Schizosaccharomyces pombe." Eukaryot Cell **5**(11): 1866-1881.
Mitchell, P., E. Petfalski, A. Shevchenko, M. Mann and D. Tollervey (1997). "The exosome: a conserved eukaryotic RNA processing complex containing multiple 3'-->5' exoribonucleases." Cell **91**(4): 457-466.
Miyamoto, M., K. Tanaka and H. Okayama (1994). "res2+, a new member of the cdc10+/SWI4 family, controls the 'start' of mitotic and meiotic cycles in fission yeast." EMBO J **13**(8): 1873-1880.
Mochizuki, N. and M. Yamamoto (1992). "Reduction in the intracellular cAMP level triggers initiation of sexual development in fission yeast." Mol Gen Genet **233**(1-2): 17-24.
Mudge, D. K., C. A. Hoffman, T. J. Lubinski and C. S. Hoffman (2012). "Use of a ura5+-lys7+ cassette to construct unmarked gene knock-ins in Schizosaccharomyces pombe." Curr Genet **58**(1): 59-64.
Nakashima, N., K. Tanaka, S. Sturm and H. Okayama (1995). "Fission yeast Rep2 is a putative transcriptional activator subunit for the cell cycle 'start' function of Res2-Cdc10." EMBO J **14**(19): 4794-4802.
Neiman, A. M., B. J. Stevenson, H. P. Xu, G. F. Sprague, Jr., I. Herskowitz, M. Wigler and S. Marcus (1993). "Functional homology of protein kinases required for sexual differentiation in Schizosaccharomyces pombe and Saccharomyces cerevisiae suggests

a conserved signal transduction module in eukaryotic organisms." Mol Biol Cell **4**(1): 107-120.
Nurse, P. (1985). "Mutants of the fission yeast Schizosaccharomyces pombe which alter the shift between cell proliferation and sporulation." Molecular and General Genetics MGG **198**(3): 497-502.
Obara, T., M. Nakafuku, M. Yamamoto and Y. Kaziro (1991). "Isolation and characterization of a gene encoding a G-protein alpha subunit from Schizosaccharomyces pombe: involvement in mating and sporulation pathways." Proc Natl Acad Sci U S A **88**(13): 5877-5881.
Pelletier, B., J. Beaudoin, C. C. Philpott and S. Labbe (2003). "Fep1 represses expression of the fission yeast Schizosaccharomyces pombe siderophore-iron transport system." Nucleic Acids Res **31**(15): 4332-4344.
Peng, J. C. and H. Lin (2013). "Beyond transposons: the epigenetic and somatic functions of the Piwi-piRNA mechanism." Curr Opin Cell Biol **25**(2): 190-194.
Phillips, S. and J. S. Butler (2003). "Contribution of domain structure to the RNA 3' end processing and degradation functions of the nuclear exosome subunit Rrp6p." RNA **9**(9): 1098-1107.
Puig, S., E. Askeland and D. J. Thiele (2005). "Coordinated remodeling of cellular metabolism during iron deficiency through targeted mRNA degradation." Cell **120**(1): 99-110.
Puig, S., S. V. Vergara and D. J. Thiele (2008). "Cooperation of two mRNA-binding proteins drives metabolic adaptation to iron deficiency." Cell Metab **7**(6): 555-564.
Robinson, J. T., H. Thorvaldsdottir, W. Winckler, M. Guttman, E. S. Lander, G. Getz and J. P. Mesirov (2011). "Integrative genomics viewer." Nat Biotechnol **29**(1): 24-26.
Roman, D. G., A. Dancis, G. J. Anderson and R. D. Klausner (1993). "The fission yeast ferric reductase gene frp1+ is required for ferric iron uptake and encodes a protein that is homologous to the gp91-phox subunit of the human NADPH phagocyte oxidoreductase." Mol Cell Biol **13**(7): 4342-4350.
Rouault, T. A., M. W. Hentze, S. W. Caughman, J. B. Harford and R. D. Klausner (1988). "Binding of a cytosolic protein to the iron-responsive element of human ferritin messenger RNA." Science **241**(4870): 1207-1210.
Saito, T. T., T. Tougan, D. Okuzaki, T. Kasama and H. Nojima (2005). "Mcp6, a meiosis-specific coiled-coil protein of Schizosaccharomyces pombe, localizes to the spindle pole body and is required for horsetail movement and recombination." J Cell Sci **118**(Pt 2): 447-459.
Saldanha, A. J. (2004). "Java Treeview--extensible visualization of microarray data." Bioinformatics **20**(17): 3246-3248.
Sato, M., S. Shinozaki-Yabana, A. Yamashita, Y. Watanabe and M. Yamamoto (2001). "The fission yeast meiotic regulator Mei2p undergoes nucleocytoplasmic shuttling." FEBS Lett **499**(3): 251-255.
Sato, M., Y. Watanabe, Y. Akiyoshi and M. Yamamoto (2002). "14-3-3 protein interferes with the binding of RNA to the phosphorylated form of fission yeast meiotic regulator Mei2p." Curr Biol **12**(2): 141-145.

Schmid, M. and T. H. Jensen (2008). "The exosome: a multipurpose RNA-decay machine." Trends Biochem Sci **33**(10): 501-510.
Segalla, S., S. Pivetti, K. Todoerti, M. A. Chudzik, E. C. Giuliani, F. Lazzaro, V. Volta, D. Lazarevic, G. Musco, M. Muzi-Falconi, A. Neri, S. Biffo and G. Tonon (2015). "The ribonuclease DIS3 promotes let-7 miRNA maturation by degrading the pluripotency factor LIN28B mRNA." Nucleic Acids Res **43**(10): 5182-5193.
Selth, L. A., C. Gilbert and J. Q. Svejstrup (2009). "RNA immunoprecipitation to determine RNA-protein associations in vivo." Cold Spring Harb Protoc **2009**(6): pdb prot5234.
Shichino, Y., A. Yamashita and M. Yamamoto (2014). "Meiotic long non-coding meiRNA accumulates as a dot at its genetic locus facilitated by Mmi1 and plays as a decoy to lure Mmi1." Open Biol **4**(6): 140022.
Shimada, T., A. Yamashita and M. Yamamoto (2003). "The fission yeast meiotic regulator Mei2p forms a dot structure in the horse-tail nucleus in association with the sme2 locus on chromosome II." Mol Biol Cell **14**(6): 2461-2469.
Shimoda, C., A. Hirata, M. Kishida, T. Hashida and K. Tanaka (1985). "Characterization of meiosis-deficient mutants by electron microscopy and mapping of four essential genes in the fission yeast Schizosaccharomyces pombe." Mol Gen Genet **200**(2): 252-257.
Shimoda, C., M. Uehira, M. Kishida, H. Fujioka, Y. Iino, Y. Watanabe and M. Yamamoto (1987). "Cloning and analysis of transcription of the mei2 gene responsible for initiation of meiosis in the fission yeast Schizosaccharomyces pombe." J Bacteriol **169**(1): 93-96.
Sinclair, A. H., P. Berta, M. S. Palmer, J. R. Hawkins, B. L. Griffiths, M. J. Smith, J. W. Foster, A. M. Frischauf, R. Lovell-Badge and P. N. Goodfellow (1990). "A gene from the human sex-determining region encodes a protein with homology to a conserved DNA-binding motif." Nature **346**(6281): 240-244.
Sipiczki, M. (1988). "The role of sterility genes (ste and aff) in the initiation of sexual development in Schizosaccharomyces pombe." Mol Gen Genet **213**(2-3): 529-534.
St-Andre, O., C. Lemieux, A. Perreault, D. H. Lackner, J. Bahler and F. Bachand (2010). "Negative regulation of meiotic gene expression by the nuclear poly(a)-binding protein in fission yeast." J Biol Chem **285**(36): 27859-27868.
Sugimoto, A., Y. Iino, T. Maeda, Y. Watanabe and M. Yamamoto (1991). "Schizosaccharomyces pombe ste11+ encodes a transcription factor with an HMG motif that is a critical regulator of sexual development." Genes Dev **5**(11): 1990-1999.
Sugiyama, A., K. Tanaka, K. Okazaki, H. Nojima and H. Okayama (1994). "A zinc finger protein controls the onset of premeiotic DNA synthesis of fission yeast in a Mei2-independent cascade." EMBO J **13**(8): 1881-1887.
Sugiyama, T. and R. Sugioka-Sugiyama (2011). "Red1 promotes the elimination of meiosis-specific mRNAs in vegetatively growing fission yeast." EMBO J **30**(6): 1027-1039.
Sugiyama, T., R. Sugioka-Sugiyama, K. Hada and R. Niwa (2012). "Rhn1, a nuclear protein, is required for suppression of meiotic mRNAs in mitotically dividing fission yeast." PLoS One **7**(8): e42962.

Tanaka, K., K. Okazaki, N. Okazaki, T. Ueda, A. Sugiyama, H. Nojima and H. Okayama (1992). "A new cdc gene required for S phase entry of Schizosaccharomyces pombe encodes a protein similar to the cdc 10+ and SWI4 gene products." EMBO J **11**(13): 4923-4932.
Tashiro, S., T. Asano, J. Kanoh and F. Ishikawa (2013). "Transcription-induced chromatin association of RNA surveillance factors mediates facultative heterochromatin formation in fission yeast." Genes Cells **18**(4): 327-339.
Thompson, J. D., T. J. Gibson and D. G. Higgins (2002). "Multiple sequence alignment using ClustalW and ClustalX." Curr Protoc Bioinformatics **Chapter 2**: Unit 2 3.
Thorvaldsdottir, H., J. T. Robinson and J. P. Mesirov (2013). "Integrative Genomics Viewer (IGV): high-performance genomics data visualization and exploration." Brief Bioinform **14**(2): 178-192.
Tomecki, R., K. Drazkowska, I. Kucinski, K. Stodus, R. J. Szczesny, J. Gruchota, E. P. Owczarek, K. Kalisiak and A. Dziembowski (2014). "Multiple myeloma-associated hDIS3 mutations cause perturbations in cellular RNA metabolism and suggest hDIS3 PIN domain as a potential drug target." Nucleic Acids Res **42**(2): 1270-1290.
Trapnell, C., D. G. Hendrickson, M. Sauvageau, L. Goff, J. L. Rinn and L. Pachter (2013). "Differential analysis of gene regulation at transcript resolution with RNA-seq." Nat Biotechnol **31**(1): 46-53.
Trapnell, C., A. Roberts, L. Goff, G. Pertea, D. Kim, D. R. Kelley, H. Pimentel, S. L. Salzberg, J. L. Rinn and L. Pachter (2012). "Differential gene and transcript expression analysis of RNA-seq experiments with TopHat and Cufflinks." Nat Protoc **7**(3): 562-578.
Van Heeckeren, W. J., D. R. Dorris and K. Struhl (1998). "The mating-type proteins of fission yeast induce meiosis by directly activating mei3 transcription." Mol Cell Biol **18**(12): 7317-7326.
Wasmuth, E. V., K. Januszyk and C. D. Lima (2014). "Structure of an Rrp6-RNA exosome complex bound to poly(A) RNA." Nature **511**(7510): 435-439.
Wasmuth, E. V. and C. D. Lima (2012). "Exo- and endoribonucleolytic activities of yeast cytoplasmic and nuclear RNA exosomes are dependent on the noncatalytic core and central channel." Mol Cell **48**(1): 133-144.
Watanabe, T. and H. Lin (2014). "Posttranscriptional regulation of gene expression by Piwi proteins and piRNAs." Mol Cell **56**(1): 18-27.
Watanabe, Y., Y. Lino, K. Furuhata, C. Shimoda and M. Yamamoto (1988). "The S.pombe mei2 gene encoding a crucial molecule for commitment to meiosis is under the regulation of cAMP." EMBO J **7**(3): 761-767.
Watanabe, Y., S. Shinozaki-Yabana, Y. Chikashige, Y. Hiraoka and M. Yamamoto (1997). "Phosphorylation of RNA-binding protein controls cell cycle switch from mitotic to meiotic in fission yeast." Nature **386**(6621): 187-190.
Watanabe, Y. and M. Yamamoto (1994). "S. pombe mei2+ encodes an RNA-binding protein essential for premeiotic DNA synthesis and meiosis I, which cooperates with a novel RNA species meiRNA." Cell **78**(3): 487-498.

Waterhouse, A. M., J. B. Procter, D. M. Martin, M. Clamp and G. J. Barton (2009). "Jalview Version 2--a multiple sequence alignment editor and analysis workbench." Bioinformatics **25**(9): 1189-1191.
Weissbach, S., C. Langer, B. Puppe, T. Nedeva, E. Bach, M. Kull, R. Bargou, H. Einsele, A. Rosenwald, S. Knop and E. Leich (2015). "The molecular spectrum and clinical impact of DIS3 mutations in multiple myeloma." Br J Haematol **169**(1): 57-70.
Willer, M., L. Hoffmann, U. Styrkarsdottir, R. Egel, J. Davey and O. Nielsen (1995). "Two-step activation of meiosis by the mat1 locus in Schizosaccharomyces pombe." Mol Cell Biol **15**(9): 4964-4970.
Yamamoto, M. (1996). "Regulation of meiosis in fission yeast." Cell Struct Funct **21**(5): 431-436.
Yamanaka, S., A. Yamashita, Y. Harigaya, R. Iwata and M. Yamamoto (2010). "Importance of polyadenylation in the selective elimination of meiotic mRNAs in growing S. pombe cells." EMBO J **29**(13): 2173-2181.
Yamashita, A., Y. Shichino, H. Tanaka, E. Hiriart, L. Touat-Todeschini, A. Vavasseur, D. Q. Ding, Y. Hiraoka, A. Verdel and M. Yamamoto (2012). "Hexanucleotide motifs mediate recruitment of the RNA elimination machinery to silent meiotic genes." Open Biol **2**(3): 120014.
Yamashita, A., T. Takayama, R. Iwata and M. Yamamoto (2013). "A novel factor Iss10 regulates Mmi1-mediated selective elimination of meiotic transcripts." Nucleic Acids Res **41**(21): 9680-9687.
Yamashita, A., Y. Watanabe, N. Nukina and M. Yamamoto (1998). "RNA-assisted nuclear transport of the meiotic regulator Mei2p in fission yeast." Cell **95**(1): 115-123.
Yu, G., J. Li and D. Young (1994). "The Schizosaccharomyces pombe pka1 gene, encoding a homolog of cAMP-dependent protein kinase." Gene **151**(1-2): 215-220.
Zhu, Y., T. Takeda, K. Nasmyth and N. Jones (1994). "pct1+, which encodes a new DNA-binding partner of p85cdc10, is required for meiosis in the fission yeast Schizosaccharomyces pombe." Genes Dev **8**(8): 885-898.
Zofall, M., S. Yamanaka, F. E. Reyes-Turcu, K. Zhang, C. Rubin and S. I. Grewal (2012). "RNA elimination machinery targeting meiotic mRNAs promotes facultative heterochromatin formation." Science **335**(6064): 96-100.

# APPENDIX

## Table 1. Rrp6 mRNA Targets

| Systematic ID | WT fpkm | rrp6-del fpkm | rrp6-cat fpkm | dis3-4 30C fpkm | rrp6-cat dis3-4 30C fpkm | del/wt ratio | cat/del ratio |
|---|---|---|---|---|---|---|---|
| SPBC29A10.02 | 4.71 | 627.87 | 15.90 | 25.84 | 15.28 | 133.42 | 0.03 |
| SPAC1F8.02c | 1.00 | 110.07 | 3.11 | 0.00 | 25.36 | 110.07 | 0.03 |
| SPBC29A10.14 | 6.59 | 388.15 | 13.16 | 18.27 | 17.71 | 58.92 | 0.03 |
| SPAC13A11.03 | 13.19 | 481.92 | 41.02 | 36.28 | 44.01 | 36.55 | 0.09 |
| SPAC57A10.04 | 8.29 | 283.47 | 41.71 | 53.38 | 41.22 | 34.18 | 0.15 |
| SPBC32H8.11 | 6.77 | 205.17 | 30.32 | 119.14 | 90.85 | 30.29 | 0.15 |
| SPAC922.09 | 1.00 | 28.05 | 9.39 | 8.20 | 24.67 | 28.05 | 0.33 |
| SPAC1F8.03c | 3.76 | 84.14 | 7.66 | 0.99 | 31.74 | 22.38 | 0.09 |
| SPAC23D3.10c | 28.69 | 547.10 | 42.19 | 29.83 | 31.02 | 19.07 | 0.08 |
| SPBC1347.12 | 4.98 | 94.82 | 11.79 | 19.43 | 24.38 | 19.06 | 0.12 |
| SPAC32A11.01 | 18.43 | 349.93 | 37.14 | 74.25 | 58.18 | 18.98 | 0.11 |
| SPCC965.07c | 23.70 | 399.96 | 170.11 | 69.20 | 275.79 | 16.88 | 0.43 |
| SPAC29E6.07 | 1.00 | 15.87 | 12.34 | 5.05 | 15.48 | 15.87 | 0.78 |
| SPBC646.17c | 4.64 | 67.51 | 16.27 | 39.39 | 33.80 | 14.54 | 0.24 |
| SPAC1F7.08 | 3.02 | 40.04 | 6.79 | 2.95 | 15.84 | 13.25 | 0.17 |
| SPBC2D10.06 | 5.99 | 77.00 | 20.76 | 39.27 | 33.09 | 12.86 | 0.27 |
| SPBC1683.09c | 10.32 | 130.03 | 24.55 | 11.52 | 26.02 | 12.60 | 0.19 |
| SPAC343.20 | 40.99 | 437.33 | 123.34 | 197.31 | 276.60 | 10.67 | 0.28 |
| SPAC27D7.13c | 8.75 | 88.69 | 18.40 | 32.30 | 44.47 | 10.14 | 0.21 |
| SPBC1711.15c | 20.87 | 210.11 | 79.36 | 209.98 | 272.27 | 10.07 | 0.38 |
| SPBC1D7.01 | 9.79 | 94.47 | 26.28 | 56.56 | 34.04 | 9.65 | 0.28 |
| SPAC23C4.07 | 8.76 | 84.14 | 33.81 | 46.45 | 57.07 | 9.61 | 0.40 |
| SPBC23G7.10c | 14.14 | 130.07 | 78.69 | 41.27 | 8.45 | 9.20 | 0.60 |
| SPAC22H10.13 | 64.67 | 587.08 | 172.54 | 19.16 | 139.30 | 9.08 | 0.29 |
| SPBC16A3.13 | 13.27 | 101.11 | 10.05 | 11.96 | 19.19 | 7.62 | 0.10 |
| SPBPB21E7.04c | 5.32 | 39.69 | 8.27 | 1.22 | 11.81 | 7.46 | 0.21 |
| SPAC1556.06 | 12.66 | 91.64 | 17.62 | 45.16 | 27.08 | 7.24 | 0.19 |
| SPBP26C9.03c | 5.04 | 34.94 | 9.84 | 11.13 | 17.24 | 6.93 | 0.28 |
| SPCC1393.07c | 7.29 | 46.30 | 12.34 | 18.08 | 12.49 | 6.35 | 0.27 |
| SPBC215.11c | 31.02 | 195.29 | 147.65 | 39.82 | 217.86 | 6.30 | 0.76 |
| SPBC725.15 | 60.85 | 380.05 | 85.09 | 133.63 | 72.24 | 6.25 | 0.22 |
| SPCC663.06c | 6.56 | 40.79 | 14.73 | 14.28 | 42.17 | 6.22 | 0.36 |
| SPAC23H3.02c | 29.79 | 179.94 | 127.90 | 122.38 | 146.63 | 6.04 | 0.71 |
| SPAC16E8.16 | 24.27 | 146.31 | 95.97 | 145.80 | 203.91 | 6.03 | 0.66 |

| | | | | | | | |
|---|---|---|---|---|---|---|---|
| SPBC106.02c | 27.72 | 166.09 | 52.81 | 21.93 | 73.98 | 5.99 | 0.32 |
| SPBC1773.06c | 10.80 | 62.40 | 21.03 | 32.12 | 29.37 | 5.78 | 0.34 |
| SPAP27G11.08c | 9.32 | 50.92 | 15.19 | 27.25 | 37.33 | 5.47 | 0.30 |
| SPAC6G10.03c | 15.26 | 80.54 | 33.72 | 17.33 | 64.01 | 5.28 | 0.42 |
| SPAC17A5.04c | 20.54 | 108.01 | 24.15 | 33.29 | 30.38 | 5.26 | 0.22 |
| SPAC27D7.09c | 121.23 | 542.66 | 452.34 | 117.49 | 280.88 | 4.48 | 0.83 |
| SPAC5D6.08c | 21.04 | 92.45 | 19.38 | 21.40 | 15.78 | 4.39 | 0.21 |
| SPAC19G12.07c | 25.85 | 112.91 | 48.84 | 94.70 | 95.14 | 4.37 | 0.43 |
| SPAP8A3.04c | 769.21 | 3207.59 | 978.67 | 1104.80 | 1716.25 | 4.17 | 0.31 |
| SPBC947.05c | 5.21 | 21.32 | 9.51 | 8.91 | 10.15 | 4.09 | 0.45 |
| SPBC16C6.14 | 24.81 | 100.50 | 25.81 | 19.93 | 26.97 | 4.05 | 0.26 |
| SPBC4F6.09 | 31.57 | 125.26 | 38.89 | 16.08 | 36.87 | 3.97 | 0.31 |
| SPAC17A5.18c | 15.95 | 62.49 | 29.53 | 63.31 | 54.12 | 3.92 | 0.47 |
| SPCC338.12 | 53.60 | 208.34 | 86.80 | 77.96 | 89.20 | 3.89 | 0.42 |
| SPAC1250.05 | 154.45 | 576.99 | 431.09 | 548.64 | 426.13 | 3.74 | 0.75 |
| SPAC4G9.07 | 4.75 | 17.47 | 6.61 | 3.65 | 7.07 | 3.68 | 0.38 |
| SPBC4C3.04c | 14.60 | 53.48 | 31.63 | 50.83 | 41.30 | 3.66 | 0.59 |
| SPAC9E9.12c | 23.56 | 85.71 | 68.41 | 98.93 | 98.23 | 3.64 | 0.80 |
| SPAPB24D3.08c | 47.57 | 169.75 | 83.71 | 77.39 | 88.32 | 3.57 | 0.49 |
| SPCC1620.02 | 6.66 | 23.54 | 12.65 | 2.24 | 8.81 | 3.53 | 0.54 |
| SPCC1020.03 | 13.10 | 46.15 | 18.45 | 28.26 | 34.75 | 3.52 | 0.40 |
| SPBC428.08c | 8.79 | 30.26 | 10.00 | 8.24 | 9.60 | 3.44 | 0.33 |
| SPAC6B12.06c | 13.59 | 46.63 | 38.39 | 46.64 | 40.42 | 3.43 | 0.82 |
| SPBC16E9.16c | 32.99 | 112.77 | 39.92 | 37.93 | 69.38 | 3.42 | 0.35 |
| SPBC1271.09 | 7.83 | 25.98 | 17.53 | 32.01 | 79.63 | 3.32 | 0.67 |
| SPBC32H8.07 | 7.51 | 24.91 | 12.17 | 5.54 | 25.63 | 3.32 | 0.49 |
| SPBC2G2.10c | 25.46 | 83.04 | 17.05 | 12.79 | 17.78 | 3.26 | 0.21 |
| SPAC22F3.03c | 8.43 | 27.45 | 13.15 | 19.61 | 20.61 | 3.26 | 0.48 |
| SPAC29E6.08 | 131.17 | 415.81 | 263.07 | 389.58 | 505.16 | 3.17 | 0.63 |
| SPBC337.08c | 27.24 | 85.24 | 43.73 | 301.95 | 46.09 | 3.13 | 0.51 |
| SPCC417.11c | 7.95 | 24.66 | 16.20 | 25.67 | 17.65 | 3.10 | 0.66 |
| SPCC63.04 | 17.43 | 53.98 | 17.27 | 15.87 | 12.45 | 3.10 | 0.32 |
| SPCC330.06c | 83.17 | 255.00 | 235.15 | 287.17 | 296.70 | 3.07 | 0.92 |
| SPAC15E1.02c | 22.49 | 68.59 | 34.09 | 73.37 | 61.81 | 3.05 | 0.50 |
| SPAC13G6.12c | 9.58 | 29.00 | 20.67 | 19.68 | 24.99 | 3.03 | 0.71 |
| SPAC25H1.05 | 23.57 | 70.84 | 45.44 | 42.99 | 45.93 | 3.01 | 0.64 |
| SPAC1002.19 | 14.69 | 42.26 | 25.65 | 12.74 | 66.03 | 2.88 | 0.61 |
| SPBC646.06c | 43.47 | 124.89 | 46.22 | 52.64 | 39.50 | 2.87 | 0.37 |
| SPCC4G3.10c | 13.88 | 39.63 | 27.35 | 32.57 | 72.03 | 2.86 | 0.69 |

| | | | | | | | |
|---|---|---|---|---|---|---|---|
| SPBC660.06 | 52.10 | 146.58 | 83.55 | 67.64 | 128.15 | 2.81 | 0.57 |
| SPCC11E10.09c | 10.73 | 30.05 | 13.86 | 11.56 | 9.04 | 2.80 | 0.46 |
| SPAC1006.01 | 42.12 | 117.74 | 117.98 | 84.16 | 98.12 | 2.80 | 1.00 |
| SPCC830.09c | 34.36 | 95.70 | 44.91 | 74.79 | 55.12 | 2.79 | 0.47 |
| SPAC3G9.11c | 15.17 | 42.01 | 23.57 | 32.08 | 51.88 | 2.77 | 0.56 |
| SPCC18B5.01c | 19.75 | 54.64 | 45.70 | 48.72 | 31.02 | 2.77 | 0.84 |
| SPAC4A8.04 | 38.37 | 105.82 | 61.87 | 52.62 | 73.46 | 2.76 | 0.58 |
| SPAC869.05c | 5.18 | 14.25 | 4.86 | 11.97 | 8.06 | 2.75 | 0.34 |
| SPCC1183.09c | 52.85 | 145.28 | 62.76 | 43.75 | 58.60 | 2.75 | 0.43 |
| SPCC613.11c | 14.83 | 40.70 | 26.82 | 16.80 | 23.03 | 2.75 | 0.66 |
| SPAC3C7.05c | 14.60 | 39.64 | 27.77 | 25.49 | 27.45 | 2.72 | 0.70 |
| SPAC19G12.09 | 217.04 | 586.11 | 394.74 | 189.83 | 356.33 | 2.70 | 0.67 |
| SPAC16A10.04 | 14.85 | 39.97 | 20.44 | 35.19 | 32.14 | 2.69 | 0.51 |
| SPBC3H7.09 | 32.90 | 87.51 | 34.21 | 35.06 | 25.53 | 2.66 | 0.39 |
| SPAC3A12.08 | 20.17 | 53.26 | 31.95 | 36.02 | 57.74 | 2.64 | 0.60 |
| SPCC965.06 | 33.94 | 89.47 | 50.56 | 44.57 | 87.23 | 2.64 | 0.57 |
| SPAC24H6.13 | 12.37 | 32.16 | 10.99 | 21.60 | 17.97 | 2.60 | 0.34 |
| SPAPB17E12.10c | 15.80 | 41.09 | 21.10 | 22.47 | 18.40 | 2.60 | 0.51 |
| SPAC18B11.04 | 54.03 | 139.77 | 55.32 | 59.42 | 61.93 | 2.59 | 0.40 |
| SPBC2A9.02 | 55.41 | 142.15 | 119.72 | 106.73 | 129.62 | 2.57 | 0.84 |
| SPAC977.14c | 335.40 | 860.41 | 1123.69 | 724.75 | 1193.95 | 2.57 | 1.31 |
| SPBC1773.03c | 8.93 | 22.66 | 12.98 | 20.81 | 23.96 | 2.54 | 0.57 |
| SPAC22G7.07c | 8.14 | 20.62 | 10.33 | 10.08 | 8.13 | 2.53 | 0.50 |
| SPBC19C7.04c | 104.81 | 264.71 | 93.44 | 108.96 | 134.28 | 2.53 | 0.35 |
| SPBC1652.01 | 11.28 | 28.39 | 31.46 | 54.33 | 49.29 | 2.52 | 1.11 |
| SPAC4F10.12 | 29.24 | 72.74 | 36.18 | 69.97 | 61.24 | 2.49 | 0.50 |
| SPAC1F7.07c | 30.07 | 74.06 | 16.46 | 7.36 | 25.46 | 2.46 | 0.22 |
| SPCC1393.04 | 18.77 | 46.18 | 37.05 | 38.79 | 37.54 | 2.46 | 0.80 |
| SPBC713.11c | 205.97 | 500.92 | 279.31 | 271.06 | 410.74 | 2.43 | 0.56 |
| SPAC513.02 | 19.47 | 47.26 | 49.49 | 27.81 | 30.21 | 2.43 | 1.05 |
| SPAC27D7.03c | 5.86 | 13.99 | 4.75 | 4.13 | 4.80 | 2.39 | 0.34 |
| SPAC4H3.08 | 18.95 | 44.75 | 22.41 | 23.77 | 16.90 | 2.36 | 0.50 |
| SPBC1604.01 | 16.33 | 38.41 | 22.86 | 43.93 | 38.70 | 2.35 | 0.60 |
| SPBC119.03 | 68.01 | 158.85 | 87.51 | 85.63 | 81.64 | 2.34 | 0.55 |
| SPCC1020.13c | 19.33 | 45.06 | 24.92 | 20.87 | 27.67 | 2.33 | 0.55 |
| SPAC18B11.06 | 33.69 | 78.45 | 54.75 | 66.40 | 124.93 | 2.33 | 0.70 |
| SPAC20G8.10c | 17.45 | 40.13 | 24.18 | 15.67 | 27.10 | 2.30 | 0.60 |
| SPAC1006.03c | 61.27 | 138.68 | 196.05 | 104.15 | 110.16 | 2.26 | 1.41 |

| | | | | | | | |
|---|---|---|---|---|---|---|---|
| SPAC1610.01 | 30.20 | 68.26 | 53.56 | 62.02 | 78.27 | 2.26 | 0.78 |
| SPAC4F10.20 | 162.58 | 367.20 | 466.69 | 650.44 | 294.01 | 2.26 | 1.27 |
| SPCC1393.12 | 59.61 | 134.23 | 60.34 | 66.14 | 87.78 | 2.25 | 0.45 |
| SPAC17G8.11c | 17.50 | 39.32 | 25.35 | 26.40 | 42.19 | 2.25 | 0.64 |
| SPCC1682.08c | 30.94 | 68.96 | 30.18 | 59.19 | 91.00 | 2.23 | 0.44 |
| SPAC20G4.03c | 9.79 | 21.79 | 13.63 | 14.02 | 11.07 | 2.23 | 0.63 |
| SPAC1705.02 | 215.85 | 480.02 | 450.71 | 433.85 | 359.09 | 2.22 | 0.94 |
| SPAC1F7.12 | 31.94 | 70.66 | 41.27 | 44.83 | 54.00 | 2.21 | 0.58 |
| SPBP8B7.24c | 246.62 | 541.46 | 261.49 | 135.03 | 154.85 | 2.20 | 0.48 |
| SPAC23G3.02c | 10.97 | 24.08 | 10.65 | 13.12 | 12.74 | 2.20 | 0.44 |
| SPCC1672.09 | 58.65 | 127.92 | 44.35 | 30.84 | 34.32 | 2.18 | 0.35 |
| SPAC20G4.06c | 291.50 | 634.41 | 620.10 | 755.98 | 559.54 | 2.18 | 0.98 |
| SPBC3B9.17 | 48.69 | 105.72 | 88.51 | 57.53 | 48.78 | 2.17 | 0.84 |
| SPAC222.04c | 119.32 | 254.52 | 158.92 | 194.30 | 179.82 | 2.13 | 0.62 |
| SPAC6B12.05c | 60.31 | 128.39 | 76.41 | 86.51 | 96.61 | 2.13 | 0.60 |
| SPBC3E7.02c | 255.14 | 541.99 | 424.48 | 912.57 | 372.94 | 2.12 | 0.78 |
| SPAC19G12.11 | 53.93 | 114.52 | 80.20 | 91.99 | 63.74 | 2.12 | 0.70 |
| SPAC2C4.15c | 31.73 | 67.06 | 46.50 | 41.81 | 69.27 | 2.11 | 0.69 |
| SPAC19G12.13c | 20.47 | 43.04 | 34.46 | 33.10 | 22.14 | 2.10 | 0.80 |
| SPAC29B12.13 | 77.48 | 162.20 | 123.70 | 259.44 | 154.48 | 2.09 | 0.76 |
| SPBC12C2.04 | 100.46 | 209.66 | 172.77 | 116.21 | 97.04 | 2.09 | 0.82 |
| SPAC23D3.12 | 22.83 | 47.47 | 37.34 | 14.52 | 38.43 | 2.08 | 0.79 |
| SPAC4F8.01 | 108.02 | 223.99 | 173.02 | 145.09 | 116.27 | 2.07 | 0.77 |
| SPAC4G8.02c | 125.79 | 257.97 | 342.11 | 395.16 | 238.83 | 2.05 | 1.33 |
| SPAC22F3.08c | 34.09 | 68.26 | 62.67 | 69.15 | 114.09 | 2.00 | 0.92 |
| SPBC1709.11c | 76.26 | 152.22 | 115.07 | 83.42 | 87.63 | 2.00 | 0.76 |
| SPBC405.04c | 111.51 | 222.38 | 141.22 | 135.60 | 131.03 | 1.99 | 0.64 |
| SPBC337.12 | 53.05 | 104.95 | 62.90 | 60.89 | 65.56 | 1.98 | 0.60 |
| SPAC19A8.06 | 37.45 | 73.92 | 62.94 | 56.75 | 53.83 | 1.97 | 0.85 |
| SPBC1271.10c | 22.97 | 44.91 | 37.48 | 38.80 | 80.42 | 1.95 | 0.83 |
| SPCC1840.09 | 38.03 | 74.26 | 60.16 | 62.81 | 52.44 | 1.95 | 0.81 |
| SPBC29A10.12 | 259.43 | 505.74 | 312.37 | 207.92 | 244.38 | 1.95 | 0.62 |
| SPAC1527.02 | 58.11 | 113.28 | 75.72 | 90.99 | 68.93 | 1.95 | 0.67 |
| SPAC26F1.07 | 291.83 | 568.59 | 921.99 | 329.41 | 305.16 | 1.95 | 1.62 |
| SPBC29A3.01 | 24.83 | 47.75 | 28.07 | 48.24 | 69.39 | 1.92 | 0.59 |
| SPAC22F8.05 | 22.14 | 42.53 | 28.10 | 20.74 | 47.17 | 1.92 | 0.66 |
| SPCC1393.10 | 50.61 | 96.97 | 151.61 | 351.89 | 262.82 | 1.92 | 1.56 |
| SPAC25B8.01 | 84.82 | 161.96 | 152.30 | 130.31 | 152.68 | 1.91 | 0.94 |
| SPAC12B10.16c | 29.31 | 55.95 | 26.18 | 31.78 | 23.28 | 1.91 | 0.47 |

| | | | | | | | |
|---|---|---|---|---|---|---|---|
| SPBC543.06c | 54.31 | 101.95 | 85.12 | 90.09 | 96.83 | 1.88 | 0.83 |
| SPCC11E10.07c | 73.25 | 137.24 | 124.72 | 117.78 | 121.94 | 1.87 | 0.91 |
| SPAC8C9.16c | 41.10 | 76.39 | 41.89 | 23.78 | 30.74 | 1.86 | 0.55 |
| SPBC17D11.08 | 46.43 | 84.17 | 39.47 | 38.21 | 33.69 | 1.81 | 0.47 |
| SPCPB16A4.07 | 252.42 | 453.58 | 449.62 | 277.63 | 342.24 | 1.80 | 0.99 |
| SPBC577.10 | 150.35 | 265.54 | 211.86 | 257.94 | 226.51 | 1.77 | 0.80 |
| SPBP8B7.16c | 126.34 | 222.89 | 186.88 | 247.38 | 506.25 | 1.76 | 0.84 |

## Table 2. Rrp6 non coding RNA targets

| Systematic ID | WT fpkm | rrp6-del fpkm | rrp6-cat fpkm | dis3-4 30C fpkm | rrp6-cat dis3-4 30C fpkm | cat/del ratio |
|---|---|---|---|---|---|---|
| SPATRNAILE.02 | 1.00 | 74.46 | 111.37 | 32.64 | 81.89 | 1.50 |
| SPBTRNAGLY.09 | 1.00 | 78.91 | 16.70 | 0.00 | 6.88 | 0.21 |
| SPNCRNA.1415 | 1.00 | 58.92 | 26.00 | 17.68 | 88.62 | 0.44 |
| SPNCRNA.173 | 1.00 | 158.11 | 21.21 | 100.37 | 57.84 | 0.13 |
| SPNCRNA.209 | 1.00 | 20.04 | 25.01 | 59.53 | 29.61 | 1.25 |
| SPNCRNA.220 | 1.00 | 91.25 | 15.92 | 25.55 | 4.12 | 0.17 |
| SPNCRNA.281 | 1.00 | 10.71 | 7.74 | 14.15 | 5.26 | 0.72 |
| SPNCRNA.392 | 1.00 | 25.82 | 15.71 | 41.27 | 24.39 | 0.61 |
| SPNCRNA.603 | 1.00 | 10.98 | 1.24 | 5.26 | 4.96 | 0.11 |
| SPSNORNA.53 | 1.00 | 288.91 | 27.54 | 0.00 | 67.97 | 0.10 |
| SPNCRNA.901 | 51.29 | 4496.88 | 1868.13 | 3719.84 | 2450.84 | 0.42 |
| SPSNORNA.32 | 97.17 | 7795.34 | 2568.01 | 3549.59 | 3115.46 | 0.33 |
| SPNCRNA.1511 | 60.99 | 3440.40 | 1723.10 | 3297.66 | 2426.65 | 0.50 |
| SPNCRNA.942 | 48.14 | 2419.01 | 885.09 | 2549.66 | 1523.90 | 0.37 |
| SPNCRNA.965 | 40.88 | 1954.20 | 1454.09 | 991.08 | 1308.10 | 0.74 |
| SPNCRNA.507 | 371.62 | 15032.50 | 12290.30 | 827.71 | 1878.33 | 0.82 |
| SPNCRNA.1436 | 22.60 | 616.23 | 651.09 | 947.52 | 656.93 | 1.06 |
| SPNCRNA.893 | 34.62 | 912.56 | 788.10 | 1417.61 | 964.57 | 0.86 |
| SPNCRNA.445 | 58.64 | 1439.78 | 1046.05 | 916.43 | 962.10 | 0.73 |
| SPSNORNA.35 | 239.19 | 5073.34 | 2748.80 | 3841.92 | 2681.36 | 0.54 |
| SPNCRNA.1444 | 107.57 | 1532.56 | 1027.29 | 1119.75 | 1169.36 | 0.67 |
| SPNCRNA.727 | 29.51 | 394.50 | 267.36 | 289.40 | 278.85 | 0.68 |
| SPNCRNA.1397 | 8.70 | 101.74 | 16.59 | 37.48 | 28.91 | 0.16 |
| SPNCRNA.475 | 138.49 | 1374.90 | 3166.53 | 4807.34 | 2512.12 | 2.30 |
| SPNCRNA.1696 | 27.29 | 249.55 | 156.78 | 392.20 | 249.47 | 0.63 |

| | | | | | | |
|---|---|---|---|---|---|---|
| SPNCRNA.906 | 137.33 | 1171.80 | 1387.01 | 1903.81 | 1233.84 | 1.18 |
| SPNCRNA.1153 | 18.62 | 121.62 | 76.73 | 29.05 | 105.06 | 0.63 |
| SPNCRNA.659 | 27.73 | 181.67 | 66.79 | 52.71 | 73.74 | 0.37 |
| SPNCRNA.1236 | 44.48 | 265.65 | 176.33 | 221.51 | 215.75 | 0.66 |
| SPNCRNA.584 | 18.59 | 106.42 | 24.38 | 26.02 | 37.39 | 0.23 |
| SPNCRNA.793 | 162.85 | 909.06 | 427.76 | 374.00 | 464.63 | 0.47 |
| SPNCRNA.605 | 18.38 | 95.60 | 26.90 | 21.17 | 75.80 | 0.28 |
| SPNCRNA.1213 | 16.52 | 76.32 | 37.62 | 33.48 | 82.96 | 0.49 |
| SPNCRNA.1095 | 658.36 | 2122.55 | 6073.27 | 2581.32 | 4468.36 | 2.86 |
| SPNCRNA.844 | 45.59 | 119.74 | 84.91 | 122.83 | 110.19 | 0.71 |
| SPNCRNA.348 | 1.00 | 16.00 | 10.86 | 12.31 | 5.46 | 0.68 |
| SPNCRNA.29 | 16.47 | 235.07 | 39.39 | 85.88 | 31.15 | 0.17 |
| SPNCRNA.267 | 1.00 | 14.16 | 10.62 | 5.31 | 13.86 | 0.75 |
| SPNCRNA.723 | 16.30 | 281.43 | 75.47 | 226.52 | 151.90 | 0.27 |
| SPNCRNA.667 | 44.94 | 228.16 | 195.89 | 243.77 | 201.30 | 0.86 |
| SPNCRNA.388 | 52.75 | 137.94 | 73.36 | 72.92 | 4.66 | 0.53 |
| SPSNORNA.40 | 43.85 | 2906.30 | 514.33 | 1252.93 | 650.89 | 0.18 |
| SPNCRNA.1238 | 14.25 | 233.65 | 14.83 | 17.99 | 14.33 | 0.06 |
| SPNCRNA.713 | 19.42 | 58.14 | 57.90 | 90.86 | 69.28 | 1.00 |
| SPNCRNA.118 | 1.00 | 65.38 | 1.00 | 0.00 | 0.00 | 0.02 |
| SPNCRNA.1580 | 17.81 | 56.30 | 32.07 | 30.07 | 33.74 | 0.57 |
| SPNCRNA.710 | 28.14 | 73.13 | 32.74 | 32.49 | 38.50 | 0.45 |
| SPNCRNA.1615 | 89.36 | 179.96 | 135.88 | 171.18 | 124.30 | 0.76 |
| SPNCRNA.1483 | 18.24 | 82.97 | 92.43 | 38.38 | 76.04 | 1.11 |
| SPNCRNA.771 | 28.05 | 68.07 | 40.58 | 93.43 | 62.66 | 0.60 |
| SPNCRNA.1197 | 16.87 | 1180.45 | 61.01 | 207.48 | 138.68 | 0.05 |
| SPSNORNA.46 | 39.20 | 814.01 | 171.59 | 210.88 | 166.56 | 0.21 |
| SPSNORNA.37 | 51.70 | 4482.50 | 1959.63 | 3785.72 | 2590.30 | 0.44 |
| SPNCRNA.1435 | 6.56 | 34.10 | 19.21 | 17.44 | 72.62 | 0.56 |
| SPBTRNAASN.04 | 1.00 | 45.52 | 57.45 | 14.56 | 23.52 | 1.26 |
| SPNCRNA.989 | 6.96 | 32.65 | 10.76 | 12.33 | 13.55 | 0.33 |
| SPNCRNA.510 | 78.07 | 3793.02 | 1618.39 | 2597.96 | 2453.14 | 0.43 |
| SPNCRNA.316 | 28.16 | 87.10 | 118.87 | 91.08 | 88.88 | 1.36 |
| SPRRNA.15 | 118.41 | 927.38 | 1682.59 | 317.11 | 712.78 | 1.81 |
| SPNCRNA.1651 | 23.98 | 2098.28 | 963.32 | 1611.81 | 1274.85 | 0.46 |
| SPNCRNA.606 | 5.24 | 306.70 | 10.75 | 8.00 | 10.11 | 0.04 |
| SPNCRNA.708 | 20.54 | 47.37 | 54.10 | 71.24 | 60.83 | 1.14 |
| SPNCRNA.103 | 9.69 | 2522.37 | 122.76 | 285.35 | 205.25 | 0.05 |
| SPSNORNA.21 | 52.73 | 2359.63 | 366.60 | 44.03 | 166.03 | 0.16 |

| | | | | | | |
|---|---|---|---|---|---|---|
| SPNCRNA.1042 | 45.10 | 190.06 | 166.72 | 114.55 | 146.01 | 0.88 |
| SPNCRNA.1293 | 26.67 | 81.72 | 61.17 | 171.63 | 116.99 | 0.75 |
| SPNCRNA.751 | 13.21 | 113.17 | 59.63 | 140.35 | 109.07 | 0.53 |
| SPNCRNA.1663 | 22.34 | 109.56 | 32.70 | 27.74 | 25.11 | 0.30 |
| SPNCRNA.1394 | 19.44 | 471.12 | 274.77 | 277.72 | 304.87 | 0.58 |
| SPNCRNA.666 | 25.91 | 56.33 | 36.86 | 80.99 | 64.77 | 0.65 |
| SPNCRNA.301 | 14.22 | 77.56 | 49.55 | 81.10 | 71.42 | 0.64 |
| SPNCRNA.648 | 51.31 | 178.53 | 122.31 | 255.29 | 262.46 | 0.69 |
| SPNCRNA.58 | 52.84 | 146.16 | 90.51 | 148.56 | 101.47 | 0.62 |
| SPNCRNA.629 | 171.56 | 320.79 | 231.27 | 230.12 | 201.64 | 0.72 |
| SPSNORNA.44 | 41.23 | 2599.80 | 1475.50 | 2676.06 | 814.13 | 0.57 |
| SPNCRNA.762 | 4.64 | 48.96 | 9.32 | 4.89 | 7.34 | 0.19 |
| SPSNORNA.13 | 59.77 | 3183.24 | 1535.22 | 38.93 | 779.60 | 0.48 |
| SPSNORNA.36 | 38.66 | 1992.45 | 958.85 | 1263.64 | 1277.00 | 0.48 |
| SPNCRNA.513 | 10.85 | 139.26 | 125.39 | 122.11 | 80.53 | 0.90 |
| SPNCRNA.1469 | 9.09 | 20.71 | 16.49 | 24.71 | 28.00 | 0.80 |
| SPNCRNA.1578 | 215.02 | 412.23 | 243.49 | 416.36 | 493.01 | 0.59 |
| SPNCRNA.1114 | 31.82 | 663.18 | 534.93 | 862.32 | 773.19 | 0.81 |
| SPATRNAALA.06 | 1.00 | 29.46 | 50.70 | 12.98 | 16.37 | 1.72 |
| SPNCRNA.1685 | 20.68 | 91.74 | 22.49 | 22.46 | 25.66 | 0.25 |
| SPSNORNA.42 | 62.24 | 1576.51 | 995.50 | 968.86 | 492.36 | 0.63 |
| SPNCRNA.760 | 7.69 | 28.16 | 14.09 | 24.02 | 24.48 | 0.50 |
| SPNCRNA.1094 | 200.78 | 419.78 | 800.76 | 617.43 | 1037.39 | 1.91 |
| SPNCRNA.692 | 100.51 | 182.06 | 150.67 | 162.03 | 155.20 | 0.83 |
| SPNCRNA.877 | 10.25 | 55.04 | 30.10 | 94.23 | 175.28 | 0.55 |
| SPNCRNA.1356 | 7.47 | 57.52 | 17.92 | 27.05 | 24.36 | 0.31 |
| SPNCRNA.1584 | 19.72 | 48.00 | 29.30 | 34.96 | 25.51 | 0.61 |
| SPNCRNA.411 | 8.23 | 56.01 | 32.84 | 20.24 | 39.97 | 0.59 |
| SPNCRNA.412 | 24.84 | 69.89 | 62.62 | 72.14 | 37.93 | 0.90 |
| SPNCRNA.1588 | 14.77 | 54.01 | 17.83 | 12.83 | 11.61 | 0.33 |
| SPATRNALEU.01 | 1.00 | 22.82 | 31.36 | 11.46 | 30.04 | 1.37 |
| SPNCRNA.1198 | 5.48 | 39.31 | 11.80 | 15.28 | 14.96 | 0.30 |
| SPNCRNA.243 | 6.60 | 44.76 | 26.62 | 57.77 | 37.73 | 0.59 |
| SPNCRNA.431 | 10.03 | 65.46 | 33.82 | 38.37 | 38.97 | 0.52 |
| SPNCRNA.1461 | 82.17 | 172.81 | 120.95 | 126.91 | 120.97 | 0.70 |
| SPNCRNA.1402 | 28.03 | 102.68 | 75.52 | 101.32 | 86.91 | 0.74 |
| SPNCRNA.427 | 27.61 | 81.71 | 81.65 | 83.20 | 95.03 | 1.00 |
| SPNCRNA.1299 | 20.19 | 58.89 | 79.01 | 32.77 | 204.07 | 1.34 |
| SPNCRNA.1129 | 22.72 | 52.60 | 49.72 | 69.17 | 39.35 | 0.95 |

## Table 3. GO results for Rrp6 targets

| GO ID | TERM | P-VALUE | No. of Annotations | Tot. Annotations in Category |
|---|---|---|---|---|
| GO:0055072 | iron ion homeostasis | 2.13E-07 | 9 | 22 |
| GO:0055076 | transition metal ion homeostasis | 4.21E-07 | 11 | 41 |
| GO:0006879 | cellular iron ion homeostasis | 2.61E-06 | 8 | 20 |
| GO:0046916 | cellular transition metal ion homeostasis | 4.18E-06 | 10 | 39 |
| GO:0000003 | reproduction | 2.67E-05 | 25 | 332 |
| GO:0033212 | iron assimilation | 5.38E-05 | 5 | 7 |
| GO:0055065 | metal ion homeostasis | 5.41E-05 | 11 | 63 |
| GO:0055080 | cation homeostasis | 0.000139282 | 12 | 84 |
| GO:0048878 | chemical homeostasis | 0.000151283 | 13 | 101 |
| GO:0098771 | inorganic ion homeostasis | 0.000159129 | 12 | 85 |
| GO:0050801 | ion homeostasis | 0.000206533 | 12 | 87 |
| GO:1903046 | meiotic cell cycle process | 0.000280604 | 17 | 184 |
| GO:0006875 | cellular metal ion homeostasis | 0.000390755 | 10 | 61 |
| GO:0030001 | metal ion transport | 0.00045715 | 10 | 62 |
| GO:0051321 | meiotic cell cycle | 0.000486312 | 19 | 236 |
| GO:0055082 | cellular chemical homeostasis | 0.00068656 | 12 | 97 |
| GO:0030003 | cellular cation homeostasis | 0.000756763 | 11 | 81 |
| GO:0006873 | cellular ion homeostasis | 0.000970003 | 11 | 83 |
| GO:0006826 | iron ion transport | 0.001853573 | 5 | 12 |
| GO:0000041 | transition metal ion transport | 0.002058223 | 7 | 31 |
| GO:0019725 | cellular homeostasis | 0.002646558 | 12 | 110 |
| GO:0033215 | iron assimilation by reduction and transport | 0.005567091 | 3 | 3 |
| GO:1901678 | iron coordination entity transport | 0.005567091 | 3 | 3 |
| GO:0034755 | iron ion transmembrane transport | 0.007969543 | 4 | 8 |
| GO:0022414 | reproductive process | 0.008978605 | 15 | 189 |

## Table 4. Rrp6 target iron homeostasis mRNAs

| GENE | wt | del | cat | dis3-30 | rrp6-dis3-30 | cat/del |
|---|---|---|---|---|---|---|
| SPAC1F8.03c | 3.76 | 84.14 | 7.66 | 0.99 | 31.74 | 0.09 |
| SPBC1683.09c | 10.32 | 130.03 | 24.55 | 11.52 | 26.02 | 0.19 |
| SPAC1F7.08 | 3.02 | 40.04 | 6.79 | 2.95 | 15.84 | 0.17 |
| SPBC947.05c | 5.21 | 21.32 | 9.51 | 8.91 | 10.15 | 0.45 |

| | | | | | | |
|---|---|---|---|---|---|---|
| SPCC1020.03 | 13.10 | 46.15 | 18.45 | 28.26 | 34.75 | 0.40 |
| SPBC4F6.09 | 31.57 | 125.26 | 38.89 | 16.08 | 36.87 | 0.31 |
| SPAC1F7.07c | 30.07 | 74.06 | 16.46 | 7.36 | 25.46 | 0.22 |
| SPBP26C9.03c | 5.04 | 34.94 | 9.84 | 11.13 | 17.24 | 0.28 |
| SPAC23G3.02c | 10.97 | 24.08 | 10.65 | 13.12 | 12.74 | 0.44 |

## Table 5. RNA accumulation of Mmi1 target mRNAs in *rrp6* and *dis3* mutants

| GENE | wt | del | cat | dis3-30 | rrp6-dis3-30 |
|---|---|---|---|---|---|
| SPBC29A10.02 | 4.71 | 627.87 | 15.90 | 26.84 | 16.28 |
| SPBC29A10.14 | 6.59 | 388.15 | 13.16 | 19.27 | 18.71 |
| SPAC13A11.03 | 13.19 | 481.92 | 41.02 | 37.28 | 45.01 |
| SPAC32A11.01 | 18.43 | 349.93 | 37.14 | 75.25 | 59.18 |
| SPBC1347.12 | 4.98 | 94.82 | 11.79 | 20.43 | 25.38 |
| SPAC57A10.04 | 8.29 | 283.47 | 41.71 | 54.38 | 42.22 |
| SPBC32H8.11 | 6.77 | 205.17 | 30.32 | 120.14 | 91.85 |
| SPAC1556.06 | 12.66 | 91.64 | 17.62 | 46.16 | 28.08 |
| SPAC27D7.13c | 8.75 | 88.69 | 18.40 | 33.30 | 45.47 |
| SPBC646.17c | 4.64 | 67.51 | 16.27 | 40.39 | 34.80 |
| SPCC1393.07c | 7.29 | 46.30 | 12.34 | 19.08 | 13.49 |
| SPBC2D10.06 | 5.99 | 77.00 | 20.76 | 40.27 | 34.09 |
| SPAP27G11.08c | 9.32 | 50.92 | 15.19 | 28.25 | 38.33 |
| SPAC23C4.07 | 8.76 | 84.14 | 33.81 | 47.45 | 58.07 |
| SPAC17A5.18c | 15.95 | 62.49 | 29.53 | 64.31 | 55.12 |
| SPAC458.04c | 12.18 | 42.12 | 22.27 | 37.79 | 24.00 |
| SPBC582.06c | #N/A | #N/A | #N/A | #N/A | #N/A |
| SPAC25G10.04c | 8.08 | 55.41 | 22.85 | 22.84 | 23.80 |
| SPCC11E10.03 | #N/A | #N/A | #N/A | #N/A | #N/A |
| SPBC216.02 | #N/A | #N/A | #N/A | #N/A | #N/A |
| SPAC14C4.03 | 4.00 | 37.42 | 12.09 | 29.50 | 17.55 |
| SPCC70.09c | 5.26 | 126.89 | 19.79 | 45.25 | 36.77 |
| SPAC6C3.05 | #N/A | #N/A | #N/A | #N/A | #N/A |
| SPBC577.05c | 4.12 | 27.95 | 10.01 | 23.77 | 18.51 |
| SPAC222.15 | 3.74 | 76.05 | 12.27 | 10.71 | 16.62 |
| SPBC2G2.09c | 1.99 | 88.69 | 6.25 | 18.23 | 17.22 |
| SPCC4E9.01c | 2.27 | 17.92 | 5.03 | 10.24 | 9.25 |

| | | | | | |
|---|---|---|---|---|---|
| SPBP8B7.04 | 6.31 | 41.15 | 23.99 | 52.11 | 27.57 |
| SPBC1921.04c | 1.00 | 58.27 | 19.33 | 22.06 | 8.99 |
| SPNCRNA.103 | 9.69 | 2522.37 | 122.76 | 285.35 | 205.25 |

## Table 6. Genes in GO categories

| GO ID | TERM | ANNOTATED_GENES |
|---|---|---|
| GO:0055072 | iron ion homeostasis | SPAC1F8.03c, SPBC1683.09c, SPAC1F7.08, SPBC947.05c, SPCC1020.03, SPBC4F6.09, SPAC1F7.07c, SPBP26C9.03c, SPAC23G3.02c |
| GO:0055076 | transition metal ion homeostasis | SPBC29A3.01, SPBC1683.09c, SPBC947.05c, SPCC1020.03, SPAC1F7.07c, SPBP26C9.03c, SPAC22H10.13, SPAC1F8.03c, SPAC1F7.08, SPBC4F6.09, SPAC23G3.02c |
| GO:0006879 | cellular iron ion homeostasis | SPAC1F8.03c, SPBC1683.09c, SPAC1F7.08, SPBC947.05c, SPCC1020.03, SPBC4F6.09, SPAC1F7.07c, SPAC23G3.02c |
| GO:0046916 | cellular transition metal ion homeostasis | SPBC29A3.01, SPBC1683.09c, SPBC947.05c, SPCC1020.03, SPAC1F7.07c, SPAC22H10.13, SPAC1F8.03c, SPAC1F7.08, SPBC4F6.09, SPAC23G3.02c |
| GO:0000003 | reproduction | SPAC17A5.04c, SPBC646.06c, SPBC428.08c, SPAC27D7.13c, SPBP8B7.24c, SPAC23C4.07, SPAC17A5.18c, SPAC13G6.12c, SPBC32H8.07, SPCC1682.08c, SPBC29A10.14, SPAC23D3.10c, SPCC63.04, SPAC18B11.04, SPBC337.08c, SPBC32H8.11, SPBC646.17c, SPBC2D10.06, SPBC29A10.02, SPAC5D6.08c, SPAC13A11.03, SPAC27D7.03c, SPBC16C6.14, SPAC22F3.03c, SPAC4A8.04 |
| GO:0033212 | iron assimilation | SPAC1F8.03c, SPBC1683.09c, SPAC1F7.08, SPBC4F6.09, SPAC1F7.07c |
| GO:0055065 | metal ion homeostasis | SPBC29A3.01, SPBC1683.09c, SPBC947.05c, SPCC1020.03, SPAC1F7.07c, SPBP26C9.03c, SPAC22H10.13, SPAC1F8.03c, SPAC1F7.08, SPBC4F6.09, SPAC23G3.02c |
| GO:0055080 | cation homeostasis | SPBC29A3.01, SPBC1683.09c, SPBC947.05c, SPCC1020.03, SPAC1F7.07c, SPBP26C9.03c, SPBC405.04c, SPAC22H10.13, SPAC1F8.03c, SPAC1F7.08, SPBC4F6.09, SPAC23G3.02c |
| GO:0048878 | chemical homeostasis | SPBC32H8.07, SPBC29A3.01, SPBC1683.09c, SPBC947.05c, SPCC1020.03, SPAC1F7.07c, SPBP26C9.03c, SPBC405.04c, SPAC22H10.13, SPAC1F8.03c, SPAC1F7.08, SPBC4F6.09, SPAC23G3.02c |
| GO:0098771 | inorganic ion homeostasis | SPBC29A3.01, SPBC1683.09c, SPBC947.05c, SPCC1020.03, SPAC1F7.07c, SPBP26C9.03c, SPBC405.04c, SPAC22H10.13, SPAC1F8.03c, SPAC1F7.08, SPBC4F6.09, SPAC23G3.02c |
| GO:0050801 | ion homeostasis | SPBC29A3.01, SPBC1683.09c, SPBC947.05c, SPCC1020.03, SPAC1F7.07c, SPBP26C9.03c, SPBC405.04c, SPAC22H10.13, SPAC1F8.03c, SPAC1F7.08, SPBC4F6.09, SPAC23G3.02c |
| GO:1903046 | meiotic cell cycle process | SPAC17A5.04c, SPBC646.06c, SPBC428.08c, SPAC27D7.13c, SPAC17A5.18c, SPBC29A10.14, SPAC13G6.12c, SPCC63.04, SPBC32H8.11, SPBC646.17c, SPBC2D10.06, SPBC29A10.02, SPAC5D6.08c, SPAC13A11.03, SPAC27D7.03c, SPBC16C6.14, SPAC22F3.03c |
| GO:000687 | cellular metal | SPBC29A3.01, SPBC1683.09c, SPBC947.05c, SPCC1020.03, SPAC1F7.07c, |

| | | |
|---|---|---|
| 5 | ion homeostasis | SPAC22H10.13, SPAC1F8.03c, SPAC1F7.08, SPBC4F6.09, SPAC23G3.02c |
| GO:0030001 | metal ion transport | SPCC965.06, SPBC29A3.01, SPAC18B11.04, SPBC1683.09c, SPBC947.05c, SPCC1020.03, SPAC1F7.07c, SPBP26C9.03c, SPAC1F7.08, SPAC25H1.05 |
| GO:0051321 | meiotic cell cycle | SPAC17A5.04c, SPBC646.06c, SPBC428.08c, SPAC27D7.13c, SPAC17A5.18c, SPBC29A10.14, SPCC1682.08c, SPAC13G6.12c, SPCC63.04, SPBC337.08c, SPBC32H8.11, SPBC646.17c, SPBC2D10.06, SPBC29A10.02, SPAC5D6.08c, SPAC13A11.03, SPAC27D7.03c, SPBC16C6.14, SPAC22F3.03c |
| GO:0055082 | cellular chemical homeostasis | SPBC32H8.07, SPBC29A3.01, SPBC1683.09c, SPBC947.05c, SPCC1020.03, SPAC1F7.07c, SPBC405.04c, SPAC22H10.13, SPAC1F8.03c, SPAC1F7.08, SPBC4F6.09, SPAC23G3.02c |
| GO:0030003 | cellular cation homeostasis | SPBC29A3.01, SPBC1683.09c, SPBC947.05c, SPCC1020.03, SPAC1F7.07c, SPBC405.04c, SPAC22H10.13, SPAC1F8.03c, SPAC1F7.08, SPBC4F6.09, SPAC23G3.02c |
| GO:0006873 | cellular ion homeostasis | SPBC29A3.01, SPBC1683.09c, SPBC947.05c, SPCC1020.03, SPAC1F7.07c, SPBC405.04c, SPAC22H10.13, SPAC1F8.03c, SPAC1F7.08, SPBC4F6.09, SPAC23G3.02c |
| GO:0006826 | iron ion transport | SPAC1F7.08, SPBC947.05c, SPCC1020.03, SPAC1F7.07c, SPBP26C9.03c |
| GO:0000041 | transition metal ion transport | SPBC29A3.01, SPBC1683.09c, SPAC1F7.08, SPBC947.05c, SPCC1020.03, SPAC1F7.07c, SPBP26C9.03c |
| GO:0019725 | cellular homeostasis | SPBC32H8.07, SPBC29A3.01, SPBC1683.09c, SPBC947.05c, SPCC1020.03, SPAC1F7.07c, SPBC405.04c, SPAC22H10.13, SPAC1F8.03c, SPAC1F7.08, SPBC4F6.09, SPAC23G3.02c |
| GO:0033215 | iron assimilation by reduction and transport | SPBC1683.09c, SPAC1F7.08, SPAC1F7.07c |
| GO:1901678 | iron coordination entity transport | SPAC1F8.02c, SPBC947.05c, SPBC4F6.09 |
| GO:0034755 | iron ion transmembrane transport | SPAC1F7.08, SPBC947.05c, SPAC1F7.07c, SPBP26C9.03c |
| GO:0022414 | reproductive process | SPAC13G6.12c, SPBC32H8.07, SPAC18B11.04, SPCC63.04, SPAC17A5.04c, SPAC23D3.10c, SPBC646.17c, SPBC646.06c, SPBC428.08c, SPAC27D7.13c, SPBC29A10.02, SPBP8B7.24c, SPAC23C4.07, SPBC16C6.14, SPAC4A8.04 |